

3835

NATIONAL LIBRARY
PUBLIC ARCHIVES BUILDING
OTTAWA 2



BIBLIOTHÈQUE NATIONALE
ÉDIFICE DES ARCHIVES PUBLIQUES
OTTAWA 2

NAME OF AUTHOR.....Gerard de Vries.....
TITLE OF THESIS...A Study of Visco. and.....
.....Pseudo-Plastic Flow.....
.....
UNIVERSITY...of Alberta - Edmonton.....
DEGREE.....Ph. D. YEAR GRANTED ...1969.....

Permission is hereby granted to THE NATIONAL
LIBRARY OF CANADA to microfilm this thesis and to
lend or sell copies of the film.

The author reserves other publication rights,
and neither the thesis nor extensive extracts from
it may be printed or otherwise reproduced without
the author's written permission.

(Signed)..........

PERMANENT ADDRESS:

Dept. of Mech. Eng.
U. of Calgary..
CALGARY, Alta

DATED...Jan. 10..... 1969

NL-91

THE UNIVERSITY OF ALBERTA

A STUDY OF VISCO AND PSEUDO-PLASTIC FLOW

by

 GERARD DE VRIES

A THESIS


SUBMITTED TO THE FACULTY OF GRADUATE STUDIES
IN PARTIAL FULFILMENT OF THE REQUIREMENTS FOR THE DEGREE
OF DOCTOR OF PHILOSOPHY

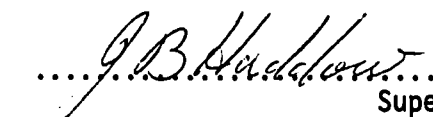
DEPARTMENT OF MECHANICAL ENGINEERING

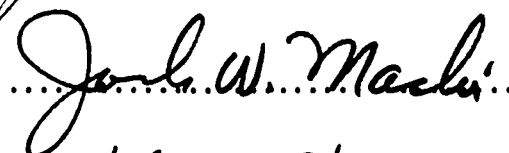
EDMONTON, ALBERTA
December, 1968

UNIVERSITY OF ALBERTA
FACULTY OF GRADUATE STUDIES

The undersigned certify that they have read, and recommend
to the Faculty of Graduate Studies for acceptance, a thesis entitled
"A STUDY OF VISCO AND PSEUDO-PLASTIC FLOW" submitted by GERARD DE VRIES
in partial fulfilment of the requirements for the degree of Doctor of
Philosophy.

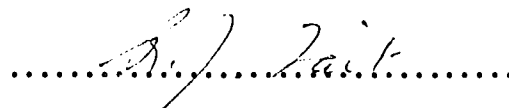



Supervisor

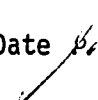









External Examiner

Date  June 8th 1969....

ABSTRACT

It is shown that solutions to the plane, radial, steady, quasi-static flow of a Bingham solid in a converging channel, and to the axially symmetric, radial, steady, quasi-static, converging flow in a circular cone do not exist, at least if the material is incompressible, and there are no body forces.

The velocity and stress fields for the corresponding power law pseudo-plastic flow problems are obtained. A new numerical technique is developed to solve the non-linear boundary value problem that arises in the determination of these fields.

The results are applied to hydraulic extrusions and wire drawing processes.

ACKNOWLEDGMENTS

The author wishes to extend his appreciation to Dr. J.B. Haddow for his guidance and supervision of this thesis. He also gratefully acknowledges the financial support for this research by the National Research Council and by the University of Alberta.

Thanks are extended to the members of the Mechanical Engineering Shop who made the experimental apparatus and particularly to R. Haswell who assisted in all stages of the experimental work.

Additional thanks are also extended to Dr. J.M. Chudobiak who on numerous occasions curtailed his own research in order to aid the author, and to Miss H. Wozniuk for her patience in typing the thesis.

The author would like also to express his appreciation to his wife, Ineke, for her encouragement and considerations.

TABLE OF CONTENTS

	<u>Page</u>
CHAPTER I INTRODUCTION	1
1.1 The Bingham Solid	4
1.2 The Pseudo-Plastic Material	8
1.3 Aim of the Thesis	10
1.4 Consideration of Related Problems	11
Plane Viscous Flow - Hamel's Problem	12
Axially Symmetric Analog to Hamel's Problem	12
Plane Rigid Perfectly Plastic Flow	13
Axially Symmetric Rigid Perfectly Plastic Flow	13
 CHAPTER II VISCO-PLASTIC FLOW	 15
2.1 Plane Visco-Plastic Flow	15
2.2 Axially Symmetric Visco-Plastic Flow	24
 CHAPTER III PSEUDO-PLASTIC FLOW	 33
3.1 Plane Pseudo-Plastic Flow	33
3.2 Axially Symmetric Pseudo-Plastic Flow	42
3.3 Integration Procedure	50
3.4 On the Inclusion of Inertia Effects	52
3.5 On the Neglect of Inertia Effects	54

TABLE OF CONTENTS (continued)

	<u>Page</u>
CHAPTER IV APPLICATION TO WIRE DRAWING AND HYDRAULIC EXTRUSION	63
4.1 Wire Drawing	68
4.2 Hydraulic Extrusion	78
 CHAPTER V EXPERIMENTAL INVESTIGATION	82
5.1 Experimental Apparatus	83
5.2 Results of Experiments	88
The Specimens	88
Lead Extrusions	89
Wax Extrusions	90
5.3 Conclusions	91
 CHAPTER VI CONCLUDING REMARKS	93
6.1 Results	93
6.2 Error Analysis of the Numerical Results	128
6.3 Objections to the Power Law Model	130
6.4 Wire Drawing and Hydraulic Extrusion	132
6.5 Suggestions for Future Work	141
 BIBLIOGRAPHY	147

TABLE OF CONTENTS (continued)

		<u>Page</u>
APPENDIX	NUMERICAL INTEGRATION OF ORDINARY DIFFERENTIAL EQUATIONS	
	A.1 Introduction	152
	A.2 The First Order Ordinary Differential Equation	152
	A.3 Equations Governing the Constants and Weighting Factors	154
	A.4 Determination of the Constants and Weighting Factors	158
	A.5 The System of First Order Ordinary Differential Equations	165
	A.6 Gill's Variation of the Runge-Kutta Fourth Order Method	169
	A.7 Brief Discussion on the Accuracy of the Method	174
	A.8 Subroutine DRKGS	177

LIST OF TABLES

<u>Table</u>		<u>Page</u>
A.1	Typical Terms and their Coefficients	169

LIST OF FIGURES

<u>Figure</u>		<u>Page</u>
1.1	Stress-Strain Rate Relationships for Simple Shear	4
2.1	Visco-Plastic Flow in a Converging Channel	16
2.2	Visco-Plastic Flow in a Circular Cone	25
3.1	Pseudo-Plastic Flow in a Converging Channel	34
3.2	Compression of a Pseudo-Plastic Material Between Inclined Plates	42
3.3	Pseudo-Plastic Flow in a Circular Cone	43
3.4	Pseudo-Plastic Flow in a Circular Tube	56
3.5	Velocity Components in a Circular Cone of Small Semi-Angle α	60
4.1	Flow Curves for the Power Law Model	64
4.2	Flow Curve for the "Rigid" Pseudo-Plastic Material	66
4.3	Cross-Section of a Conical Reducing Die	67
5.1	Typical Half of the Die	85
5.2	The Separation Plate	86
5.3	The Piston and the Piston Housing	87
6.1	Possible Negative Normal Stresses at the Walls	134
6.2	The Cone of Finite Length	142

LIST OF FIGURES (continued)

<u>Figure</u>	<u>Page</u>
A.1 Geometrical Construction of δy	154
Results of Plane Pseudo-Plastic Flow in a Converging Channel	
6.II-1 $m''(0)$ versus n	99
6.II-2 $m(\theta)$ versus θ : $\alpha = 15^\circ$	100
6.II-3 $m(\theta)$ versus θ : $\alpha = 30^\circ$	101
6.II-4 $m(\theta)$ versus θ : $\alpha = 45^\circ$	102
6.II-5 $m(\theta)$ versus θ : $\alpha = 60^\circ$	103
6.II-6 $\tau_{r\theta}(\alpha) r^{2n}/\mu Q^n$ versus n	104
6.II-7 $\tau_{r\theta}(\alpha) r^{2n}/\mu Q^n$ versus α : $\alpha = 0^\circ-30^\circ$	105
6.II-8 $\tau_{r\theta}(\alpha) r^{2n}/\mu Q^n$ versus α : $\alpha = 30^\circ-60^\circ$	106
6.II-9 $\alpha \tau_{r\theta}(\alpha) r^{2n}/\mu Q^n$ versus α : $\alpha = 0^\circ-25^\circ$	107
6.II-10 $\sigma_{ij} r^{2n}/\mu Q^n$ versus θ : $\alpha = 15^\circ$, $n = 0.1$	108
6.II-11 $\sigma_{ij} r^{2n}/\mu Q^n$ versus θ : $\alpha = 30^\circ$, $n = 0.1$	109
6.II-12 $\sigma_{ij} r^{2n}/\mu Q^n$ versus θ : $\alpha = 45^\circ$, $n = 0.1$	110
6.II-13 $\sigma_{ij} r^{2n}/\mu Q^n$ versus θ : $\alpha = 60^\circ$, $n = 0.1$	111
Results of Axially Symmetric Pseudo-Plastic Flow in a Circular Cone	
6.III-1 $m''(0)$ versus n	113
6.III-2 $m(\phi)$ versus ϕ : $\alpha = 15^\circ$	114
6.III-3 $m(\phi)$ versus ϕ : $\alpha = 30^\circ$	115
6.III-4 $m(\phi)$ versus ϕ : $\alpha = 45^\circ$	116

LIST OF FIGURES (continued)

<u>Figure</u>	<u>Page</u>
6.III-5 $m(\phi)$ versus ϕ : $\alpha = 60^\circ$	117
6.III-6 $\tau_{r\phi}(\alpha) r^{3n}/\mu Q^n$ versus n	118
6.III-7 $\tau_{r\phi}(\alpha) r^{3n}/\mu Q^n$ versus α : $\alpha = 0^\circ-30^\circ$	119
6.III-8 $\tau_{r\phi}(\alpha) r^{3n}/\mu Q^n$ versus α : $\alpha = 30^\circ-60^\circ$	120
6.III-9 $\alpha \tau_{r\phi}(\alpha) r^{3n}/\mu Q^n$ versus α : $\alpha = 0^\circ-20^\circ$	121
6.III-10 $\sigma_{ij} r^{3n}/\mu Q^n$ versus ϕ : $\alpha = 15^\circ$, $n = 0.1$	122
6.III-11 $\sigma_{ij} r^{3n}/\mu Q^n$ versus ϕ : $\alpha = 30^\circ$, $n = 0.1$	123
6.III-12 $\sigma_{ij} r^{3n}/\mu Q^n$ versus ϕ : $\alpha = 45^\circ$, $n = 0.1$	124
6.III-13 $\sigma_{ij} r^{3n}/\mu Q^n$ versus ϕ : $\alpha = 60^\circ$, $n = 0.1$	125
6.III-14 $m(\phi)$ versus ϕ : $\alpha = 5^\circ$, $n = 0.1$	126
6.III-15 $\sigma_{ij} r^{3n}/\mu Q^n$ versus ϕ : $\alpha = 5^\circ$, $n = 0.1$	127
Results of Wire Drawing and Hydraulic Extrusion	
6.A-1 Maximum Percentage Reduction versus α	138
6.A-2 Drawing Stress $\times D_1^{3n}/\mu Q^n$ versus α	139
6.A-3 $P_{ram} D_1^{3n}/\mu Q^n$ versus α	140

NOMENCLATURE

σ_{ij}	components of a stress tensor
s_{ij}	components of a deviatoric stress tensor
$-p$	hydrostatic part of the stress tensor
d_{ij}	components of a strain rate tensor
ρ	density
f_i	body forces per unit mass
v_i	components of a velocity vector
a_i	components of an acceleration vector
μ	(apparent) coefficient of viscosity
k	yield stress in pure shear
Y	tensile yield stress
I	$\sqrt{2d_{ij}d_{ij}}$ a strain rate invariant
J	$\sqrt{\frac{1}{2}s_{ij}s_{ij}}$ a stress invariant
$\frac{D}{Dt}$	material derivative
$v_{i,j}$	covariant differentiation
n	parameter in power law model
α	semi-angle of the channel or cone
D_1	exit diameter of the circular cone in wire drawing and hydraulic extrusion
Q	volume flow (per unit length)
$\sigma_{ij}r^{2n}/\mu Q^n$	components of a non-dimensional stress tensor for plane flow
$\sigma_{ij}r^{3n}/\mu Q^n$	components of a non-dimensional stress tensor for axially symmetric flow

NOMENCLATURE (continued)

$P_{ram} D_1^{3n} / \mu Q^n$ non-dimensional ram pressure in hydraulic extrusion

Drawing stress $\times D_1^{3n} / \mu Q^n$ non-dimensional drawing stress in wire
drawing

CHAPTER I

INTRODUCTION

Analysis of the deformation and flow of matter is facilitated by the assumption that matter is a continuum and by further introducing the broad classification of matter as being either a fluid or a solid.

A continuum is a hypothetical representation of matter as a continuous medium; a study based upon the assumption of a continuum is termed a phenomenological approach. A fluid, according to the classical definition, is a substance that flows under the action of any anisotropic stress system, no matter how small (1)*. A material is said to flow if it deforms continuously with time (1). A solid, according to the classical definition, is a substance that requires a definite non-zero anisotropic stress level to produce flow; a stress below this level produces deformation, which may be reversible or irreversible, but no flow.

The classification of a "real" substance as a solid is to some extent an idealization; this becomes more evident as experiments, employing more refined measuring techniques, show that the application of an anisotropic stress system to a "real" solid results in continuous deformation. Indeed the motto of the Society of Rheology is "Everything flows";** and this is termed by Reiner (1) as "the second axiom of rheology". The state-

*Numbers without decimal enclosed by brackets designate the references listed in the Bibliography.

**The motto of the Society of Rheology had its origin in the strictly philosophical deduction by Heraclitus (3), that "Everything flows".

ment "Everything flows" is justified since the essential difference between the tendency to flow of a fluid and a solid is quantitative and not qualitative. Thus, according to Reiner (2), it is equally as justifiable to claim that "Everything is solid".

The analysis of the deformation and flow, resulting from the application of forces to a material in bulk, is based on the following equations:

$$\sigma_{ij,j} + \rho f_i = \rho a_i , \quad (1.1)$$

$$\sigma_{ij} = \sigma_{ji} , \quad (1.2)$$

$$\frac{D\rho}{Dt} + \rho v_{i,i} = 0 , \quad (1.3)$$

and equations resulting from the first and second law of thermodynamics, which are not included since thermodynamic effects are neglected in the analysis presented in this thesis. Equation (1.2) is valid since the body moments per unit mass and couple stresses are assumed to be zero. The relations (1.1), (1.2), and (1.3) provide seven equations for the thirteen unknowns σ_{ij} , v_i , and ρ , if the distribution of the body force per unit mass, f_i , is known. The problem, therefore, remains six degrees indeterminate. To proceed further, the material response has to be considered; consequently what are known as constitutive equations are introduced. Eringen (4) notes that "The character of the material is brought into the formulation through appropriate constitutive equations for each material

with the constitutive variables being restricted in their regions of definitions."

Constitutive equations cannot be formulated arbitrarily, but must satisfy certain physical and mathematical requirements based on the axioms of constitutive theory as described by Eringen (4). The constitutive equations are relations between the stress and strain tensors and their time derivatives. For an arbitrary element these equations must be independent of any superimposed rigid body motion. In the constitutive equations certain rheological properties appear as parameters; these are elasticity, viscosity, and plasticity. These properties are termed by Reiner (5) as fundamental and other properties, which are combinations of the fundamental properties, as complex properties. Some examples of complex properties are retardation, relaxation, delayed elasticity, visco-plasticity, visco-elasticity, and anelasticity.

A "real" material exhibits all of the fundamental rheological properties to some extent (6). The inclusion of certain specific rheological properties in the constitutive equation of a "real" material is justified if it is observed experimentally that these properties dominate. This thesis considers visco-plastic and pseudo-plastic materials. These are inelastic materials for which plastic and viscous properties dominate. According to the classical definitions, the visco-plastic material considered in this thesis is an example of a solid, and the pseudo-plastic material is an example of a fluid. The relationships between shearing stress, τ_{xy} , and shearing strain rate, d_{xy} , in simple shear for these materials are indicated in FIG. 1.1, where, for the purpose of comparison, the Newtonian

viscous liquid is also shown.

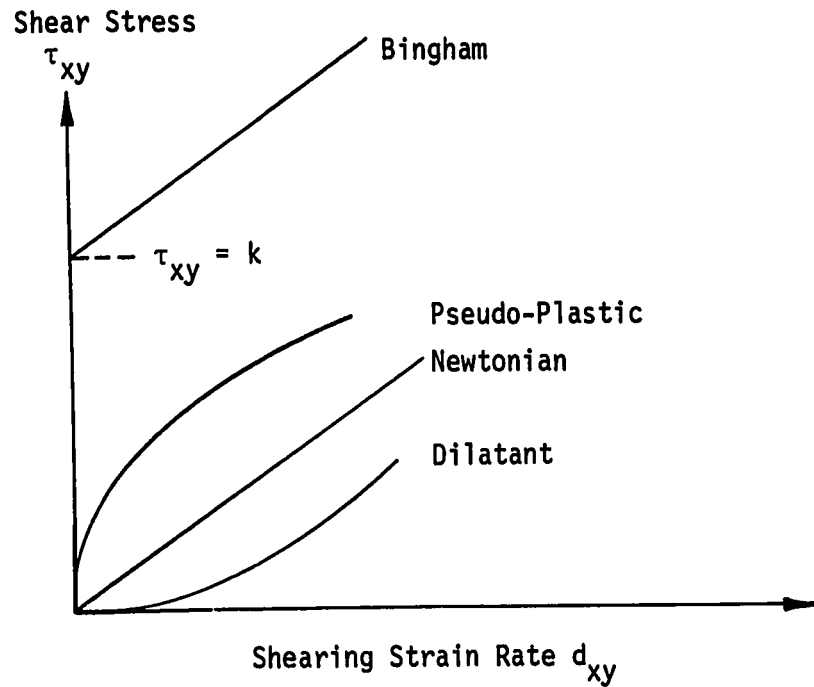


FIGURE 1.1

Stress-Strain Rate Relationships for Simple Shear

The remainder of this chapter presents a brief discussion of the Bingham solid and the pseudo-plastic material, respectively.

1.1 The Bingham Solid

In FIG. 1.1 the flow curve for a Newtonian viscous liquid is shown. The Newtonian liquid is a viscous material and its constitutive equation in simple shear is

$$\tau_{xy} = 2\mu d_{xy} .$$

The coefficient μ , which depends only on temperature and pressure, and not on rate of deformation, is called the Newtonian coefficient of viscosity, and it completely characterizes the fluid if the fluid can be considered incompressible.

The fundamental rheological properties may be associated with the manner in which mechanical energy is dissipated by the material. A material which is classified as perfectly elastic does not dissipate energy*; the Newtonian viscous liquid dissipates energy by the transfer of momentum on a molecular scale. Gases and liquids of low molecular weight are contained in the viscous category (7).

An inelastic dissipative material, whose behavior is not even approximately described by the Newtonian constitutive equation, is paint (8). Paint is required to possess the following practical properties:

- (i) it must brush without too much effort,
- (ii) it must flow in order that brushmarks disappear, i.e. it must possess "leveling" properties, and
- (iii) it must not run when applied to a vertical wall.

Reiner (8) points out that a low viscosity is required for the first two properties, and a high viscosity for the third; the viscosity requirements seem to be in conflict. The solution to this problem was found by Bingham and Green (9) and was presented by them in a paper entitled: "Paint, a Plastic Material and not a Viscous Liquid". The basis of the solution rested upon the experimentally determined fact that the viscosity of paint is not a constant for different rates of flow.

*At least if thermal effects are neglected.

The one-dimensional model, which Bingham and Green (9) suggested to describe the behavior of paint, has as its rheological equation in simple shear (10)

$$\tau_{xy} = 2\mu d_{xy} + \tau_0 \operatorname{sgn} d_{xy}, \text{ if } |\tau_{xy}| > \tau_0,$$

$$d_{xy} = 0, \text{ if } |\tau_{xy}| < \tau_0.$$

This two-parameter model is now termed the Bingham solid. A generalization of this model to three dimensions was suggested by Hohenemser and Prager (11). In three dimensions Prager (12) has characterized the mechanical behavior as follows: "Let a Newtonian viscous liquid, a perfectly plastic Mises solid, and a visco-plastic Bingham solid be subjected to the same velocity strain. The stress in the Bingham solid is then obtained by adding the stresses in the Newtonian liquid and the Mises solid". The constitutive equations for this generalization are

$$s_{ij} = 2\left(\mu + \frac{k}{I}\right) d_{ij}, \text{ if } I \neq 0, \quad (1.4)$$

where

$$I = (2d_{mn} d_{mn})^{1/2}.$$

Clearly the Newtonian viscous liquid and the perfectly plastic von Mises solid are special cases of the Bingham solid; this is consistent with the third axiom of rheology, which states that the constitutive equation of a

more simple body can be derived from that of a less simple body (13).

The constitutive equation (1.4) may be inverted as follows.

Squaring both sides of (1.4) gives

$$\mu I = \begin{cases} 0 & , \text{ if } J < k, \\ J-k & , \text{ if } J \geq k, \end{cases}$$

where

$$J = \left(\frac{1}{2} s_{mn} s_{mn} \right)^{1/2} .$$

Substituting in the original equation (1.4) gives

$$2\mu d_{ij} = \begin{cases} 0 & , \text{ if } J < k, \\ (1 - \frac{k}{J}) s_{ij} & , \text{ if } J \geq k . \end{cases}$$

Few non-trivial problems have been solved for the Bingham solid. Oldroyd (14) considered some two-dimensional boundary layer and rectilinear flow problems. Carlson (15) has treated the axial compression of a disc. Carlson used a piecewise linearized yield criterion introduced by Prager (16) in 1961. Haddow (17) extended Carlson's solution to include inertia effects. The linearization theory was extended by Haddow (18) and was applied by Haddow and Hrudef (19) to solve the flow problem of a thin circular plate subjected to a uniformly distributed transverse load. Prager (20) derived extremum principles for the Bingham solid; these extremum principles were extended by Haddow and Luming (21).

1.2 The Pseudo-Plastic Material

Comparison of the Bingham constitutive equation,

$$s_{ij} = 2\left(\mu + \frac{k}{\sqrt{2d_{mn}d_{mn}}}\right) d_{ij} ,$$

with that of a Newtonian viscous liquid,

$$s_{ij} = 2\mu d_{ij} ,$$

suggests that the Bingham solid can be considered to be a material with a variable coefficient of viscosity that depends on the strain rate invariant I,

$$\mu + \frac{k}{\sqrt{2d_{mn}d_{mn}}} ,$$

which can be termed the "apparent" viscosity. Other examples of materials with a variable coefficient of viscosity are the pseudo-plastic model, which describes a material for which viscosity decreases with an increasing shear rate, and the dilatant fluid, for which the viscosity increases with an increasing rate of shear (7). These effects were originally noted in colloidal solutions and their explanation is due to Ostwald (22). Ostwald hypothesized that a "structure" in the fluid altered with flow and introduced the term "Strukturviskosität" or "Structural viscosity" to denote this phenomenon. Fluids exhibiting this kind of variable viscosity have been designated by Reiner (23) as "Non-Newtonian fluids"; this "Non-Newtonian"

classification includes the Bingham solid, pseudo-plastics and dilatant fluids* (7).

Ostwald (10) suggested a two-parameter power law model as a means of characterizing the pseudo-plastic or the dilatant fluid; this power law is commonly written in simple shear as

$$\tau_{xy} = \mu |2d_{xy}|^{n-1} d_{xy} . \quad (1.5)$$

For this constitutive equation the apparent viscosity is

$$\mu |2d_{xy}|^{n-1}$$

Thus, $n < 1$ characterizes a pseudo-plastic, and $n > 1$ characterizes the dilatant fluid. Reiner (24) has raised three major objections to the use of the power law and concludes that equation (1.5) is not a physical law but rather only an empirical formula. An obvious defect in this formula is that the physical dimension of μ depends on the value n .

Other empirical equations, which describe pseudo-plastic behavior in simple shear, are

$$\text{Prandtl} \quad \tau_{xy} = A \sin^{-1} \left(\frac{2d_{xy}}{C} \right) ,$$

$$\text{Eyring} \quad \tau_{xy} = \frac{2d_{xy}}{B} + C \sin \left(\frac{\tau_{xy}}{A} \right) ,$$

*Often the terminology "Non-Newtonian" fluids includes a broader class of materials such as elastico-viscous materials and models which show a cross viscosity.

Powell-Eyring $\tau_{xy} = 2Ad_{xy} + B \sinh^{-1} (2 C d_{xy}) ,$

Williamson $\tau_{xy} = 2Ad_{xy}/(B + 2d_{xy}) + \mu_{\infty} d_{xy} ,$

where A, B, and C are constants characterizing the particular fluid behavior (7).

1.3 Aim of the Thesis

The purpose of this thesis is to consider the plane flow of an incompressible visco-plastic and a pseudo-plastic material in a converging channel, and also axially symmetric converging flow in a circular cone. The visco-plastic material considered is the Bingham solid and the pseudo-plastic material is based on the power law model. The constitutive equation for the Bingham solid, which is applied, is the Hohenemser-Prager generalization

$$s_{ij} = 2\left(\mu + \frac{k}{\sqrt{2d_{mn}d_{mn}}}\right) d_{ij} .$$

The constitutive equation which is used for the pseudo-plastic material, is the power law representation (25)

$$s_{ij} = 2\mu(d_{mn}d_{mn})^{\frac{n-1}{2}} d_{ij} . \quad (1.6)$$

The special case of equation (1.6) with $n = 0$ is the perfectly plastic von Mises solid, whose yield criterion is

$$\frac{1}{2} s_{mn} s_{mn} = k^2 ,$$

where k is the yield stress in pure shear. When $n = 1$, equation (1.6) is that for a Newtonian viscous liquid.

The visco-plastic material as typified by the Bingham solid possesses a yield limit; this is to be contrasted with the pseudo-plastic material which does not possess a yield limit for values of n in the range

$$0 < n \leq 1.$$

However, the limiting case $n = 0$, the perfectly plastic von Mises solid, does possess a yield limit.

The rheological problems considered in this thesis may be applicable to hydraulic extrusion and wire drawing technologies which involve rate dependent materials.

Calculations are performed for values of n between 0 and 1; thus it is possible to study, both quantitatively and qualitatively, the transition from a Newtonian viscous liquid to a perfectly plastic von Mises solid.

1.4 Consideration of Related Problems

Various solutions have been presented for the plane flow of Newtonian viscous liquids and rigid perfectly plastic materials in a converging channel, and also axially symmetric converging flow in a circular cone. These flow problems shall now be considered briefly.

Plane Viscous Flow - Hamel's Problem

In a classic paper, and using the prior assumption of radial flow, Rosenhead (26) obtained closed form solutions for the plane, steady flow of an incompressible Newtonian viscous liquid between two inclined walls, separated by an angle of 2α . Rosenhead included inertia terms and made a thorough investigation of the change in flow characteristics due to increasing Reynold's number.

The mathematical solution is extremely complex and is obtained in terms of Weierstrassian elliptic functions. A principal result of Rosenhead's investigation is that for every pair of values α and Reynold's number, the number of mathematically possible velocity profiles is infinite. The profiles may or may not be symmetrical with respect to the central line of the channel. Further, Rosenhead found that both inflow and outflow could occur simultaneously. A solution not assuming radial flow has not been obtained as yet.

Axially Symmetric Analog to Hamel's Problem

It has been shown by Hamel (27) and others that for axially symmetric converging flow of an incompressible Newtonian viscous liquid in a circular cone, without body forces, no purely radial flow can exist, if inertia effects are considered.

The assumption of non-radial flow leads to an intractable problem. It is interesting to note that a radial flow solution is obtained upon the neglect of inertia terms. This solution has been employed by Ramacharyulu (28) as a first order approximation to the elastico-viscous flow problem in a circular cone. The second order solution yielded a non-radial flow pattern.

Plane Rigid Perfectly Plastic Flow

In 1924 Nadai (29) considered the plane, steady, quasi-static flow of an incompressible rigid perfectly plastic solid in a converging channel, of semi-angle α , with perfectly rough* walls. Nadai assumed that the stresses are a function of θ , but not of r , and this implies that the streamlines of the associated velocity field must be radial straight lines directed through the virtual apex of the channel. Furthermore, assuming that the channel is very long, and thus neglecting end effects, enabled Nadai to obtain the stress field for this flow problem. Hill (30) obtained the associated velocity field of the form

$$v_r = \frac{g(\theta)}{r}.$$

It may be shown that $g'(\theta)$ at $\theta = \alpha$ is infinite. This derivative cannot be infinite in the Bingham solid since this would imply that the shearing stresses at the wall are also infinite. Hill (30) has extended Nadai's solution to cover the cases of rough walls with a constant shearing traction mk at the walls, where

$$0 \leq m \leq 1.$$

Axially Symmetric Rigid Perfectly Plastic Flow

In 1955 Shield (31) obtained the stress field for the axially

*The coefficient of friction between a perfectly rough surface and the deforming rigid perfectly plastic material is large enough that the shearing yield stress can be developed at the surface.

symmetric converging flow of an incompressible rigid perfectly plastic material in a circular cone of semi-angle α . The wall friction is assumed to be constant at the value of mk , where

$$0 \leq m \leq 1,$$

and k is the yield stress in pure shear. The velocity field is radial, and consequently of the form

$$v_r = \frac{g(\phi)}{r^2}.$$

Shield did not obtain a closed-form solution to the governing differential equation, which is in terms of the shearing stress $\tau_{r\phi}$, but solved it numerically. Shield applied the results of the stress field to wire drawing in a manner to be discussed in Chapter IV.

As mentioned previously in this chapter, it is desired to study wire drawing and hydraulic extrusion. Most materials used in this process exhibit both plastic and viscous effects.

The remaining chapters are concerned with the application of the Bingham solid and the pseudo-plastic material to the above mentioned plane and axially symmetric flow problems.

CHAPTER II

VISCO-PLASTIC FLOW

This chapter considers plane flow of an incompressible homogeneous isotropic rigid visco-plastic material, the Bingham solid, in a converging channel, and axially symmetric converging flow in a circular cone.

It will be shown that the only possible radial flow solution is the trivial solution, with zero radial velocity, unless it is assumed that slip occurs at the walls and axially symmetric flow results for the plane problem and spherically symmetric flow for the axially symmetric problem.

The assumption of a more general velocity field, which includes both radial and tangential components, leads to extensive and cumbersome equations, which cannot be integrated analytically.

2.1 Plane Visco-Plastic Flow

The plane flow of an incompressible Bingham solid in a converging channel is considered. Polar coordinates, (r, θ) , which are taken relative to the axis of symmetry, are used to describe the flow, and the channel is bounded by the lines $\theta = \pm \alpha$. It is assumed that the flow is steady, quasi-static, and directed radially through the virtual apex of the channel, 0, see FIG. 2.1, and that the channel is long enough so that the velocity and stress fields are independent of conditions at the ends.

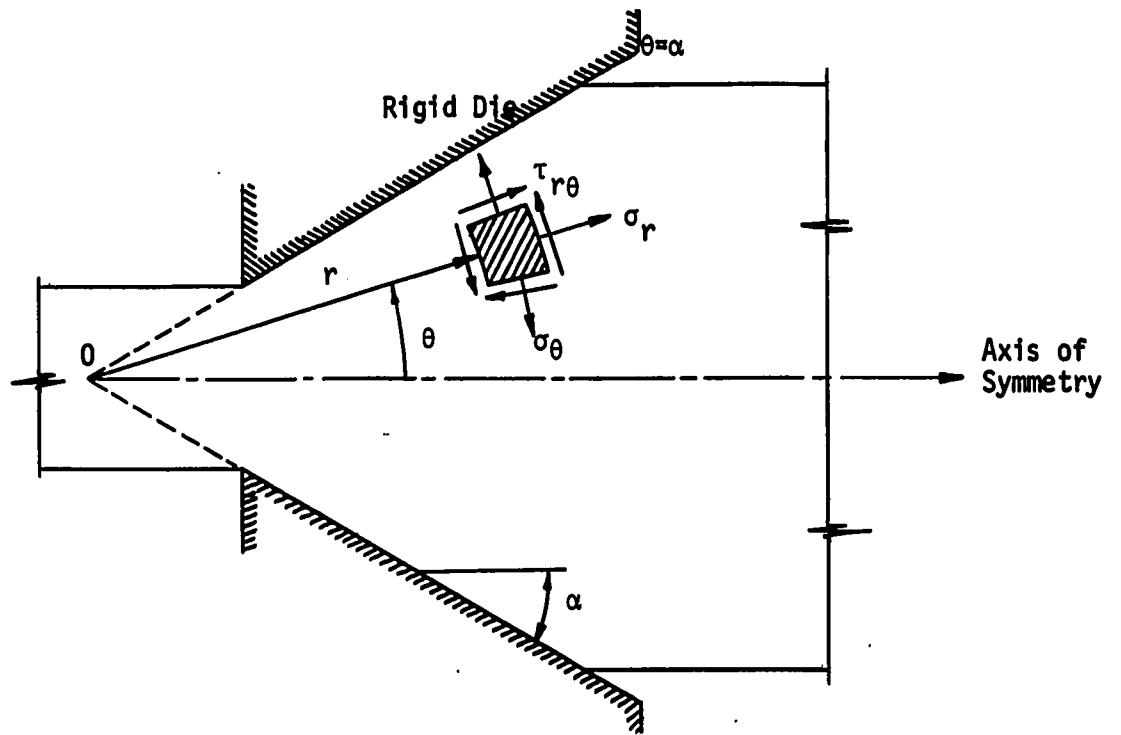


FIGURE 2.1

Visco-Plastic Flow in a Converging Channel

The components of the velocity strain tensor, defined by

$$d_{ij} = \frac{1}{2}(v_{i,j} + v_{j,i}) , \quad (2.1)$$

are

$$d_r = \frac{\partial v_r}{\partial r} ,$$

$$d_\theta = \frac{v_r}{r} , \quad (2.2)$$

$$d_{r\theta} = \frac{1}{2r} \frac{\partial v_r}{\partial \theta} .$$

The condition of incompressibility is

$$d_{ij} = v_{i,j} = 0 ,$$

which using equations (2.2) is

$$\frac{\partial v_r}{\partial r} + \frac{v_r}{r} = 0 . \quad (2.3)$$

Equation (2.3) requires that the velocity field v_r be of the form

$$v_r = \frac{g(\theta)}{r} . \quad (2.4)$$

Substitution of equation (2.4) in equations (2.2) yields

$$\begin{aligned} d_r &= - \frac{g(\theta)}{r^2} , \\ d_\theta &= - d_r = \frac{g(\theta)}{r^2} , \\ d_{r\theta} &= \frac{g'(\theta)}{2r^2} , \end{aligned} \quad (2.5)$$

where ' denotes differentiation with respect to θ .

The components of the stress tensor, which do not vanish identically, are σ_r , σ_θ , and $\tau_{r\theta}$. Assuming steady, quasi-static flow, and neg-

lecting body forces, the equilibrium equations are

$$r \frac{\partial \sigma_r}{\partial r} + \frac{\partial \tau_{r\theta}}{\partial \theta} + \sigma_r - \sigma_\theta = 0 ,$$

$$r \frac{\partial \tau_{r\theta}}{\partial r} + \frac{\partial \sigma_\theta}{\partial \theta} + 2\tau_{r\theta} = 0 .$$

Also

$$\sigma_{ij} = s_{ij} - p\delta_{ij} , \quad (2.6)$$

where

$$p = - \frac{\sigma_{kk}}{3}$$

is the hydrostatic part of the stress tensor, and s_{ij} is the deviatoric part. Using equation (2.6), the equilibrium equations reduce to

$$\frac{\partial p}{\partial r} = \frac{\partial s_r}{\partial r} + \frac{1}{r} \frac{\partial s_{r\theta}}{\partial \theta} + \frac{s_r - s_\theta}{r} ,$$

$$\frac{\partial p}{\partial \theta} = r \frac{\partial s_{r\theta}}{\partial r} + \frac{\partial s_\theta}{\partial \theta} + 2s_{r\theta} ,$$

which, upon noting that

$$s_\theta = -s_r ,$$

become

$$\frac{\partial p}{\partial r} = \frac{\partial s_r}{\partial r} + \frac{2s_r}{r} + \frac{1}{r} \frac{\partial s_{r\theta}}{\partial \theta}, \quad (2.7)$$

$$\frac{\partial p}{\partial \theta} = -\frac{\partial s_r}{\partial \theta} + 2s_{r\theta} + r \frac{\partial s_{r\theta}}{\partial r}.$$

In terms of the strain rates, given by equations (2.5), the invariant I becomes

$$I = [4d_r^2 + 4d_{r\theta}^2]^{1/2} = \frac{1}{r^2} [4g^2 + (g')^2]^{1/2}. \quad (2.8)$$

Substitution of the relation (2.8) and the strain rates (2.5) in the constitutive equations (1.4) gives for the components of the stress deviators

$$s_r = -\frac{2\mu g}{r^2} - 2kg/[4g^2 + (g')^2]^{1/2}, \quad (2.9)$$

$$s_{r\theta} = \frac{\mu g'}{r^2} + kg'/[4g^2 + (g')^2]^{1/2}.$$

The hydrostatic pressure p can be eliminated from equations (2.7), and the final result is

$$2 \frac{\partial^2 s_r}{\partial r \partial \theta} + \frac{2}{r} \frac{\partial s_r}{\partial \theta} + \frac{1}{r} \frac{\partial^2 s_{r\theta}}{\partial \theta^2} - r \frac{\partial^2 s_{r\theta}}{\partial r^2} - 3 \frac{\partial s_{r\theta}}{\partial r} = 0. \quad (2.10)$$

Upon substitution of the stress deviators (2.9) in equation (2.10), an ordinary differential equation is obtained for $g(\theta)$; the differential

equation is

$$\frac{\mu}{r^2} [g'''' + 4g'] + k \left[\left\{ \frac{g'}{[4g^2 + (g')^2]^{1/2}} \right\}'' - 4 \left\{ \frac{g}{[4g^2 + (g')^2]^{1/2}} \right\}' \right] = 0. \quad (2.11)$$

Clearly $g = \text{const.}$ satisfies equation (2.11), consequently this solution cannot depend on μ or k and the corresponding flow is axially symmetric. Alternatively in order that the differential equation (2.11) be satisfied, it is therefore necessary that $g(\theta)$ satisfies both

$$g'''' + 4g' = 0, \quad (2.12a)$$

and

$$\left\{ \frac{g'}{[4g^2 + (g')^2]^{1/2}} \right\}'' - 4 \left\{ \frac{g}{[4g^2 + (g')^2]^{1/2}} \right\}' = 0. \quad (2.12b)$$

It is noted that $g(\theta)$ is governed by two ordinary differential equations, whereas for the velocity field obtained by Hill (30) for the plane rigid perfectly plastic solution, there is no r dependence, and $g(\theta)$ is defined by one equation.

Further constraints on $g(\theta)$ are obtained from the boundary conditions at $\theta = 0$, $\theta = \alpha$, and from a specification of the volume flow per unit length.

From symmetry

$$g'(0) = 0. \quad (2.13)$$

Further, since the Bingham solid may be regarded as a viscous medium with a variable coefficient of viscosity, it appears reasonable to impose the

no-slip boundary condition, usually assumed for viscous flow, that is

$$g(\alpha) = 0.$$

If the volume flow per unit length is Q , then

$$Q = 2 \int_0^\alpha g(s) ds.$$

The solution to the differential equation (2.12a) is readily found to be

$$g(\theta) = A + B \cos 2\theta + C \sin 2\theta,$$

where A , B , and C are arbitrary constants of integration. The symmetry condition (2.13) requires that

$$C = 0,$$

consequently

$$g(\theta) = A + B \cos 2\theta. \quad (2.14)$$

Substitution of equation (2.14) in the differential equation (2.12b) yields

$$4B \sin 2\theta [-3A^2 B^2 \cos^2 2\theta - 2(A^3 B + 4AB^3) \cos 2\theta - (A^4 + 2B^4)] = 0. \quad (2.15)$$

Equation (2.15) possesses the real and trivial solution

$$B = 0.$$

Further, imposition of the boundary condition at $\theta = \alpha$ implies that

$$A = 0.$$

Thus the assumption of radial flow, subject to the no-slip boundary condition at $\theta = \alpha$, has yielded the trivial solution.

Alternatively, one might attempt to employ the solution

$$g(\theta) = D,$$

in the region

$$|\theta| \leq |\beta| < |\alpha| ,$$

where D is a constant, and the solution

$$g(\theta) = A + B \cos 2\theta + C \operatorname{sgn}\theta \sin 2\theta$$

in the region

$$|\beta| \leq |\theta| \leq |\alpha| ,$$

subject to the constraints noted, plus the requirements that $g(\theta)$ and $g'(\theta)$ be continuous at $\theta = \pm \beta$.

Continuity of $g'(\theta)$ at $\theta = \beta$, therefore, requires that

$$g'(\beta) = 0.$$

This condition requires that

$$C = B \operatorname{sgn} \beta \tan 2\beta. \quad (2.16)$$

In order to retain continuity in the velocity, and hence in $g(\theta)$, at $\theta = \beta$, it is required that

$$D = A + B \cos 2\beta + C \operatorname{sgn} \beta \sin 2\beta,$$

or using relation (2.16)

$$D = A + \frac{B}{\cos 2\beta},$$

consequently

$$g(\theta) = A + B [\cos 2\theta + \tan 2\beta \sin 2\theta]. \quad (2.17)$$

The expression, which is obtained by substitution of equation (2.17) in the differential equation (2.12b), is very complex and is not reproduced

here. It can be shown that the non-trivial solution to this expression results in

$$B = 0.$$

This case, however, has been considered before and gives rise to the trivial solution, with zero radial velocity. Hence a solution of the assumed form does not exist.

2.2 Axially Symmetric Visco-Plastic Flow

This section deals with the axially symmetric converging flow of an incompressible Bingham solid in a circular cone. The z-axis is taken along the axis of symmetry and spherical polar coordinates, (r, ϕ, θ) , are used in considering the flow. The flow is assumed to be radial, steady, and quasi-static. It is further assumed that the cone is long enough to neglect any end effects. The cone may be described as the part bounded by $\phi = \alpha$ and $\phi = -\alpha$, where α is the semi-angle of the cone, see FIG. 2.2.

Denoting the outward radial velocity by v_r , then by the velocity strain tensor (2.1), the only non-vanishing strain rates are given by

$$\begin{aligned} d_r &= \frac{\partial v_r}{\partial r} , \\ d_\phi &= d_\theta = \frac{v_r}{r} , \\ d_{r\phi} &= \frac{1}{2r} \frac{\partial v_r}{\partial \phi} . \end{aligned} \tag{2.18}$$

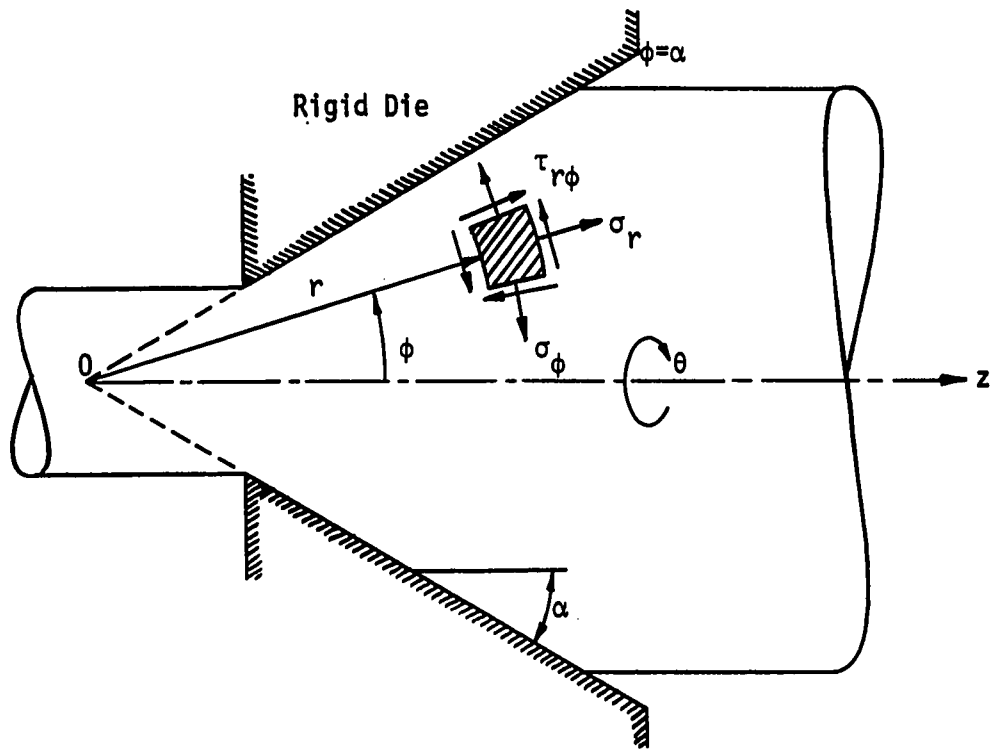


FIGURE 2.2
Visco-Plastic Flow in a Circular Cone

The continuity equation,

$$\frac{\partial v_r}{\partial r} + \frac{2v_r}{r} = 0 ,$$

requires that

$$v_r = \frac{g(\phi)}{r^2} . \quad (2.19)$$

Substitution of this velocity field (2.19) in the strain rate relationships

(2.18) gives

$$\begin{aligned} d_r &= -2 \frac{g(\phi)}{r^3}, \\ d_\phi &= d_\theta = \frac{g(\phi)}{r^3}, \\ d_{r\phi} &= \frac{g'(\phi)}{2r^3}, \text{ where } ' \equiv \frac{d}{d\phi}. \end{aligned} \quad (2.20)$$

The non-vanishing components of the stress tensor are σ_r , σ_ϕ , σ_θ , and $\tau_{r\phi}$. Neglecting inertia terms and body forces, the equations of equilibrium are

$$\begin{aligned} \frac{\partial \sigma_r}{\partial r} + \frac{1}{r} \frac{\partial \tau_{r\phi}}{\partial \phi} + \frac{1}{r} (2\sigma_r - \sigma_\phi - \sigma_\theta + \tau_{r\phi} \cot \phi) &= 0, \\ \frac{\partial \tau_{r\phi}}{\partial r} + \frac{1}{r} \frac{\partial \sigma_\phi}{\partial \phi} + \frac{1}{r} [(\sigma_\phi - \sigma_\theta) \cot \phi + 3\tau_{r\phi}] &= 0. \end{aligned} \quad (2.21)$$

Substitution of relation (2.6) in the equations (2.21) yields

$$\begin{aligned} \frac{\partial p}{\partial r} &= \frac{\partial s_r}{\partial r} + \frac{1}{r} \frac{\partial s_{r\phi}}{\partial \phi} + \frac{1}{r} (2s_r - s_\phi - s_\theta + s_{r\phi} \cot \phi), \\ \frac{\partial p}{\partial \phi} &= r \frac{\partial s_{r\phi}}{\partial r} + \frac{\partial s_\phi}{\partial \phi} + (s_\phi - s_\theta) \cot \phi + 3s_{r\phi}, \end{aligned} \quad (2.22)$$

and upon noting that

$$s_\theta = -(s_r + s_\phi)$$

equation (2.22) becomes

$$\frac{\partial p}{\partial r} = \frac{\partial s_r}{\partial r} + \frac{3s_r}{r} + \frac{1}{r} \frac{\partial s_{r\phi}}{\partial \phi} + \frac{1}{r} s_{r\phi} \cot \phi, \quad (2.23)$$

$$\frac{\partial p}{\partial \phi} = r \frac{\partial s_{r\phi}}{\partial r} + \frac{\partial s_\phi}{\partial \phi} + 3s_{r\phi}.$$

In terms of the strain rates, as given by equations (2.20), the invariant I becomes

$$I = [2d_r^2 + 2d_\phi^2 + 2d_\theta^2 + 4d_{r\phi}^2]^{1/2} = \frac{1}{r^3} [12g^2 + (g')^2]^{1/2}. \quad (2.24)$$

Substitution of the relation (2.24) and the strain rates (2.20) in the constitutive equations (1.4) gives for the components of the stress deviators

$$\begin{aligned} s_r &= -\frac{4\mu g}{r^3} - 4kg/[12g^2 + (g')^2]^{1/2}, \\ s_\phi &= s_\theta = \frac{2\mu g}{r^3} + 2kg/[12g^2 + (g')^2]^{1/2}, \\ s_{r\phi} &= \frac{\mu g'}{r^3} + kg'/[12g^2 + (g')^2]^{1/2}. \end{aligned} \quad (2.25)$$

The hydrostatic pressure p may be eliminated from equations (2.23), and the resulting partial differential equation in terms of the stress deviators is

$$\frac{\partial^2 s_r}{\partial r \partial \phi} + \frac{3}{r} \frac{\partial s_r}{\partial \phi} - \frac{\partial^2 s_\phi}{\partial r \partial \phi} + \frac{1}{r} \frac{\partial^2 s_{r\phi}}{\partial \phi^2} - r \frac{\partial^2 s_{r\phi}}{\partial r^2} +$$

$$+ \frac{1}{r} \frac{\partial}{\partial \phi} [s_{r\phi} \cot \phi] - 4 \frac{\partial s_{r\phi}}{\partial r} = 0. \quad (2.26)$$

Substitution of the stress deviator components (2.25) in the equation (2.26) results in the following ordinary differential equation for $g(\phi)$:

$$\begin{aligned} & \frac{\mu}{r^3} [g'''' + (g' \cot \phi)' + 6g'] + \\ & + k \left[\left\{ \frac{g'}{[12g^2 + (g')^2]^{1/2}} \right\}'' + \left\{ \frac{g' \cot \phi}{[12g^2 + (g')^2]^{1/2}} \right\}' - 12 \left\{ \frac{g}{[12g^2 + (g')^2]^{1/2}} \right\}' \right] = 0, \end{aligned}$$

Again $g = \text{const.}$ satisfies this equation and the flow corresponding to this solution is spherically symmetric. Alternatively it follows that

$$g'''' + (g' \cot \phi)' + 6g' = 0,$$

which upon integration gives

$$g'' + g' \cot \phi + 6g = \text{const.}, \quad (2.27a)$$

and

$$\left\{ \frac{g'}{[12g^2 + (g')^2]^{1/2}} \right\}'' + \left\{ \frac{g' \cot \phi}{[12g^2 + (g')^2]^{1/2}} \right\}' - 12 \left\{ \frac{g}{[12g^2 + (g')^2]^{1/2}} \right\}' = 0. \quad (2.27b)$$

Again, as is the case for the plane flow problem, $g(\phi)$ must obey two ordinary differential equations.

The condition that the flow be symmetric with respect to the $\phi = 0$ axis gives

$$g'(0) = 0. \quad (2.28)$$

As was pointed out in the previous section, a logical boundary condition to assume at $\phi = \alpha$ is

$$g(\alpha) = 0 . \quad (2.29)$$

Furthermore, the volume flow condition is

$$Q = 2\pi \int_0^\alpha g(\phi) \sin\phi \, d\phi. \quad (2.30)$$

The problem of finding the unknown function $g(\phi)$ then reduces to solving the ordinary differential equation (2.27a), subject to the differential equation (2.27b), and boundary conditions (2.28) and (2.29), and volume flow condition (2.30). The solution to the differential equation (2.27a) is made up of two parts, the particular solution

$$g_p(\phi) = \text{constant},$$

and the homogeneous solution, $g_H(\phi)$, which satisfies

$$g_H'' + g_H' \cot\phi + 6g_H = 0. \quad (2.31)$$

Under the substitution

$$x = \cos\phi,$$

equation (2.31) becomes

$$(1 - x^2)g_H'' - 2xg_H' + 2(2 + 1)g_H = 0, \quad (2.32)$$

where $' \equiv \frac{d}{dx}$, and is recognized as Legendre's ordinary differential equation. The solution to equation (2.32) may be written in the form

$$g_H(x) = A P_2(x) + B Q_2(x),$$

where $P_2(x)$ and $Q_2(x)$ are the Legendre's functions of degree 2, of the first and second kinds, respectively, and A and B are arbitrary constants of integration. Returning to the ϕ variable, this solution reduces to

$$g_H(\phi) = A P_2(\cos\phi) + B Q_2(\cos\phi),$$

where

$$P_2(\cos\phi) = \frac{1}{2}(3\cos^2\phi - 1),$$

and

$$Q_2(\cos\phi) = \frac{1}{4}(3\cos^2\phi - 1) \log \frac{1 + \cos\phi}{1 - \cos\phi} - \frac{3}{2} \cos\phi.$$

The general solution to the differential equation (2.27a),

$$g(\phi) = g_p(\phi) + g_H(\phi),$$

then reduces to

$$g(\phi) = A(3\cos^2\phi - 1) + B[(3\cos^2\phi - 1)\log \frac{1 + \cos\phi}{1 - \cos\phi} - 6\cos\phi] + C,$$

where A, B, and C are to be determined such that the boundary conditions (2.28) and (2.29), and the differential equation (2.27b) are satisfied, and further that $g(\phi)$ be finite.

The latter condition requires that $B = 0$. The symmetry condition is satisfied automatically. There remains the problem to find A and C such that the differential equation (2.27b) is satisfied along with the boundary condition (2.29). Substitution of

$$g(\phi) = A(3\cos^2\phi - 1) + C$$

in the differential equation (2.27b) gives

$$\begin{aligned} 64A\sin\phi\cos\phi[(68A^3C - 22A^4)\cos^6\phi + (348A^2C^2 + 7A^4 + 111A^3C)\cos^4\phi \\ + (A^3C + 318AC^3 + 153A^2C^2)\cos^2\phi + (108C^4 + 18A^2C^2 + 111AC^3)] = 0. \end{aligned} \quad (2.33)$$

The real and non-trivial solution to equation (2.33) gives

$$A = 0.$$

The solution common to both differential equations therefore reduces to

$$g(\phi) = C,$$

and the boundary condition (2.29) requires that C be zero. Consequently the assumption of radial flow subject to the no-slip boundary condition at $\phi = \alpha$ has yielded the trivial solution in both the plane and axially symmetric problems.

It can be shown that an attempt to treat the flow as composed of two regions, as was discussed in the plane flow case, again leads to the trivial solution.

The solution of both visco-plastic problems clearly involves curved streamlines, and to obtain a solution it is probable that the inlet (or exit) velocity profile must be known. A numerical approach, using a relaxation procedure, was attempted but was abandoned since the solution rapidly diverged.

CHAPTER III

PSEUDO-PLASTIC FLOW

In CHAPTER II the plane radial flow of an incompressible Bingham solid in a converging channel, and the axially symmetric converging flow in a circular cone were introduced. It is recalled that $g(\theta)$ in both cases was constrained by two ordinary differential equations. It was shown that under the no-slip boundary condition only the trivial solutions, with zero radial velocities, were obtained. It was then suggested that a more general formulation assuming non-radial flow is intractable.

An alternative model, the pseudo-plastic material, is now considered. This model exhibits rate effects and under the assumption of radial flow removes the r -dependence in the governing equations and yields one ordinary differential equation for the required function. The absence of the r -dependence is similar to that obtained by Nadai (29) and Shield (31) for the rigid perfectly plastic materials.

It is shown in the body of this chapter that the boundary value problem for the required function can be reformulated as an initial value problem for a third order non-linear ordinary differential equation in $g(\theta)$. This problem is readily solved numerically by employing Gill's variation of the Runge-Kutta fourth order method.

3.1 Plane Pseudo-Plastic Flow

The plane, radial, steady, quasi-static flow of an incompressible pseudo-plastic material in a converging channel is considered. FIGURE 3.1 shows some necessary notation. As previously discussed, the channel is as-

sumed to be sufficiently long, so that the velocity field and the state of stress are independent of the conditions occurring at the entry and exit sections.

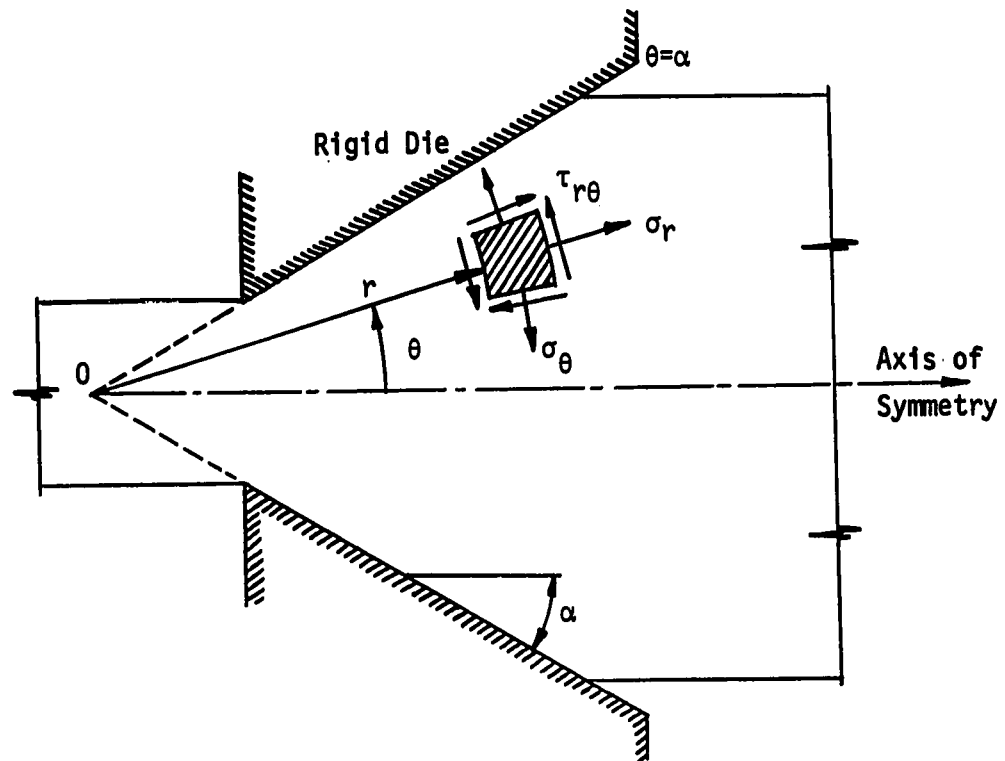


FIGURE 3.1

Pseudo-Plastic Flow in a Converging Channel

The constitutive equation for the pseudo-plastic material is

$$s_{ij} = 2\mu(d_{mn} d_{mn})^{\frac{n-1}{2}} d_{ij} ,$$

which upon applying equations (2.5),

$$\begin{aligned} d_r &= - \frac{g(\theta)}{r^2} , \\ d_\theta &= - d_r = \frac{g(\theta)}{r^2} , \\ d_{r\theta} &= \frac{g'(\theta)}{2r^2} , \end{aligned} \tag{2.5}$$

yields

$$\begin{aligned} s_r = - s_\theta &= - \frac{2}{r^{2n}} \mu^{\frac{3-n}{2}} \{ g[4g^2 + (g')^2]^{\frac{n-1}{2}} \} , \\ s_{r\theta} &= \frac{2}{r^{2n}} \mu^{\frac{1-n}{2}} \{ g' [4g^2 + (g')^2]^{\frac{n-1}{2}} \} . \end{aligned}$$

Let

$$g(\theta) = Am(\theta) , \tag{3.1}$$

where $m(\theta)$ is a non-dimensional function of θ , and A is a constant to be determined by the volume flow per unit length condition

$$Q = A \{ 2 \int_0^\alpha m(\theta) d\theta \} .$$

Using equation (3.1), the stress deviator components become

$$\begin{aligned}
 s_r = -s_\theta &= -\frac{2^{\frac{3-n}{2}} \mu A^n}{r^{2n}} mG, \\
 s_{r\theta} &= \frac{2^{\frac{1-n}{2}} \mu A^n}{r^{2n}} m'G,
 \end{aligned} \tag{3.2}$$

where

$$G = [4m^2 + (m')^2]^{\frac{n-1}{2}}.$$

The differential equation governing $m(\theta)$ is obtained by substitution of equations (3.2) in equation (2.10), and is

$$(m'G)'' + 4n(1-n)m'G + 4(2n-1)(mG)' = 0. \tag{3.3}$$

It is significant that there is no r -dependence in equation (3.3), unlike the governing differential equations for the problems considering the Bingham solid. Upon replacement of the stress deviator components in equations (2.7) by the relations given by equations (3.2), the expression for the hydrostatic pressure p is found to be

$$p = \frac{2^{\frac{1-n}{2}} \mu A^n}{r^{2n}} \left[\frac{2}{n}(1-n) mG - \frac{1}{2n} (m'G)' \right] + C,$$

where the constant C depends on the prescribed pressure at some point in the flow field.

If $n = 0$, equation (3.3) reduces to the equation for Nadai's

problem*, and $n = 1$ yields the governing differential equation for the creeping flow of a Newtonian viscous liquid.

The equation (3.3) appears to be in general analytically intractable, but the case $n = \frac{1}{2}$ can be integrated and becomes

*Substituting

$$n = 0$$

reduces equation (3.3) to

$$\left[\frac{m'}{\sqrt{4m^2 + (m')^2}} \right]'' - 4 \left[\frac{m}{\sqrt{4m^2 + (m')^2}} \right]' = 0 ,$$

and with the change in the dependent variable

$$h = \frac{m'}{2m} ,$$

this becomes

$$\left[\frac{h}{\sqrt{1 + h^2}} \right]'' - 2 \left[\frac{1}{\sqrt{1 + h^2}} \right]' = 0 .$$

With the substitution

$$h = - \tan 2\psi ,$$

the differential equation for ψ becomes

$$\psi' = c \sec 2\psi - 1 ,$$

where c is a constant of integration, and the corresponding differential equation for m is

$$\frac{m'}{2m} = - \tan 2\psi .$$

It is readily verified that the two ordinary differential equations for ψ and m are the same as those obtained by Nadai (29) and Hill (30) respectively, thus illustrating the third axiom of Rheology.

$$m'G = B\cos\theta + C\sin\theta, \quad (3.4)$$

where B and C are constants of integration. Since

$$m'(0) = 0,$$

equation (3.4) reduces to

$$m'G = C\sin\theta,$$

and the shear stress becomes

$$s_{r\theta} = \frac{2^{\frac{1}{4}} \mu A^{\frac{1}{2}}}{r} C \sin\theta .$$

This expression for $s_{r\theta}$ is used to estimate the accuracy of the numerical procedure used to integrate equation (3.3) for arbitrary n .

The boundary value problem now involves the determination of $m(\theta) \in C_3$, satisfying equation (3.3) in the region bounded by $\theta = \pm \alpha$, and subject to the symmetry condition

$$m'(0) = 0 ,$$

and the assumed no-slip boundary condition

$$m(\alpha) = 0 ,$$

and

$$m(0) = 1,$$

where A is obtained from the volume flow per unit length condition

$$Q = A \left\{ 2 \int_0^\alpha m(\theta) d\theta \right\}.$$

Considerable effort was expended on unseccessful attempts to solve this boundary value problem directly. The boundary value problem was therefore reformulated as the following initial value problem.

Solve equation (3.3) subject to the initial conditions:

$$m(0) = 1,$$

$$m'(0) = 0$$

from symmetry, and

$$m''(0) = \beta,$$

where β is determined by the requirement that

$$m(\alpha) = 0,$$

which is the assumed no-slip boundary condition. It is known that such a

problem may be reduced to a system of three first order differential equations, which must be satisfied subject to the prescribed initial conditions. Reducing equation (3.3) to a system of first order ordinary differential equations gives

$$y_1'(\theta) = y_2(\theta) ,$$

$$y_2'(\theta) = y_3(\theta) ,$$

$$y_3'(\theta) = F[y_1(\theta), y_2(\theta), y_3(\theta)] ,$$

where

$$y_1(\theta) = m(\theta) ,$$

$$y_2(\theta) = m'(\theta) ,$$

$$y_3(\theta) = m''(\theta) ,$$

and

$$\begin{aligned} F[y_1(\theta), y_2(\theta), y_3(\theta)] = & \frac{1}{M + (n-1)(m')^2} \{ (4n^2 - 12n + 4)m'M \\ & - [(4n^2 - 6n + 2)m + (n-1)m'']M' - (n-1)(n-3)m'(M')^2 / 4M \\ & - (n-1)m'[4(m')^2 + 4mm'' + (m'')^2] \} , \end{aligned}$$

where

$$M = 4m^2 + (m')^2 .$$

The initial values become

$$y_1(0) = 1 ,$$

$$y_2(0) = 0 ,$$

$$y_3(0) = \beta .$$

This formulation is readily amendable to numerical treatment using Gill's variation of the Runge-Kutta fourth order method.

The method of solution is similar to that used for the axially symmetric converging flow in a circular cone, and the details are included in the discussion of that problem.

The stress and flow fields obtained for the plane flow case are applicable to the compression of a pseudo-plastic material between two inclined plates. Letting U be the velocity of the plates normal to their lengths, see FIG. 3.2, then the velocity field is obtained by superimposing a velocity $U/\sin\alpha$ to the diverging flow field obtained above. The corresponding stress field is that obtained for diverging flow. This solution will be valid if the plates are large, and the flow is considered far enough away from the ends, so that end effects do not influence the solution.

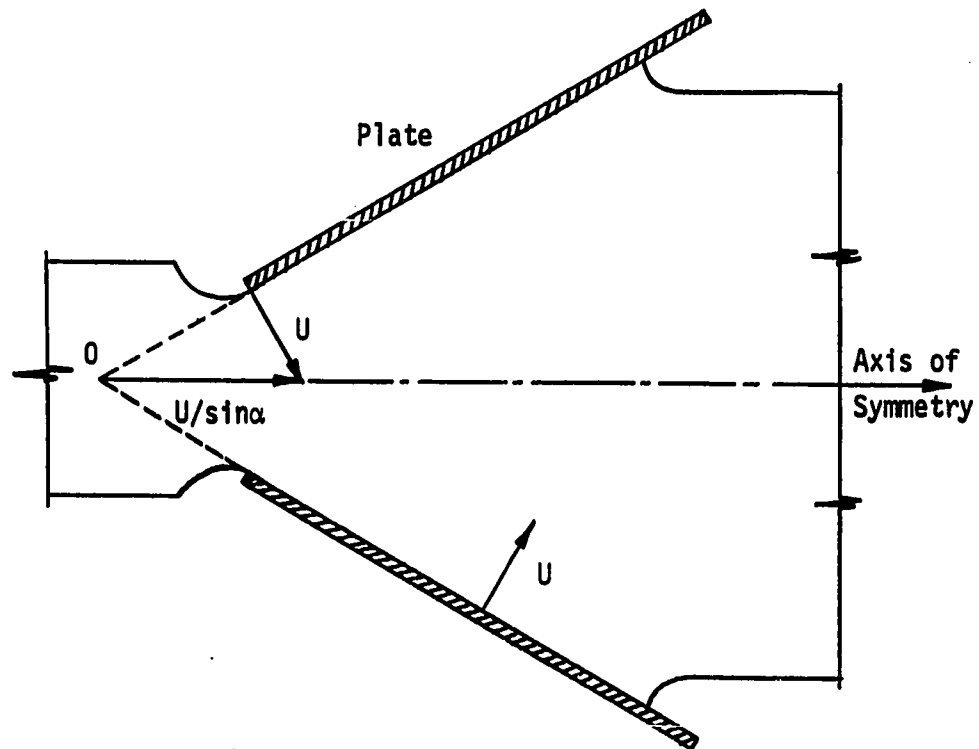


FIGURE 3.2
Compression of a Pseudo-Plastic Material
Between Inclined Plates

3.2 Axially Symmetric Pseudo-Plastic Flow

The problem, now considered, is that of the axially symmetric, radial, steady, quasi-static, converging flow of an incompressible pseudo-plastic material in a circular cone. Some pertinent notation is shown in FIG. 3.2. As in the previously discussed flow problems, the cone is assumed to be long enough so that the end effects may be neglected. The non-vanishing strain rates, for radial flow, are

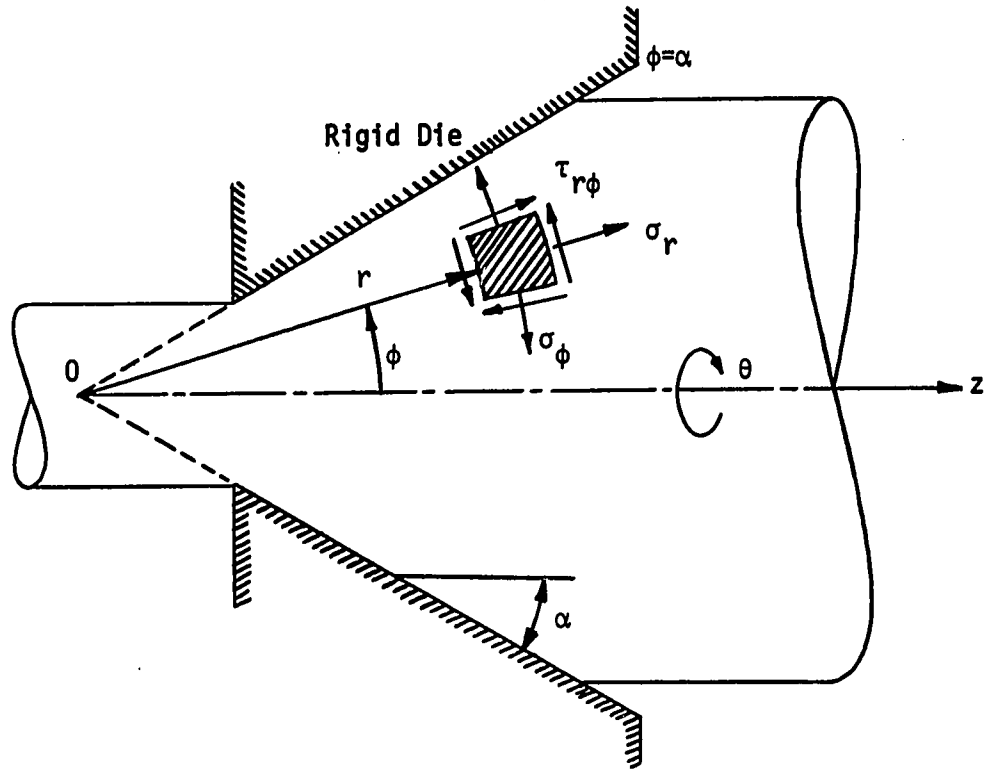


FIGURE 3.3

Pseudo-Plastic Flow in a Circular Cone

$$d_r = - \frac{2g(\phi)}{r^3} ,$$

$$d_\phi = d_\theta = \frac{g(\phi)}{r^3} , \quad (2.20)$$

$$d_{r\phi} = \frac{g'(\phi)}{2r^3} , \text{ where } ' \equiv \frac{d}{d\phi} .$$

Substitution of equations (2.20) in the constitutive equations (1.6) results

in

$$\begin{aligned}
 s_r &= - \frac{2^{\frac{5-n}{2}} \mu}{r^{3n}} \{g[12g^2 + (g')^2]^{\frac{n-1}{2}}\} , \\
 s_\phi = s_\theta &= \frac{2^{\frac{3-n}{2}} \mu}{r^{3n}} \{g[12g^2 + (g')^2]^{\frac{n-1}{2}}\} , \\
 s_{r\phi} &= \frac{2^{\frac{1-n}{2}} \mu}{r^{3n}} \{g'[12g^2 + (g')^2]^{\frac{n-1}{2}}\} .
 \end{aligned} \tag{3.5}$$

Substituting in equations (3.5)

$$g(\phi) = Am(\phi) ,$$

where $m(\phi)$ is a non-dimensional function of ϕ :

$$\begin{aligned}
 s_r &= - \frac{2^{\frac{5-n}{2}} \mu A^n}{r^{3n}} mG , \\
 s_\phi = s_\theta &= \frac{2^{\frac{3-n}{2}} \mu A^n}{r^{3n}} mG , \\
 s_{r\phi} &= \frac{2^{\frac{1-n}{2}} \mu A^n}{r^{3n}} m'G ,
 \end{aligned} \tag{3.6}$$

where

$$G = [12m^2 + (m')^2]^{\frac{n-1}{2}} ,$$

and A is a constant to be determined from the volume flow condition

$$Q = A\{2\pi \int_0^\alpha m(\phi) \sin\phi \, d\phi\} .$$

Substitution of equations (3.6) in equation (2.26) gives

$$(m'G)'' + (m'G \cot\phi)' + 9n(1-n)(m'G) + 6(3n-2)(mG)' = 0 . \quad (3.7)$$

Again the governing differential equation has no r -dependence.

After substitution of equations (3.6), the integration of equations (2.23) results in

$$p = \frac{2^{\frac{1-n}{2}} \mu A^n}{r^{3n}} \left[\frac{4}{n} (1-n)mG - \frac{1}{3n} \{(m'G)' + m'G \cot\phi\} \right] + C , \quad (3.8)$$

where the constant C depends on the prescribed pressure at some point in the flow field.

As a check, it is noted that the substitution $n = 0$ in equation (3.7) yields the equation obtained by Shield (31) for the perfectly plastic von Mises solid*, and the substitution $n = 1$ reduces equation (3.7) to that for the creeping flow of a Newtonian viscous liquid.

*Substituting $n = 0$ in equation (3.7) gives

$$\left[\frac{m'}{\sqrt{12m^2 + (m')^2}} \right]'' + \left[\frac{m'}{\sqrt{12m^2 + (m')^2}} \cot\phi \right]' - 12 \left[\frac{m}{\sqrt{12m^2 + (m')^2}} \right]' = 0, \quad (3.9)$$

and with the change in the dependent variable

$$\tau = \frac{m'}{\sqrt{12m^2 + m'^2}} ,$$

equation (3.9) becomes

$$\tau' + \tau \cot \phi \pm 2\sqrt{3} (1-\tau^2)^{1/2} = c,$$

where c is an arbitrary constant of integration. Integrating the above expression for m in terms of τ gives

$$m = B \exp \{ \pm 2\sqrt{3} \int \tau (1-\tau^2)^{-1/2} d\phi \}.$$

The differential equation for τ , and the expression for m in terms of τ are consistent with those obtained by Shield (31), again illustrating the third axiom of Rheology.

Returning to a consideration of equation (3.7); the boundary conditions to which the solution to this differential equation shall be subjected to, are

$$m(0) = 1,$$

$$m'(0) = 0$$

from symmetry, and

$$m(\alpha) = 0,$$

that is the no-slip boundary condition at the walls.

If $n = 2/3$, the differential equation reduces to

$$(m'G)'' + (m'G \cot \phi)' + 2m'G = 0,$$

which, under the substitution

$$x = \cos \phi,$$

becomes

$$(1-x^2)(m'G)'' - 2x(m'G)' + [1(1+1) - \frac{1^2}{1-x^2}] m'G = 0, \quad (3.10)$$

which is Legendre's equation of degree 1 and order 1. The solution to equation (3.10) is

$$m'G = BP_1^1(x) + CQ_1^1(x),$$

where P_1^1 and Q_1^1 are the associated Legendre's functions of degree 1 and order 1, of the first and second kinds, respectively, and B and C are arbitrary constants of integration. Analytically

$$P_n^m(x) = (1-x^2)^{\frac{m}{2}} \frac{d^m P_n(x)}{dx^m},$$

$$Q_n^m(x) = (1-x^2)^{\frac{m}{2}} \frac{d^m Q_n(x)}{dx^m}.$$

The general solution to the differential equation (3.10) therefore becomes

$$m'G = BP_1^1(\cos\phi) + CQ_1^1(\cos\phi).$$

The symmetry condition requires that $m'G$ be zero at $\phi = 0$; since $Q_1^1(0)$ is not bounded at $\phi = 0$, it is necessary that

$$C = 0,$$

consequently

$$m'G = B\sin\phi . \quad (3.11)$$

Applying equation (3.11), the shear stress becomes

$$s_{r\phi} = \frac{\frac{1}{6} \frac{2}{3} \mu A^{\frac{2}{3}}}{r^2} B\sin\phi . \quad (3.12)$$

It was not possible to obtain a closed form solution for other values of n in the range

$$0 \leq n < 1 ,$$

and equation (3.12) was used to estimate the accuracy of the numerical procedure used. The boundary value problem can be more readily solved by transforming it into an initial value problem.

This initial value problem requires the solution of equation (3.7) subjected to the initial values

$$m(0) = 1,$$

$$m'(0) = 0$$

from symmetry, and

$$m''(0) = \beta.$$

The parameter β is determined by the no-slip boundary condition

$$m(\alpha) = 0.$$

Letting

$$y_1(\phi) = m(\phi) ,$$

$$y_2(\phi) = m'(\phi) ,$$

$$y_3(\phi) = m''(\phi) ,$$

then equation (3.7) is equivalent to the system

$$y_1'(\phi) = y_2(\phi) ,$$

$$y_2'(\phi) = y_3(\phi) ,$$

$$y_3'(\phi) = F[\phi, y_1(\phi), y_2(\phi), y_3(\phi)],$$

where

$$F[\phi, y_1(\phi), y_2(\phi), y_3(\phi)] = \frac{1}{M + (n-1)(m')^2} \{[(9n^2 - 27n + 12)m'$$

$$\begin{aligned}
& - \cot \phi m'' + \csc^2 \phi m'] M - [(9n^2 - 15n + 6)m + (n-1)m''] \\
& + \left(\frac{n-1}{2}\right) \cot \phi m'] M' - (n-1)(n-3)m'(M')^2 / 4M \\
& - (n-1)m'[12(m')^2 + 12mm'' + (m'')^2]\},
\end{aligned}$$

and

$$M = 12m^2 + (m')^2.$$

Gill's variation of the Runge-Kutta fourth order method is used to solve the initial value problem. The precise procedure utilized is considered briefly in the next section.

After this work had been nearly completed, the author was shown a paper by Tanner (32), in which equation (3.7) was presented. The numerical method of solution is not indicated in this paper, and it does not include the partial analytical solution for the special case with $n = 2/3$.

3.3 Integration Procedure

It has been shown that both the plane and the axially symmetric boundary value problems are reducible to equivalent initial value problems involving the solution of a system of first order ordinary differential equations, subjected to prescribed initial conditions.

The initial conditions to be imposed on $m(\theta)$ and $m'(\theta)$ are clear; however, the initial value of $m''(\theta)$ is not readily prescribed. Rather, a trial and error method is adopted; various values of $m''(0)$ are assumed

until the desired boundary condition of $m(\alpha) = 0$ is obtained.

Gill's variation of the Runge-Kutta fourth order method is employed as an integration procedure. An explanation of this method, and a brief discussion on its accuracy, is contained in the Appendix. The Appendix also contains a copy of the DRKGS subroutine. This is the IBM System/360 Scientific Subroutine Package for Gill's variation of the fourth order Runge-Kutta method.

It has already been noted that possession of a closed form solution for $s_{r\phi}$, with $n = 2/3$, for the axially symmetric problem, and for $s_{r\theta}$, with $n = 1/2$, for the plane problem permits a direct comparison of the numerical solution to the closed form solution, and hence an assessment of the accuracy can be made for other values of n .

The values of n considered are

$$0 < n < 1.$$

The value $n = 0$ corresponds to the perfectly plastic von Mises solid, and $n = 1$ to the Newtonian viscous liquid; hence, it is possible to study the transition from the perfectly plastic von Mises solid to the Newtonian viscous liquid.

The results of the analysis performed in this chapter are presented in FIGS. 6.II-1 to 6.II-13 for the plane problem, and in FIGS. 6.III-1 to 6.III-15 for the axially symmetric case, and a brief discussion of these results is given in CHAPTER VI.

3.4 On the Inclusion of Inertia Effects

The solutions presented in this chapter for the flow of pseudo-plastic materials are based on the assumption that the non-linear term in the equilibrium equation can be neglected.

The inclusion of the inertia term is now considered briefly. Instead of the equilibrium equations (2.7), the equations of motion are used, which for steady flow become

$$\frac{\partial p}{\partial r} + \rho v_r \frac{\partial v_r}{\partial r} = \frac{\partial s_r}{\partial r} + \frac{2s_r}{r} + \frac{1}{r} \frac{\partial s_{r\theta}}{\partial \theta}, \quad (3.13)$$

$$\frac{\partial p}{\partial \theta} = - \frac{\partial s_r}{\partial \theta} + 2s_{r\theta} + r \frac{\partial s_{r\theta}}{\partial r},$$

where ρ is the density. Substitution of the stress deviators (3.2) in equation (3.13), gives

$$\frac{\partial p}{\partial r} = \frac{2^{\frac{1-n}{2}} \mu A^n}{r^{2n+1}} [4n(mG) - 4mG + (m'G)'] + \frac{\rho A^2 m^2}{r^3}, \quad (3.14)$$

$$\frac{\partial p}{\partial \theta} = \frac{2^{\frac{1-n}{2}} \mu A^n}{r^{2n}} [2(mG)' + 2m'G - 2nm'G]. \quad (3.15)$$

From equations (3.14) and (3.15) it follows that

$$p = \frac{2^{\frac{1-n}{2}} \mu A^n}{r^{2n}} \left[\frac{4mG - 4n(mG) - (m'G)'}{2n} \right] - \frac{\rho A^2 m^2}{2r^2} + C, \quad (3.16)$$

where the constant C depends on the prescribed pressure at some point in

the flow field, and further, from equation (3.16), that

$$\frac{\partial p}{\partial \theta} = \frac{2^{\frac{1-n}{2}} \mu A^n}{r^{2n}} \left[\frac{4(mG)' - 4n(mG)' - (m'G)''}{2n} \right] - \frac{\rho A^2 m m'}{r^2} . \quad (3.17)$$

Equating equations (3.15) and (3.17) gives

$$\frac{2^{\frac{1-n}{2}} \mu A^n}{r^{2n}} \left[\frac{1}{2n} \{ (m'G)'' + 4n(1-n)(m'G) + 4(2n-1)(mG)' \} \right] + \frac{\rho A^2 m m'}{r^2} = 0 . \quad (3.18)$$

Consequently, for $n \neq 1$

$$(m'G)'' + 4n(1-n)(m'G) + 4(2n-1)(mG)' = 0 , \quad (3.19)$$

and

$$\frac{\rho A^2 m m'}{r^2} = 0 . \quad (3.20)$$

Equation (3.20), and the no-slip boundary condition, imply that

$$m \equiv 0 .$$

Equation (3.19) is the same as that obtained if the inertia term is neglected, see equation (3.3).

It is interesting to note that if

$$n = 1 ,$$

then equation (3.18) implies that

$$m'''' + 4m' + \frac{\rho A m m'}{\mu} = 0 ,$$

since

$$G|_{n=1} = 1 ;$$

this is the governing equation for the plane, steady flow of a Newtonian viscous liquid, without body forces, in a converging channel, which was considered in detail by Rosenhead (26).

Similarly, the inclusion of the inertia term in the axially symmetric problem shows that there is no radial flow solution, not even for $n = 1$.

3.5 On the Neglect of Inertia Effects

It was shown above that, under the prior assumption of radial, steady flow, the presence of the non-linear inertia term in the equation of motion yielded the trivial solution with zero radial velocity, both for the plane, if $n \neq 1$, and the axially symmetric pseudo-plastic flow, at least if the material is assumed incompressible, and without body forces.

Solutions are obtained, both for the plane and the axially symmetric flow, with the assumption that the flow is quasi-static. This assumption is valid if certain conditions, which relate the inertia force

to the dissipative forces, are satisfied.

A comparison of the relative magnitudes of the inertia term with those of the terms retained in the equilibrium equation, leads to inequalities which are of little value since numerical results make physical interpretation of these conditions difficult. A better approach, due to Batchelor (33), who considered the inertia effects for the steady, quasi-static flow of a Newtonian viscous liquid in slowly-varying circular cones, can be applied to the pseudo-plastic flow problems considered in this thesis. This method, however, requires a knowledge of the solution for the flow of the pseudo-plastic material in a circular tube, which is considered first. This solution is then used to specify a condition, which, if satisfied, justifies neglecting the inertia term for the axially symmetric pseudo-plastic flow in slowly-varying circular cones.

Let polar coordinates, (r, θ, z) , describe the pseudo-plastic flow in the circular tube of radius R ; the z -axis is taken as the axis of symmetry, see FIG. 3.4. The flow is assumed to be steady and quasi-static; furthermore, it is assumed that the velocity profile is independent of θ and z . The incompressible pseudo-plastic material under consideration is the same as that used previously in this thesis.

Let the velocity in the z -direction be denoted by w , which by the prior assumption is a function of r only. Consequently, the only non-vanishing component of the strain rate tensor becomes, from equation (2.1),

$$d_{rz} = \frac{1}{2} \frac{dw}{dr} , \quad (3.21)$$

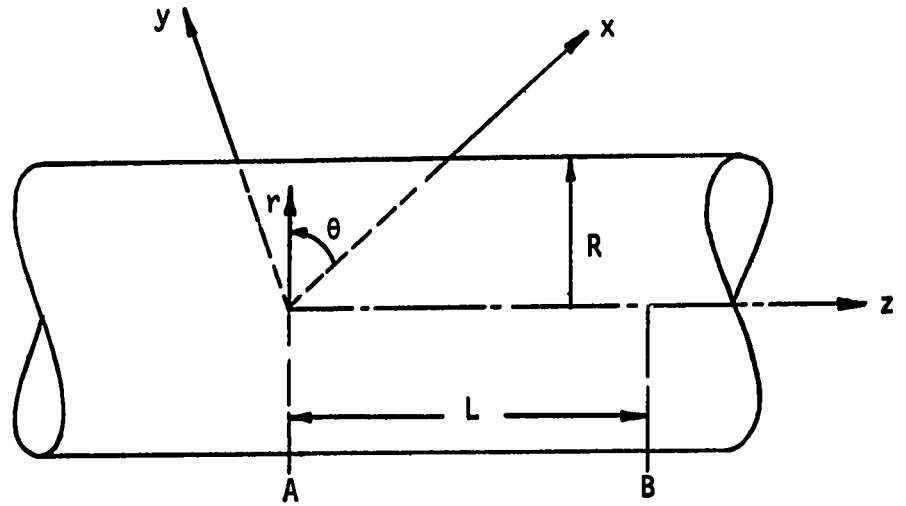


FIGURE 3.4

Pseudo-Plastic Flow in a Circular Tube

and hence the strain rate invariant I becomes

$$I = \sqrt{2d_{ij}d_{ij}} = \frac{dw}{dr}.$$

The only non-vanishing stress tensor component is s_{rz} , which by substitution of equation (3.21) in the constitutive equation (1.6) becomes

$$s_{rz} = 2^{\frac{1-n}{2}} \mu \left(\frac{dw}{dr} \right)^n. \quad (3.22)$$

Neglecting body forces, the equilibrium equations for steady, quasi-static flow are

$$\frac{\partial p}{\partial r} = 0 , \quad (3.23)$$

$$\frac{\partial p}{\partial \theta} = 0 , \quad (3.24)$$

$$\frac{\partial p}{\partial z} = \frac{\partial s_{rz}}{\partial r} + \frac{s_{rz}}{r} = \frac{1}{r} \frac{\partial}{\partial r} (rs_{rz}) . \quad (3.25)$$

Equations (3.23) and (3.24) imply that

$$p = p(z) .$$

Substitution of equation (3.22) in equation (3.25), with $n \neq 0$, results in

$$\frac{dp}{dz} = 2^{\frac{1-n}{2}} \mu \frac{1}{r} \frac{d}{dr} \left[r \left(\frac{dw}{dr} \right)^n \right] ;$$

since the left hand side is a function of z alone, and the right hand side of r alone, it follows that

$$\frac{dp}{dz} = 2^{\frac{1-n}{2}} \mu \frac{1}{r} \frac{d}{dr} \left[r \left(\frac{dw}{dr} \right)^n \right] = C , \quad (3.26)$$

where C is a constant. The constant C is associated with the pressure difference between two distant sections, A and B, see FIG. 3.4, which causes the flow. Substitution of

$$\frac{dp}{dz} = \frac{p_B - p_A}{L} = - \frac{\Delta p}{L}$$

in equation (3.26) gives

$$\frac{d}{dr} \left[r \left(\frac{dw}{dr} \right)^n \right] = - \frac{2^{\frac{n-1}{2}} \Delta p}{\mu L} r . \quad (3.27)$$

Integrating equation (3.27) once, results in

$$\left(\frac{dw}{dr} \right)^n = \frac{2^{\frac{n-1}{2}} \Delta p}{\mu L} \left(\frac{A}{r} - \frac{r}{2} \right) , \quad (3.28)$$

where A is a constant of integration. From symmetry,

$$\left. \frac{dw}{dr} \right|_{r=0} = 0 ,$$

it follows that

$$A = 0 .$$

Consequently, from equation (3.28),

$$\frac{dw}{dr} = - 2^{\frac{n-3}{2n}} \left(\frac{\Delta p}{\mu L} \right)^{\frac{1}{n}} \frac{1}{r^{\frac{1}{n}}} . \quad (3.29)$$

Integrating equation (3.29) gives, for $n \neq -1$,

$$w = 2^{\frac{n-3}{2n}} \left(\frac{\Delta p}{\mu L} \right)^{\frac{1}{n}} \left[B - \left(\frac{n}{1+n} \right) r^{\frac{1+n}{n}} \right] .$$

The parameter B is a constant of integration, which is found from the assumed no-slip boundary condition at the walls, and is

$$B = \frac{n}{1+n} R^{\frac{1+n}{n}} .$$

The velocity profile in terms of the pressure difference, therefore, is

$$w = 2^{\frac{n-3}{2n}} \left(\frac{n}{1+n} \right) \left(\frac{\Delta p}{\mu L} \right)^{\frac{1}{n}} \left[R^{\frac{1+n}{n}} - r^{\frac{1+n}{n}} \right] .$$

From the volume flow condition,

$$Q = \int_0^R 2\pi r w dr ,$$

the velocity profile may be written in terms of Q as

$$w = \frac{Q}{\pi R^2} \left(\frac{1+3n}{1+n} \right) \left[1 - \left(\frac{r}{R} \right)^{\frac{1+n}{n}} \right] . \quad (3.30)$$

It may be seen that with the substitution

$$n = 1$$

equation (3.30) reduces to the case for the Newtonian viscous flow.

The solution obtained is now used to obtain a condition, which, if satisfied, justifies neglecting inertia effects for the axially symmetric pseudo-plastic flow in circular cones of small semi-angles. The stream-

lines for slowly-varying circular cones, however, are not uniaxial, that is parallel to the z -axis, as is the case for the flow in a tube. Hence, in addition to the uniaxial velocity w , there is a radial velocity u which is of the order αw , where

$$\alpha(z) = \frac{dR}{dz}$$

is the inclination of the streamline to the z -axis, see FIG. 3.5.

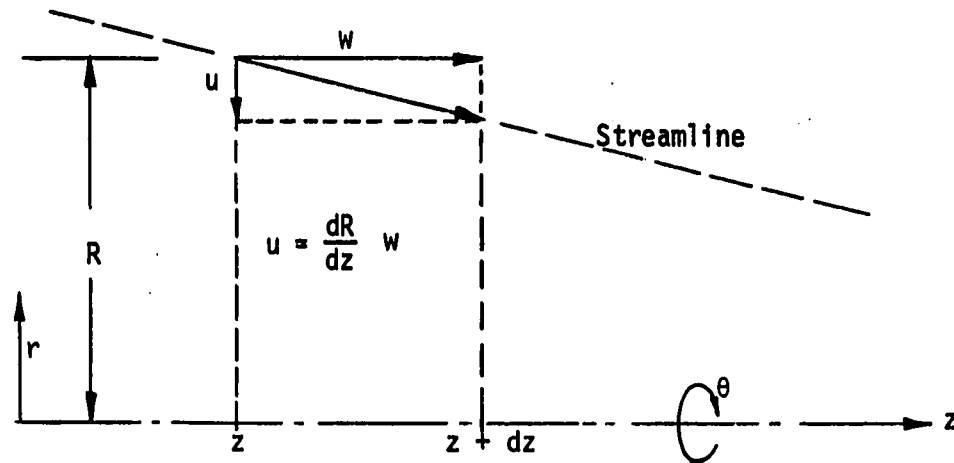


FIGURE 3.5

Velocity Components in a Circular Cone of Small
Semi-Angle α

If the flow in a circular cone, of small semi-angle, is considered, equation (3.30) is a valid approximation to the pseudo-plastic flow in that cone, provided that the neglected inertia terms are small compared to the term retained in the equilibrium equation (3.25).

The representative magnitude of each of the neglected inertia terms,

$$\rho u \frac{dw}{dr} \quad , \quad \text{and} \quad \rho w \frac{\partial w}{\partial z}$$

is

$$\rho \alpha \frac{Q^2}{R^5} \quad .$$

The representative magnitude of the term retained is

$$\mu \frac{Q^n}{R^{3n+1}} \quad .$$

Hence equation (3.30) is consistent with the neglect of the inertia term if

$$\rho \alpha \frac{Q^2}{R^5} \ll \mu \frac{Q^n}{R^{3n+1}} \quad ,$$

where α is taken as its maximum value, that is the semi-angle of the circular cone. The condition specifying the justification for neglecting the inertia term therefore becomes

$$\propto \frac{\rho Q^{2-n}}{\mu R^{4-3n}} \ll 1. \quad (3.31)$$

Upon introduction of the characteristic velocity U , defined by

$$U = \frac{Q}{\pi R^2},$$

where R is the characteristic length of the tube, the inequality (3.31) reduces to

$$\propto \frac{\rho U^{2-n} R^n}{\mu} \ll 1. \quad (3.32)$$

It is noted that for $n = 1$, which corresponds to the Newtonian viscous flow, equation (3.32) reduces to that obtained by Batchelor (33). Furthermore, it is observed that the quantity

$$\frac{\rho U^{2-n} R^n}{\mu}$$

in equation (3.32) is consistent with Reynold's number, as defined for the power law model.

Since neglecting of inertia terms for the axially symmetric pseudo-plastic flow problems is justified, if condition (3.32) is satisfied, the results should be applicable to technological processes such as wire drawing and hydraulic extrusion.

CHAPTER IV

APPLICATION TO WIRE DRAWING AND HYDRAULIC EXTRUSION

In CHAPTER III the velocity and stress fields were obtained for the plane pseudo-plastic flow in a converging channel, and axially symmetric converging flow in a circular cone.

The purpose of the present chapter is to study the application of the axially symmetric solution to wire drawing and hydraulic extrusion; the working material shall be approximated by the pseudo-plastic model with n close to zero.

FIGURE 4.1 indicates that the pseudo-plastic model,

$$s_{ij} = 2\mu(d_{mn} d_{mn})^{\frac{n-1}{2}} d_{ij} ,$$

with $n = 0.1$ should be a suitable model for a rate dependent material. This model is useful for application to extrusion processes; however, it does not possess a yield limit. This makes it difficult to apply to wire drawing problems. Since wire drawing involves uniaxial tension in the drawn material, and possibly in the undrawn material, if there is back-pull, it is difficult to consider this process if there is no yield limit. It is usually assumed that the yield limit is not exceeded in the drawn and undrawn material, but only in the deforming material passing through the die.

The following procedure can be adopted to circumvent this diffi-

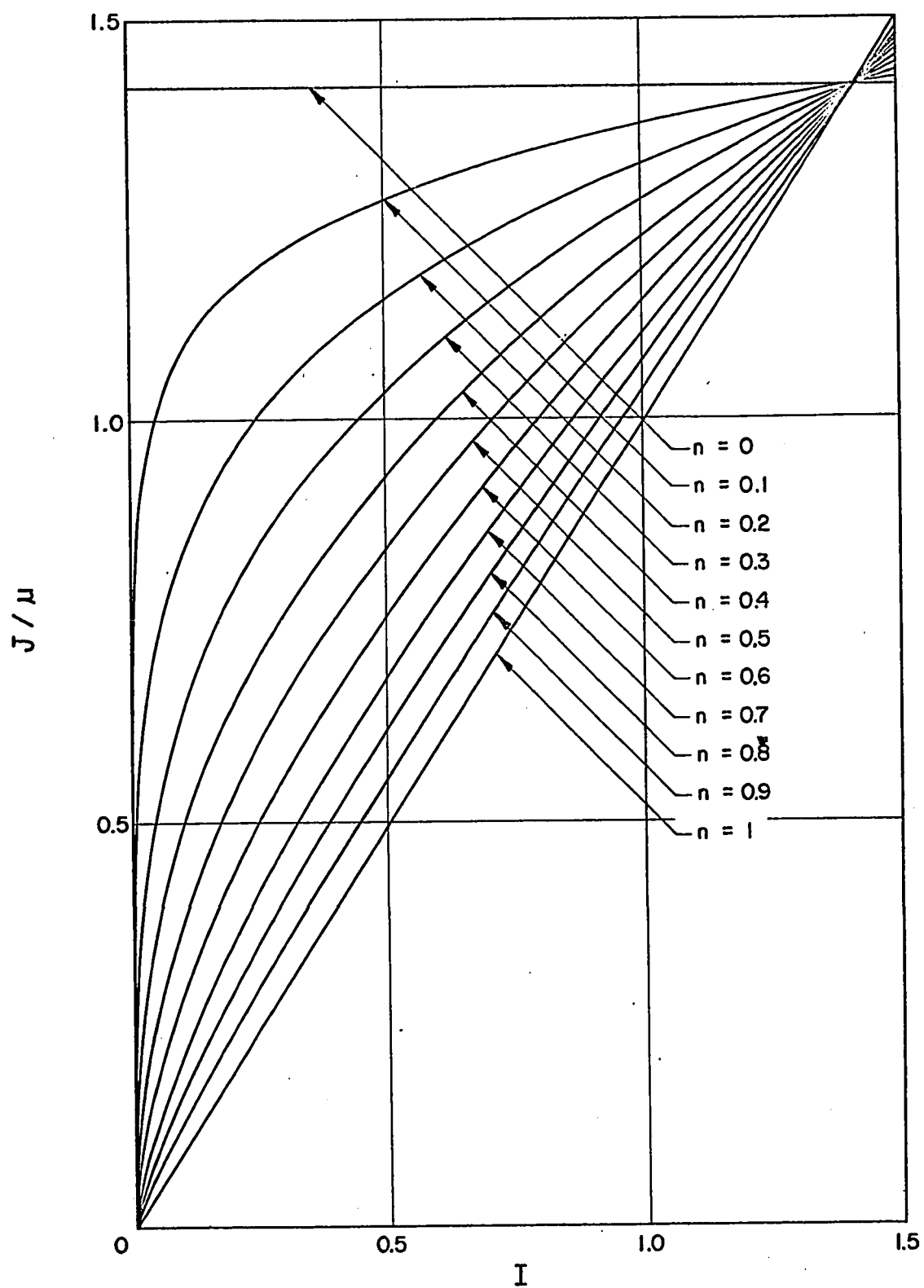


FIGURE 4.1

Flow Curves for the Power Law Model

culty and to enable the pseudo-plastic model to be applied to the wire drawing process. Consider the minimum value I_0 of I in the region ABCD, see FIG. 4.3, for the flow field obtained from equation (3.7); this minimum occurs at point E, see FIG. 4.3. The flow curve, see FIG. 4.1, gives at the point $I = I_0$ the corresponding value for J/μ , denoted by J_0/μ . The assumption is now made that the material stays rigid until J reaches its critical value $J_0^* \leq J_0$. The mean drawing stress must be less than the tensile yield stress, which, corresponding to the above assumption, is

$$\bar{Y} = \sqrt{3} J_0^* \leq \sqrt{3} J_0. \quad (4.1)$$

The assumed flow curve for the material in this drawing process, then, is as shown in FIG. 4.2.

Consider FIG. 4.3, which represents a cross-section of a conical reducing die. It is clear that severe approximations are necessary in order to analyse these processes. The method used in this thesis shall follow that of Shield. Shield (31) presented an approximation which assumes that the stress and velocity fields of the material in the region ABCD, see FIG. 4.3, can be represented by those obtained in CHAPTER III; this approximation is reasonably valid for small semi-angles and large reductions, and neglects the inlet and exit effects, sections AB and CD respectively, see FIG. 4.3. These and other approximations will become evident in the body of this chapter.

Theoretical results are presented for both wire drawing with

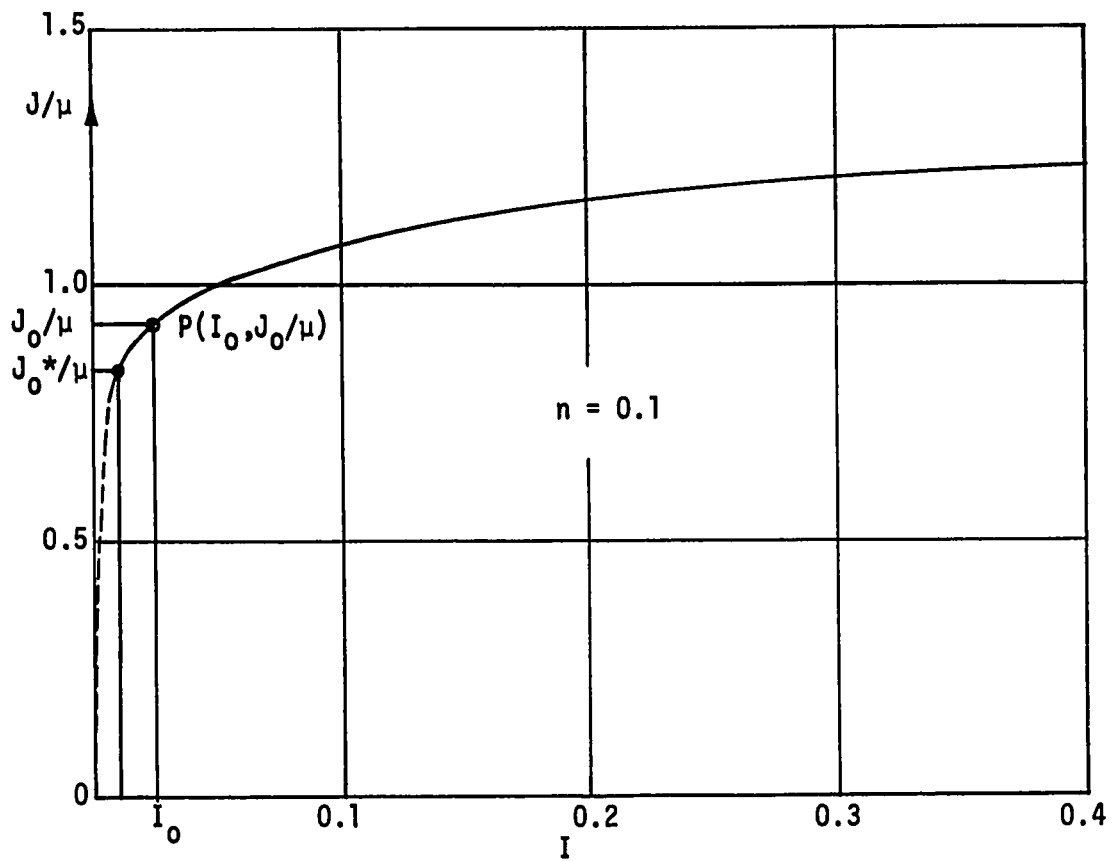


FIGURE 4.2

Flow Curve for the "Rigid" Pseudo-Plastic Material

back-pull, and hydraulic extrusion with zero drawing force. Numerical results are presented for hydraulic extrusion and for wire drawing, with $n = 0.1$; only the case of no back-pull is presented, since computations for the case including back-pull are excessively laborious.

The wire drawing analysis shall now be presented. FIGURE 4.3 serves to clarify the physical situation and to introduce the necessary

4.1 Wire Drawing

The entry and exit sections, AB and CD respectively, as shown in FIG. 4.3, are taken as plane sections, rather than circular arcs; this requires a knowledge of σ_z . The tensor transformation rule from spherical polars to cartesian coordinates gives

$$\sigma_z = \left(\frac{\sigma_r + \sigma_\phi}{2} \right) + \left(\frac{\sigma_r - \sigma_\phi}{2} \right) \cos 2\phi - \tau_{r\phi} \sin 2\phi . \quad (4.2)$$

The polar components of the stress tensor are calculated from

$$\sigma_{ij} = s_{ij} - p\delta_{ij} .$$

The deviatoric and isotropic components are given by equations (3.6) and equation (3.8) respectively, for completeness these equations are reproduced below

$$\begin{aligned} s_r &= - \frac{2^{\frac{5-n}{2}} \mu A^n}{r^{3n}} mG , \\ s_\phi &= s_\theta = \frac{2^{\frac{3-n}{2}} \mu A^n}{r^{3n}} mG , \\ s_{r\phi} &= \frac{2^{\frac{1-n}{2}} \mu A^n}{r^{3n}} m'G , \end{aligned} \quad (3.6)$$

and

$$p = \frac{2^{\frac{1-n}{2}} \mu A^n}{r^{3n}} \left[\frac{4}{n}(1-n)mG - \frac{1}{3n} \{ (m'G)' + m'G \cot \phi \} \right] + C , \quad (3.8)$$

where

$$G = [12m^2 + (m')^2]^{\frac{n-1}{2}} .$$

In expanded form the stress tensor components become

$$\begin{aligned} \sigma_r &= 2^{\frac{1-n}{2}} \mu A^n \left[\frac{1}{r^{3n}} \left\{ -\frac{4}{n} mG + \frac{1}{3n} ((m'G)') + m'G \cot \phi \right\} - H \right] , \\ \sigma_\phi = \sigma_\theta &= 2^{\frac{1-n}{2}} \mu A^n \left[\frac{1}{r^{3n}} \left\{ \frac{2(3n-2)}{n} mG + \frac{1}{3n} ((m'G)') + m'G \cot \phi \right\} - H \right] , \end{aligned} \quad (4.3)$$

$$\tau_{r\phi} = 2^{\frac{1-n}{2}} \mu A^n \left[\frac{1}{r^{3n}} (m'G) \right] .$$

The constant C in equation (3.8) has been replaced by

$$H 2^{\frac{1-n}{2}} \mu A^n ;$$

the constant H is determined by the back-pull condition.

Substitution of equations (4.3) in equation (4.2) yields

$$\sigma_z = 2^{\frac{1-n}{2}} \mu A^n \left[\frac{f(\phi)}{r^{3n}} - H \right] , \quad (4.4)$$

where

$$f(\phi) = 3mG(1 - \cos 2\phi) - \frac{4mG}{n} + \frac{1}{3n} \{ (m'G)' + m'G \cot \phi \} - m'G \sin 2\phi . \quad (4.5)$$

If the mean tensile stress over the entry section AB is given by T_0 , where T_0 must be less than the tensile yield stress, then the condition of back-pull becomes

$$T_0 = \frac{4}{\pi D_0^2} \int_{AB} \sigma_z |_{\text{at AB}} d(\text{area}) ;$$

whence

$$H = \frac{2}{z_0^{3n} \tan^2 \alpha} \int_0^\alpha f(\phi) \cos^{3n-2} \phi \tan \phi d\phi - \frac{T_0}{\frac{1-n}{2} \mu A^n} . \quad (4.6)$$

In equation (4.6), z_0 is the distance from the virtual apex of the cone, 0, to the entry section AB, as shown in FIG. 4.3. Finally, from equations (4.4) and (4.6), the expression for σ_z in terms of T_0 is

$$\sigma_z = \frac{1-n}{2} \mu A^n \left[\frac{f(\phi)}{r^{3n}} - \frac{2}{z_0^{3n} \tan^2 \alpha} \int_0^\alpha f(\phi) \cos^{3n-2} \phi \tan \phi d\phi \right] + T_0 . \quad (4.7)$$

The basic unknown of the problem is the drawing stress T_1 , which must be less than the tensile yield stress. It is found from the relation

$$T_1 = \frac{4}{\pi D_1^2} \int_{CD} \sigma_z |_{\text{at CD}} d(\text{area}) ,$$

which yields

$$T_1 = \frac{\frac{3-n}{2} \mu A^n}{z_1^{3n} \tan^2 \alpha} \left[1 - \left(\frac{z_1}{z_0} \right)^{3n} \right] \int_0^\alpha f(\phi) \cos^{3n-2} \phi \tan \phi d\phi + T_0 ,$$

where z_1 is the distance from the virtual apex of the cone to the exit section CD, as shown in FIG. 4.3. In terms of the diameters D_0 and D_1 of the entry and exit sections respectively, the expression for T_1 becomes

$$T_1 = \frac{2^{\frac{3+5n}{2}} \mu A^n \tan^{3n-2} \alpha}{D_1^{3n}} \left[1 - \left(\frac{D_1}{D_0} \right)^{3n} \right] \int_0^\alpha f(\phi) \cos^{3n-2} \phi \tan \phi d\phi + T_0 .$$

Upon the introduction of the reduction of the die, R , given by

$$R = \frac{\text{initial area} - \text{final area}}{\text{initial area}}$$

$$= \left[1 - \left(\frac{D_1}{D_0} \right)^2 \right] ,$$

gives

$$T_1 = \frac{2^{\frac{3+5n}{2}} \mu A^n \tan^{3n-2} \alpha}{D_1^{3n}} \left[1 - (1-R)^{\frac{3n}{2}} \right] \int_0^\alpha f(\phi) \cos^{3n-2} \phi \tan \phi d\phi + T_0 . \quad (4.8)$$

The drawing stress, T_1 , may not exceed the tensile yield stress, and its maximum value will now be calculated.

As previously mentioned, the minimum value of I occurs at the point E, see FIG. 4.3, and is

$$I_0 = \frac{2\sqrt{3}}{3} \frac{A}{z_0} ;$$

in terms of the diameter D_1 , and the reduction R , this becomes

$$I_0 = \frac{16\sqrt{3} A \tan^3 \alpha}{D_1^3} (1-R)^{3/2} . \quad (4.9)$$

To obtain the critical value J_0 , the equation linking the invariants J and I is required; this is obtained by squaring both sides of equation (1.6), and yields

$$J = 2^{\frac{1-n}{2}} \mu I^n . \quad (4.10)$$

Substitution of equation (4.9) in equation (4.10) results in

$$J_0 = \frac{2^{\frac{7n+1}{2}} \frac{n}{3^{\frac{n}{2}}} \mu A^n \tan^{3n} \alpha}{D_1^{3n}} (1-R)^{3n/2} .$$

As previously noted in equation (4.1), the maximum tensile yield stress is

$$Y = \sqrt{3} J_0 ,$$

which becomes

$$Y = \frac{2^{\frac{7n+1}{2}} \frac{n+1}{3^{\frac{n+1}{2}}} \mu A^n \tan^{3n} \alpha}{D_1^{3n}} (1-R)^{\frac{3n}{2}} .$$

Since T_1 may not exceed Y , the following inequality

$$\begin{aligned} & \frac{2^{\frac{3+5n}{2}} \mu A^n \tan^{3n-2} \alpha}{D_1^{3n}} [1 - (1-R)^{\frac{3n}{2}}] \int_0^\alpha f(\phi) \cos^{3n-2} \phi \tan \phi d\phi + T_0 \\ & < \frac{2^{\frac{7n+1}{2}} \frac{n+1}{3^{\frac{n+1}{2}}} \mu A^n \tan^{3n} \alpha}{D_1^{3n}} (1-R)^{\frac{3n}{2}} , \end{aligned} \quad (4.11)$$

determines the maximum reduction possible; apart from any negative normal stresses at the walls, which may occur during the process. For zero back-pull, from equation (4.11), for the maximum reduction:

$$R < 1 - \left[\frac{(2^{n-1} \frac{n+1}{3^{\frac{n+1}{2}}}) \tan^2 \alpha}{\int_0^\alpha f(\phi) \cos^{3n-2} \phi \tan \phi d\phi} + 1 \right]^{-\frac{2}{3n}} .$$

An expression for the die pressure, P_{die} , shall now be developed; this expression could be useful in a stress analysis of the die proper. By definition

$$P_{die} = (-\sigma_\phi) \Big|_{\phi=\alpha} .$$

The stress component σ_ϕ at an arbitrary point P is obtained by substitution of equation (4.6) in the second of the set of equations (4.3), which results in

$$\begin{aligned} \sigma_\phi = \sigma_\theta = 2 \frac{1-n}{2} \mu A^n \left[\frac{1}{r^{3n}} \left\{ \frac{2(3n-2)}{n} mG + \frac{1}{3n} ((m'G)' + m'G \cot \phi) \right\} \right. \\ \left. - \frac{2}{z_0^{3n} \tan^2 \alpha} \int_0^\alpha f(\phi) \cos^{3n-2} \phi \tan \phi d\phi \right] + T_0 . \end{aligned} \quad (4.12)$$

Upon substitution of $\phi = \alpha$ in equation (4.12), and noting that

$$m(\alpha) = 0 ,$$

$$G(\alpha) = (m')^{n-1} \Big|_{\phi=\alpha} ,$$

$$G'(\alpha) = (n-1)(m')^{n-2} m' \Big|_{\phi=\alpha},$$

the die pressure becomes

$$P_{die} = 2 \frac{1-n}{2} \mu A^n \left[-\frac{1}{3n} \left\{ \frac{1}{3n} (n(m')^{n-1} m' + (m')^n \cot \phi) \right\}_{\phi=\alpha} \right. \\ \left. + \frac{2}{z_0^{3n} \tan^2 \alpha} \int_0^\alpha f(\phi) \cos^{3n-2} \phi \tan \phi d\phi \right] - T_0. \quad (4.13)$$

The parameter s is measured along OCA, as shown in Fig. 4.3, and is calculated from

$$s = \gamma \frac{z_1}{\cos \alpha}, \quad (4.14)$$

where γ is a variable with the range of values given by

$$1 \leq \gamma \leq \frac{z_0}{z_1} = (1-R)^{-1/2}.$$

Under the substitution (4.14) the expression for P_{die} , in terms of the reduction R , becomes

$$P_{die} = \frac{2 \frac{1+5n}{2} \mu A^n}{D_1^{3n}} \left[-\frac{\sin 3n \alpha}{\gamma^{3n}} \left\{ \frac{1}{3n} (n(m')^{n-1} m' + (m')^n \cot \phi) \right\}_{\phi=\alpha} \right. \\ \left. + 2(1-R)^{\frac{3n}{2}} \tan^{3n-2} \alpha \int_0^\alpha f(\phi) \cos^{3n-2} \phi \tan \phi d\phi \right] - T_0. \quad (4.15)$$

Similarly, the expression for the shear stress at the boundary is given by

$$\tau_{r\phi}|_{\phi=\alpha} = \frac{2^{\frac{1+5n}{2}} \mu A^n}{D_1^{3n} \gamma^{3n}} [(m')^n \sin^{3n} \phi]_{\phi=\alpha} \quad (4.16)$$

It is noted that the integral

$$\int_0^\alpha f(\phi) \cos^{3n-2} \phi \tan \phi d\phi$$

occurs in many of the preceding expressions. It is not necessary to perform this integration numerically because the requirement of static equilibrium of the material between the entry and exit sections yields an expression for this integral in terms of α , $m'(\alpha)$, and $m''(\alpha)$. This expression is now obtained. The net axial component of the die force, F_{die} , is

$$F_{die} = 2\pi \sin^2 \alpha \int_{s=z_1/\cos \alpha}^{z_0/\cos \alpha} P_{die} s ds, \quad (4.17)$$

which, upon substitution of equation (4.13), reduces to

$$\begin{aligned} F_{die} = & 2^{\frac{5n-1}{2}} \pi \mu A^n D_1^{2-3n} \{ R[1-R]^{\frac{3n-2}{2}} \tan^{3n-2} \alpha \int_0^\alpha f(\phi) \cos^{3n-2} \phi \tan \phi d\phi \\ & - \frac{\sin^3 \alpha}{3n(2-3n)} [(1-R)^{\frac{3n-2}{2}} - 1] [n(m')^{n-1} m'' + (m')^n \cot \phi]_{\phi=\alpha} \} \\ & - \frac{\pi D_1^2}{4} \left[\frac{R}{1-R} \right] T_0. \end{aligned}$$

The net axial component of the shear force, F_{shear} , is

$$F_{\text{shear}} = 2\pi \sin \alpha \cos \alpha \int_{s=z_1/\cos \alpha}^{z_0/\cos \alpha} \tau_{r\phi} \Big|_{\phi=\alpha} s ds ,$$

which, upon substitution of $\tau_{r\phi} \Big|_{\phi=\alpha}$, reduces to

$$F_{\text{shear}} = 2 \frac{5n-1}{2} \pi \mu A^n D_1^{2-3n} [(1-R)^{\frac{3n-2}{3}} - 1] [(m')^n \frac{\sin^{3n-1} \phi \cos \phi}{(2-3n)}]_{\phi=\alpha} . (4.18)$$

The net drawing force, F_{drawing} , is

$$F_{\text{drawing}} = \frac{\pi D_1^2 T_1}{4} ,$$

which, upon substitution of the expression for T_1 , equation (4.8), reduces to

$$F_{\text{drawing}} = 2 \frac{5n-1}{2} \pi \mu A^n D_1^{2-3n} [1 - (1-R)^{\frac{3n}{2}}] \tan^{3n-2} \alpha \int_0^{\alpha} f(\phi) \cos^{3n-2} \phi \tan \phi d\phi + \frac{\pi D_1^2 T_0}{4} .$$

The condition of static equilibrium becomes

$$F_{\text{shear}} + F_{\text{die}} + \frac{\pi D_0^2 T_0}{4} - F_{\text{drawing}} = 0 . \quad (4.19)$$

Upon substitution of the above obtained expressions, there results from equation (4.19)

$$\int_0^\alpha f(\phi) \cos^{3n-2} \phi \tan \phi d\phi = \frac{\sin \alpha \cos^{3n-2} \alpha}{(2-3n)} \left\{ \frac{(m')^{n-1} m' \sin \phi}{3} + [(m')^n \cos \phi] \left[\frac{1}{3n} - 1 \right] \right\}_{\phi=\alpha} \quad (4.20)$$

It is sometimes useful to treat the boundary effects by the introduction of a coefficient of friction as is done for Coulomb friction; this has been done in various manners by Sachs (34), and also by Shield (31). Proceeding in the fashion of Shield, an average coefficient of friction, defined by

$$f_{\text{average}} = \frac{\int_{s=z_1/\cos \alpha}^{z_0/\cos \alpha} \tau_{r\phi} |_{\phi=\alpha} s ds}{\int_{s=z_1/\cos \alpha}^{z_0/\cos \alpha} P_{die} s ds}, \quad (4.21)$$

which becomes in expanded form

$$\begin{aligned} f_{\text{average}} &= (m')^n |_{\phi=\alpha} \sin^2 \alpha \left[(1-R)^{\frac{3n-2}{2}} - 1 \right] \\ &\quad \{ (2-3n)R(1-R)^{\frac{3n-2}{2}} \cos^{2-3n} \alpha \int_0^\alpha f(\phi) \cos^{3n-2} \phi \tan \phi d\phi \\ &\quad - \frac{\sin^2 \alpha}{3n} [n(m')^{n-1} m' + (m')^n \cot \phi]_{\phi=\alpha} [(1-R)^{\frac{3n-2}{2}} - 1] \\ &\quad - \frac{(2-3n)RT_0 D_1^{3n} \sin^{2-3n} \alpha}{2^{\frac{3+5n}{2}} \mu A^n (1-R)} - 1 \} \end{aligned}$$

Results for wire drawing are presented in FIGS. 6.A-1 and 6.A-2. As previously mentioned, T_0 was set equal to zero to facilitate the numerical computations.

4.2 Hydraulic Extrusion

The hydraulic extrusion of the pseudo-plastic material, under conditions of zero drawing force, that is

$$\int_{CD} \sigma_z|_{\text{at } CD} d(\text{area}) = 0 , \quad (4.22)$$

is now considered. From the above expression (4.22) the constant H in equation (4.6) is found to be

$$H = \frac{2}{z_1^{3n} \tan^2 \alpha} \int_0^\alpha f(\phi) \cos^{3n-2} \phi \tan \phi d\phi. \quad (4.23)$$

In terms of H ,

$$\sigma_z = 2^{\frac{1-n}{2}} \mu A^n \left[\frac{f(\phi)}{r^{3n}} - \frac{2}{z_1^{3n} \tan^2 \alpha} \int_0^\alpha f(\phi) \cos^{3n-2} \phi \tan \phi d\phi \right] ,$$

where $f(\phi)$ is defined by equation (4.5).

The basic unknown for the hydraulic extrusion is the ram pressure P_{ram} ; this compares to T_1 of the drawing process.

The equilibrium condition at the entry section AB is

$$P_{\text{ram}} = - \frac{4}{\pi D_0^2} \int_{AB} \sigma_z|_{\text{at } AB} d(\text{area}) ,$$

from which there is obtained in terms of the reduction R

$$P_{ram} = - \frac{2^{\frac{3+5n}{2}} \mu A^n \tan^{3n-2} \alpha}{D_1^{3n}} [(1-R)^{\frac{3n}{2}} - 1] \int_0^\alpha f(\phi) \cos^{3n-2} \phi \tan \phi d\phi.$$

Consequently, the ram force, defined by

$$F_{ram} = \frac{\pi D_o^2 P_{ram}}{4},$$

becomes

$$F_{ram} = - 2^{\frac{5n-1}{2}} \pi \mu A^n D_1^{2-3n} \tan^{3n-2} \alpha [(1-R)^{\frac{3n-2}{2}} - (1-R)^{-1}] \int_0^\alpha f(\phi) \cos^{3n-2} \phi \tan \phi d\phi.$$

From the second of the set of equations (4.3) and using equation (4.23), and evaluating at $\phi = \alpha$, there results

$$\begin{aligned} P_{die} = & \frac{2^{\frac{1+5n}{2}} \mu A^n}{D_1^{3n}} \left[- \frac{\sin^{3n} \alpha}{3n \gamma^{3n}} \{ n(m')^{n-1} m' + (m')^n \cot \phi \}_{\phi=\alpha} \right. \\ & \left. + 2 \tan^{3n-2} \alpha \int_0^\alpha f(\phi) \cos^{3n-2} \phi \tan \phi d\phi \right]. \end{aligned} \quad (4.24)$$

The net axial component of the die force, obtained by substituting equation (4.24) in equation (4.17) is

$$\begin{aligned} F_{die} = & 2^{\frac{5n-1}{2}} \pi \mu A^n D_1^{2-3n} \left\{ \frac{R}{1-R} \tan^{3n-2} \alpha \int_0^\alpha f(\phi) \cos^{3n-2} \phi \tan \phi d\phi \right. \\ & \left. - \frac{\sin^{3n} \alpha}{3n(2-3n)} [(1-R)^{\frac{3n-2}{2}} - 1] [n(m')^{n-1} m' + (m')^n \cot \phi]_{\phi=\alpha} \right\}. \end{aligned}$$

The expression for $\tau_{r\phi}|_{\phi=\alpha}$ is as previously obtained in equation (4.16), and is

$$\tau_{r\phi}|_{\phi=\alpha} = \frac{2^{\frac{1+5n}{2}} \mu A^n}{D_1 \gamma^{3n}} [(m')^n \sin^{3n} \phi]_{\phi=\alpha} \quad (4.16)$$

The net axial component of the shear force, therefore, remains unchanged and is given by equation (4.18), which for completeness is reproduced; thus,

$$F_{\text{shear}} = 2^{\frac{5n-1}{2}} \pi \mu A^n D_1^{2-3n} [(1-R)^{\frac{3n-2}{2}} - 1] [(m')^n \frac{\sin^{3n-1} \phi \cos \phi}{(2-3n)}]_{\phi=\alpha} \quad (4.18)$$

It is noted that the overall statical equilibrium condition given by equation (4.19) is essentially independent of T_0 and T_1 , and therefore of P_{ram} , hence the integral

$$\int_0^\alpha f(\phi) \cos^{3n-2} \phi \tan \phi d\phi$$

is defined in terms of boundary values by equation (4.20).

The average coefficient of friction, f_{average} , as defined by equation (4.21) becomes in expanded form

$$\begin{aligned} f_{\text{average}} &= (m')^n |_{\phi=\alpha} \sin^2 \alpha [(1-R)^{\frac{3n-2}{2}} - 1] \\ &\{ (2-3n) (\frac{R}{1-R}) \cos^{2-3n} \alpha \int_0^\alpha f(\phi) \cos^{3n-2} \phi \tan \phi d\phi \\ &- \frac{\sin^2 \alpha}{3n} [(1-R)^{\frac{3n-2}{2}} - 1] [n(m')^{n-1} m' + (m')^n \cot \phi]_{\phi=\alpha} \}^{-1} \end{aligned}$$

FIG. 6.A-3 shows the relationship between P_{ram} and semi-angle α for various reductions.

It is important to note that all calculations for both wire drawing and hydraulic extrusion are based on a constant diameter at the exit section.

CHAPTER V

EXPERIMENTAL INVESTIGATION

The experimental investigation of the axially symmetric converging flow of certain non-Newtonian materials in a circular cone is presented in this chapter.

The purpose of this experimental work is to investigate the kinematic behavior of creeping flow of non-Newtonian materials. This investigation is concerned mainly with

- (i) determining if the creeping flow of non-Newtonian materials in a circular cone yields a radial flow pattern, and
- (ii) observing whether or not the material adheres to the walls of the die during the extrusion process.

The assumption that the relative motion of a non-Newtonian material in contact with a solid body is zero, may not always be justified; this becomes more evident if pure lead is considered.

Often pure lead is used in experiments whose purpose is to examine the validity of solutions for a rigid plastic solid. At a perfectly rough boundary the solutions for flow of a rigid perfectly plastic solid indicate that there can be slip at the boundary, that is the relative motion is non-zero. The problem of flow in a converging channel (30) is an example of this. In this solution, as in other rigid plastic solutions where there is relative motion between a perfectly rough boundary and the material, the shear strain rate is infinite. This is permissible in an

inviscid material but is not permissible for a material such as a Bingham material that exhibits viscous effects. The classical perfectly plastic solid is not rate dependent. It has been shown by Luming (35) that at room temperature the behavior of pure lead can closely be approximated by that of a Bingham solid, with a low coefficient of viscosity. Consequently pure lead may be regarded as a non-Newtonian material. Possibly, the amount of slippage at the boundary should be considered as a function of the Bingham number*; this function would be of such a nature that the amount of slippage at the walls increases with increasing Bingham number. In this thesis these considerations have not been taken into account, and the classical assumption of no-slip at a boundary is used. Further experimental work is needed to study the behavior of non-Newtonian materials in contact with solid boundaries.

5.1 Experimental Apparatus

The experimental investigation consisted essentially of extruding lead and wax specimens. A rigid conical die, of circular cross-section, was designed to perform these experiments. The extruding apparatus consisted of three main parts:

- (i) The Rigid Die and Separation Plate- the die was designed so that
 - (a) removal of the specimens was possible, and
 - (b) it could be used to prepare the specimens, so that the specimens were in two halves with a grid showing on the

*The Bingham number is defined as $B = kL/\mu U$, where k , L , μ , and U are the yield stress in pure shear, the characteristic length, the Newtonian coefficient of viscosity, and the characteristic velocity, respectively (36). The Bingham number is a measure of the ratio of the relative magnitudes of the plastic forces to the viscous forces.

face of one of the halves, thus facilitating investigation of the flow behavior.

In order to facilitate the removal of the specimens, the die, approximately 8" long, was of the split type, bolted together with ten 7/16" N.C., and two 3/8" N.C. bolts, as shown in FIG. 5.1. To ensure perfect alignment of the two halves, the halves were provided with some 1/4" aligning pins. The semi-angle of the circular cone was 5°, with an exit diameter of 1/4". Due to the small exit diameter, the machining of the cone had to be done in two stages; therefore, the die had to be built up out of two parts as is shown in FIG. 5.1.

To prepare the specimens, a 1/4" plate was prepared to be clamped between the halves of the die; this way two molds were formed, so that the specimen halves could be poured with liquid lead or wax. Furthermore, the plate, provided with the appropriate holes for the aligning pins, was prepared with a grid on one of its sides; the grid consisted of radial lines at intervals of 1° - 40', and with circular arcs about the virtual apex of the cone at 1" intervals, see FIG. 5.2. A circular ring, of semi-circular cross-section, was made in the top of the die; this provided the location for the oil ring, which was clamped between the die and the piston housing, see FIG. 5.1.

(ii) The Piston Housing - the piston housing consisted essentially of a thick cylinder, approximately 3" long, see FIG. 5.3. The end of the piston housing, which is to be bolted to the die with six 7/16" N.C. bolts, was provided with a groove similar to the one on the top of the die. The outside diameter was the same as that of the die, that is 5". The inside

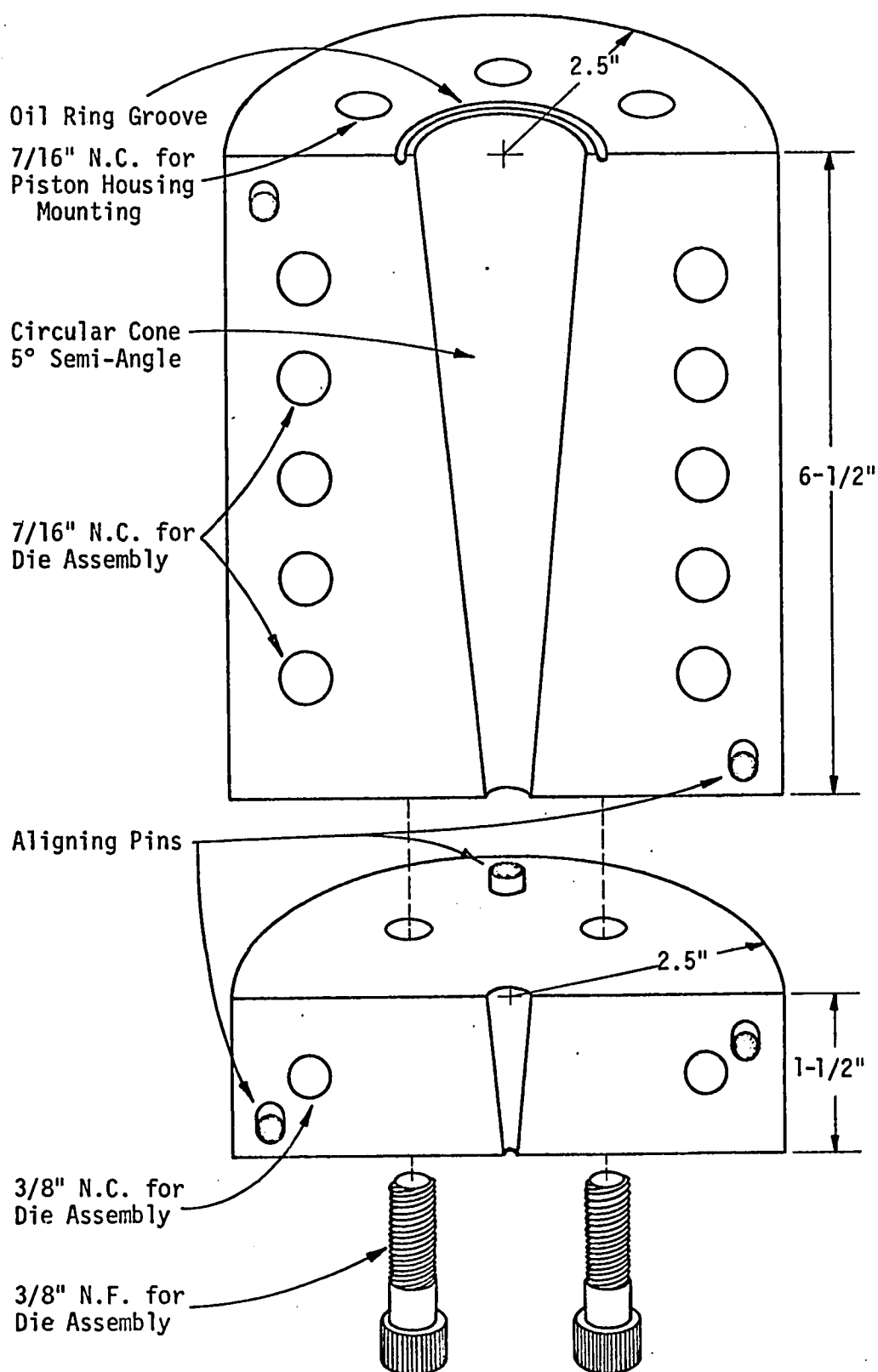


FIGURE 5.1
Typical Half of the Die

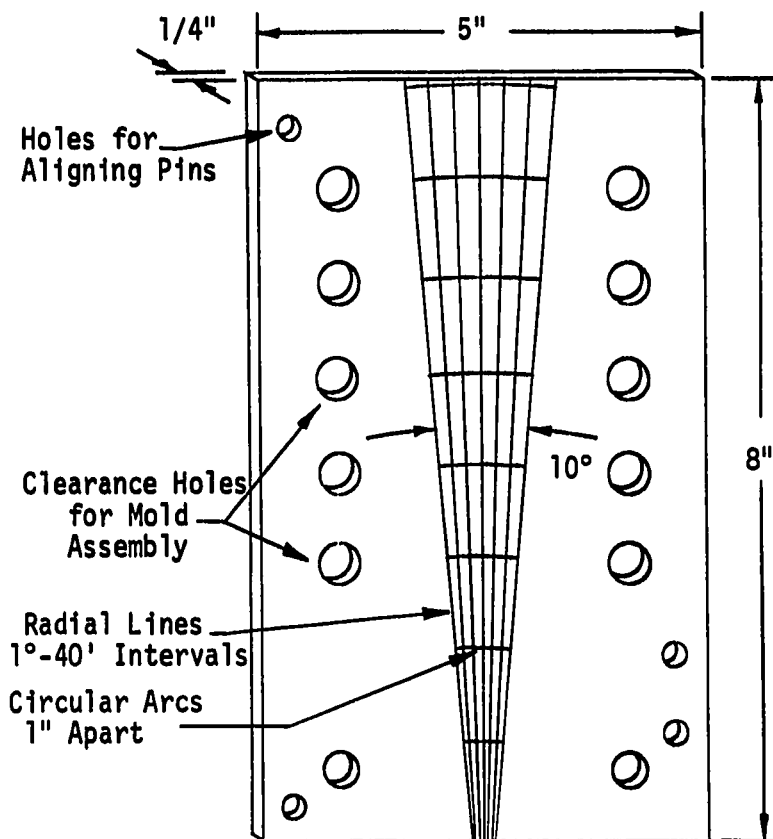


FIGURE 5.2

The Separation Plate

diameter, for the piston to be fitted in, was machined at $1 \frac{7}{16}$ ".

(iii) The Piston - the piston consisted mainly of a piece of shaft, 5" long, of circular cross-section with a diameter of $1 \frac{3}{8}$ ". At one end of the piston four grooves were provided to house the oil rings, as shown in FIG. 5.3. A hole was bored in the piston, and a hydraulic pump was attached; this enabled the extrusions to take place continuously without the

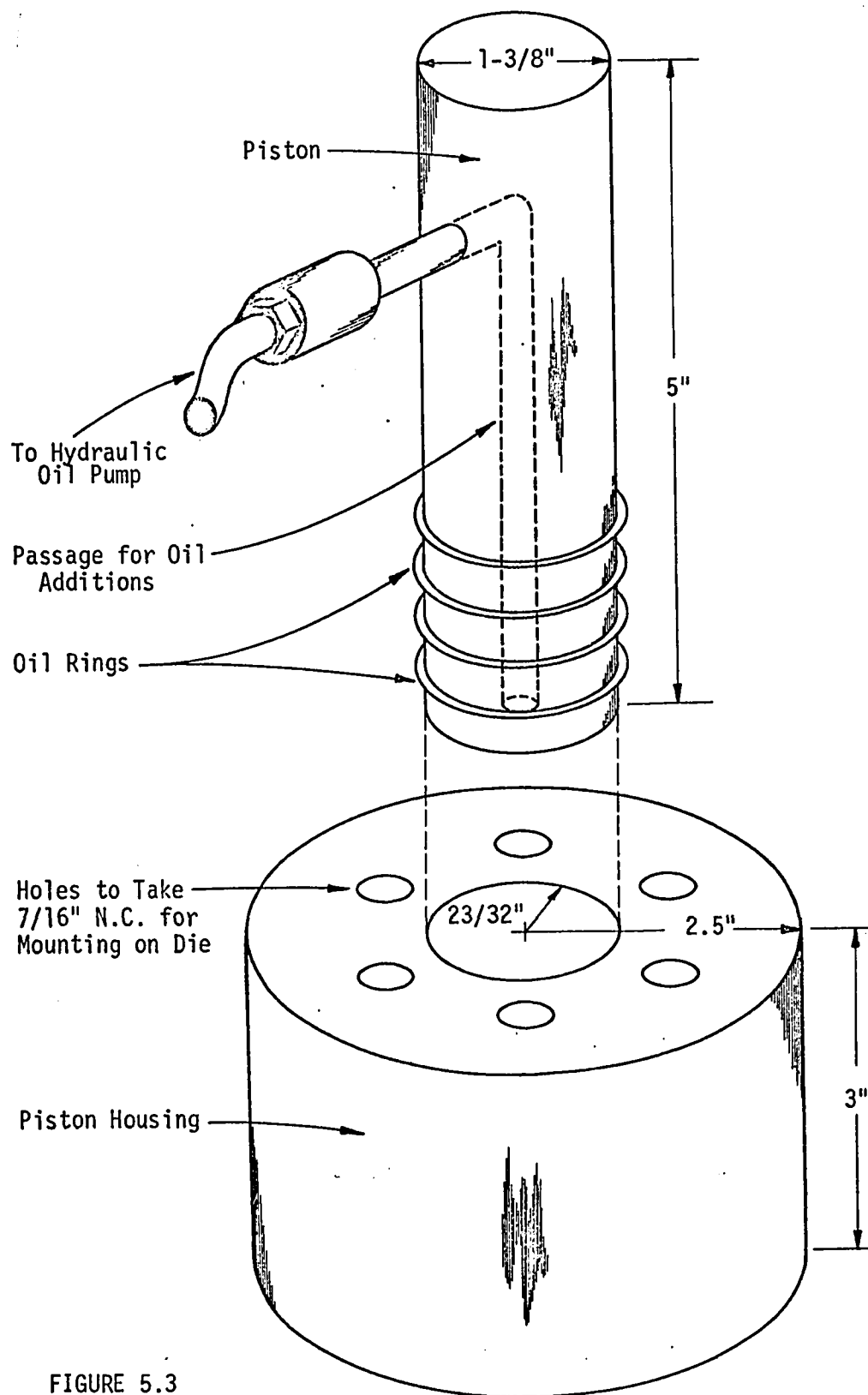


FIGURE 5.3

The Piston and the Piston Housing

disadvantage of removing the piston in order to fill up the oil level during the extrusion.

5.2 Results of Experiments

As previously mentioned, the materials used in this investigation were lead and wax. The lead used was that as supplied by Canada Metals Ltd. Its assay is 0.02% antimony, 0.015% arsenic, and 99.965% lead. The material constants were found experimentally by Luming (35) as $\mu = 1372$ psi-sec., and $k = 1170$ psi., where μ is the Newtonian coefficient of viscosity, and k is the yield stress in pure shear. The waxes used were

(i) Parowax - made by the Imperial Esso Oil Company - of which the material constants were not known, and

(ii) Bee's wax, similarly without a knowledge of its properties.

Before discussing the actual extrusions, the preparation of the specimens is considered briefly.

The Specimens

The material, lead or wax, was melted and poured into the molds; as previously discussed, these molds were obtained by the insertion of the separation plate between the two die halves. The formation of pipes, longitudinal cavities due to shrinkage toward the side of the mold during solidification, was minimized by adding molten material into the cavities during the cooling process. This technique was used throughout, both for the wax and the lead. After removing the die halves from the separation plate, some specimens had to be abandoned, in particular the waxes, since

sticking of the material to the separation plate caused some specimens to crumble.

Lead Extrusions

After the die was assembled, the two halves of the specimen were tapped in simultaneously, so that a proper fit could be ensured. The apparatus was completed by the mounting of the piston housing, with the appropriate oil ring inserted. With the insertion of the piston, extrusion could now take place. The applied load increased to approximately 4500 lbs., at which point the oil ring, separating the die and the piston housing, could not support a further increase in load, consequently the oil was seeping from the sides and extrusion of the specimen did not take place. A few more attempts were made, but all with the same result. Before attempting any more extrusions, the piston housing was milled down 0.003" so that the piston housing could be bolted to the die at a higher torque, thus providing a tighter fit for the oil ring. Extrusions were attempted again, but the problem of oil seepage remained. Before abandoning the lead extrusions completely, a lead plug was machined to fit between the specimen and the piston; this plug was used instead of the hydraulic fluid, thus removing the sealing problems of the previous extrusions. After the apparatus was assembled, extrusion could take place again. The applied load increased to approximately 45,000 lbs. before plastic flow occurred. Although some minor flashing occurred, due to a small separation of the die halves, the specimen was kept for investigation of the flow behavior.

Wax Extrusions

The hydraulic extrusions using Parowax were attempted first. Before extrusion, some coloring, using a felt pen, was applied to the grid on the specimen so that after extrusion the grid would be more distinct, thus providing easier evaluation of the flow behavior. The applied load increased to approximately 4000 - 5000 lbs., and plastic flow did indeed occur, however, the extrusion was not as expected. Due to the contraction of the specimen halves on cooling, the flat sides in contact with each other during extrusion did not seal properly, consequently the oil was forced through this opening, and extruded the bottom portion of one of the halves of the specimen. Further attempts were made, but all with the same result.

In order to overcome this difficulty, the specimens were poured to approximately 1/2" from the top, and after the two halves were fitted in the die, a wax plug was poured on top of the specimen, thus sealing any imperfections which caused oil seepage problems during the previous extrusions. Extrusions took place again with only a few useful results. It appeared that somehow the oil bypassed the plug causing either the failures as described above, or due to the uneven pressure on the specimen halves, parts of the specimen "cork-screwed" out leaving the other half crumbled in the die.

Most of the few extrusions which did indeed give good plastic flow were of no value, since the two specimen halves were fused together, and due to its brittle nature could not be separated wholly. A few specimens were kept, however, and investigated.

The extrusions using bee's wax gave the same difficulties as the ones with Parowax, except not to such a great extent. Numerous extrusions were attempted, all without success. Another complication, which was not the case with the Parowax, was that the coloring of the specimen with a felt pen was not effective. The coloring of the specimen was changed to the application of graphite in the grid on the separation plate before pouring the specimens; this indeed resulted in a good grid. More attempts were made to obtain good plastic flow of the whole specimen, most without good results; however one of such extrusions did result in a specimen which was used for the investigation of the flow behavior.

5.3 Conclusions

The lead specimen, which was retained for investigation, was obtained from the extrusion during which some minor flashing occurred. The specimen was investigated, and it was observed that the radial lines remained radial. Also the presence of relative motion between the specimen and the die was observed, notwithstanding the fact that the walls of the die were degreased before extrusion.

The specimens obtained using Parowax were investigated, and it was found that radial lines did indeed remain radial, thus predicting a radial flow pattern, at least for creeping flow. Furthermore, it was observed that the material did adhere to the walls of the die, as is the classical assumption for Newtonian viscous flow. The same flow behavior was observed with the specimen obtained from the bee's wax extrusion.

Since the specimens of the Parowax were obtained during the earlier stages of the experimental period, no photographs were taken since

it was assumed that more and better specimens would be obtained once the technique was ironed out. Furthermore, used specimens were melted and used over again. Since no other successful extrusions were attained during the many experiments performed thereafter, no photographs are available to include in this chapter. The extrusions using bee's wax, which were performed during the final stages of the experimental period, did yield one specimen which extruded rather well. However, the two halves fused together, therefore, one of the halves was cut off, taking care not to damage the grid. The grid was clear enough for investigation, and showed both radial flow and adhesion to the walls of the die. Although the visibility of the grid was good, the photographing of the same was not clear at all, and the photographs obtained do not merit inclusion in this chapter.

It may be concluded from this experimental investigation, therefore, that the flow pattern for the creeping flow of the non-Newtonian materials tested is radial, at least for small semi-angles. This conclusion is not necessarily valid for larger semi-angles; more extensive experimental work is required to investigate any possible deviations from radial flow, which may result from larger semi-angles.

Further experimental investigations of the creeping flow of lead, which may be assumed to behave as a Bingham solid for a certain range of strain rates, would be a significant contribution, especially if the theoretical investigation is considered in greater detail.

CHAPTER VI

CONCLUDING REMARKS

The main purpose of this chapter is to consider further the pseudo-plastic flow problems, which were discussed previously in this thesis.

The numerical results of these flow problems are incorporated in the first section of this chapter, while the results of wire drawing and hydraulic extrusion are presented in the section dealing with those processes. A discussion on how closely these results approximate the correct solution is given. Furthermore, the usefulness of these results is investigated by consideration of the objections, raised by Reiner (24), to the use of the power law model, which is used in this thesis. The results of the application of the axially symmetric pseudo-plastic flow to wire drawing and hydraulic extrusion are then briefly considered. In conclusion, a method due to Sutterby (37), which could possibly give an approximate solution to the axially symmetric flow of a Bingham solid in a circular cone of small semi-angle, and of finite length, is briefly discussed.

6.1 Results

Various results of the numerical procedure have been presented at the end of this section. The results for the velocity profiles, with semi-angles 15° , 30° , 45° , and 60° , and for various values of n , are presented in FIGS. 6.II-2 to 6.II-5 and in FIGS. 6.III-2 to 6.III-5 for the

plane and axially symmetric flow, respectively. It is recalled that a knowledge of $m'(0)$ was required to solve the boundary value problems. The relationships between this parameter and n for various semi-angles α are presented, therefore, in FIG. 6.II-1 for the plane flow, and for the axially symmetric flow in FIG. 6.III-1.

The velocity profiles for the limiting cases, $n = 0$, and $n = 1$, are shown for comparison. The solution for the case $n = 1$, corresponding to the Newtonian viscous liquid, may be written as

$$m(\phi) = \frac{\cos^2 \phi - \cos^2 \alpha}{\sin^2 \alpha} .$$

which is according to the expression originally obtained by Harrison(38) and Bond (39). For the plane flow, it can be shown that the solution

$$m(\theta) = \frac{\cos^2 \theta - \cos^2 \alpha}{\sin^2 \alpha}$$

satisfies the governing differential equation. The solution for the case $n = 0$, corresponding to the perfectly plastic von Mises solid, for the plane flow case may be written as

$$m(\theta) = \frac{c - 1}{c - \cos 2\psi} ,$$

where ψ is the angle between a radius and the direction of the algebraically greatest principal stress, and the parameter c is defined by

$$\frac{c}{\sqrt{c^2 - 1}} \tan^{-1} \sqrt{\frac{c+1}{c-1}} = \frac{1}{4} \pi + \alpha$$

for the case of perfectly rough walls; these equations are due to Hill (30). For the axially symmetric case, with $n = 0$, the velocity field was obtained only partially, since the derivatives at the walls are infinite. The value used for $m''(0)$, needed to start the integration procedure, was that obtained by extrapolating the curves in FIG. 6.III-1 to $n = 0$.

It is noted from the velocity profiles that there is a distinct difference between the curves $n = 0.1$ and $n = 0$. This difference is more pronounced than that between the curves $n = 0.9$ and $n = 1$. To illustrate this further, the velocity profiles for the plane flow, with $n = 0.04$ and $n = 0.07$ have been presented for a channel with a semi-angle of 15° , see FIG. 6.II-2. This marked difference can be attributed to the fact that in the range

$$0 < n \leq 1$$

the material is assumed to adhere to the walls, whereas for the case $n = 0$, there is slippage.

In the solutions of the stress fields for the plane perfectly plastic von Mises flow in a converging channel due to Nadai (29), and that for the axially symmetric flow in a circular cone, due to Shield (31), it was assumed that for perfectly rough walls, the shear stress at the walls is k , where k is the yield stress in pure shear. This, however, is not the case if a viscous medium is considered; the shear stress at the wall

is determined by the velocity field. To illustrate this further, the results presented in FIGS. 6.II-6 and 6.III-6 for the plane and axially symmetric flow, respectively, show that for $n = 0$ the shear stress at the wall is independent of the semi-angle α , whereas for values of n in the range

$$0 < n \leq 1 ,$$

the shear stress at the wall is dependent on the semi-angle of the cone. Furthermore, this dependence increases with increasing n . For completeness, results of the relationships between the shear stress at the wall and semi-angle α have been presented in FIGS. 6.II-7 to 6.II-9 for the plane flow, and in FIGS. 6.III-7 to 6.III-9 for the axially symmetric flow. It is noted that in FIGS. 6.II-9 and 6.III-9 the non-dimensional quantities $\tau_{r\theta}(\alpha) r^{2n}/\mu Q^n$ and $\tau_{r\phi}(\alpha) r^{3n}/\mu Q^n$ have been replaced by $\alpha \tau_{r\theta}(\alpha) r^{2n}/\mu Q^n$ and $\alpha \tau_{r\phi}(\alpha) r^{3n}/\mu Q^n$ for the plane and axially symmetric flow, respectively. This replacement is necessary, since the results of $\tau_{r\theta}(\alpha) r^{2n}/\mu Q^n$ versus α for the plane flow, and those of $\tau_{r\phi}(\alpha) r^{3n}/\mu Q^n$ versus α for the axially-symmetric flow yield curves which are of such a nature that only a qualitative and not a quantitative study can be made.

Since the solutions to the axially symmetric flow problems, with $n = 0.1$, are applied to wire drawing and hydraulic extrusion, the stress distributions in the material are presented only for that particular value of n . The semi-angles for this purpose were chosen to be

15°, 30°, 45°, and 60°. Although large semi-angles are of no practical consequence in the application to wire drawing, they are, nevertheless, of academic interest, and thus merit presentation. These results are presented in FIGS. 6.III-10 to 6.III-13. Similar results were obtained for the plane flow case, and are presented in FIGS. 6.II-10 to 6.II-13.

RESULTS
OF
PLANE PSEUDO-PLASTIC FLOW
IN A CONVERGING CHANNEL

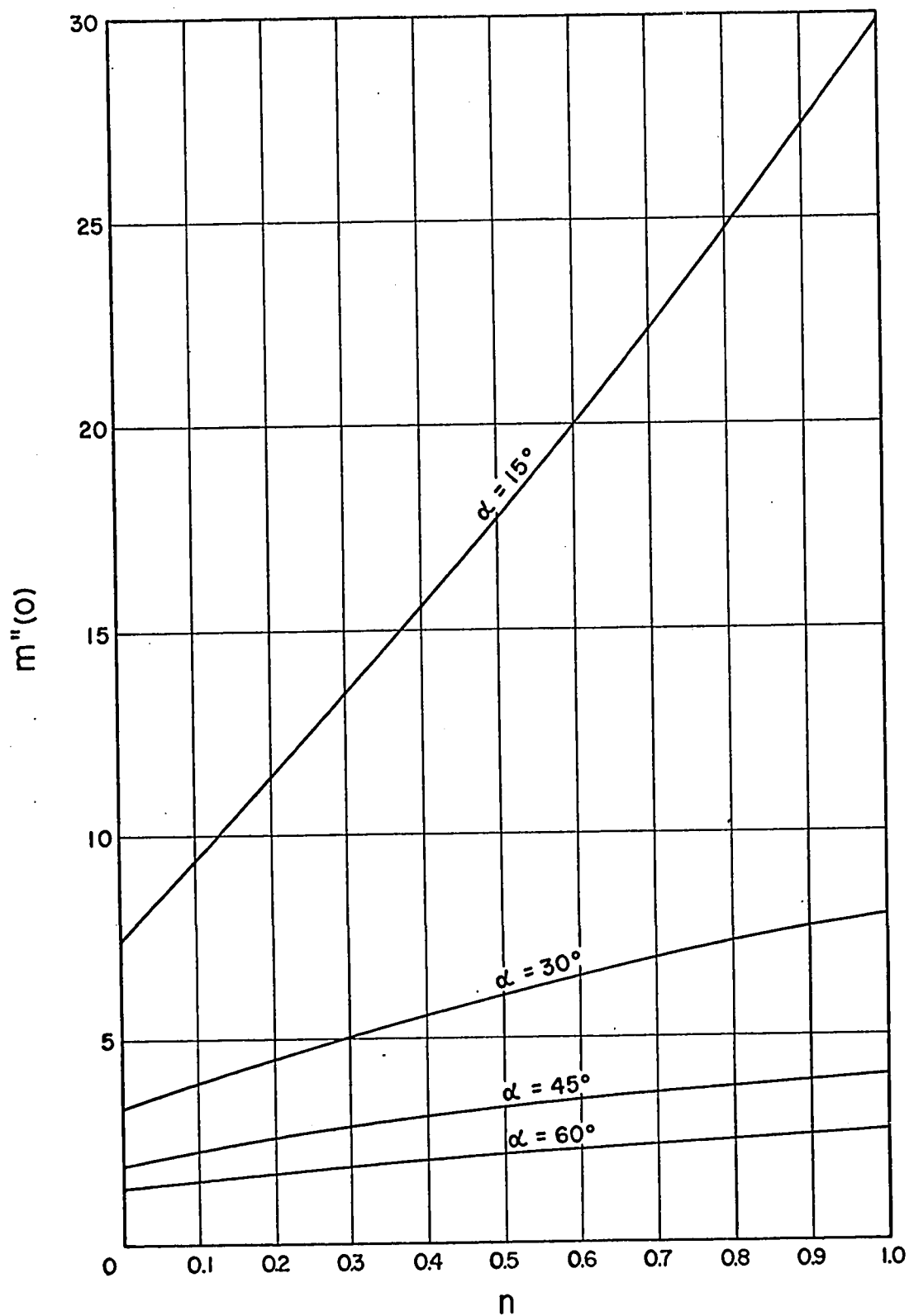


FIGURE 6. II-1
 $m''(0)$ VERSUS n

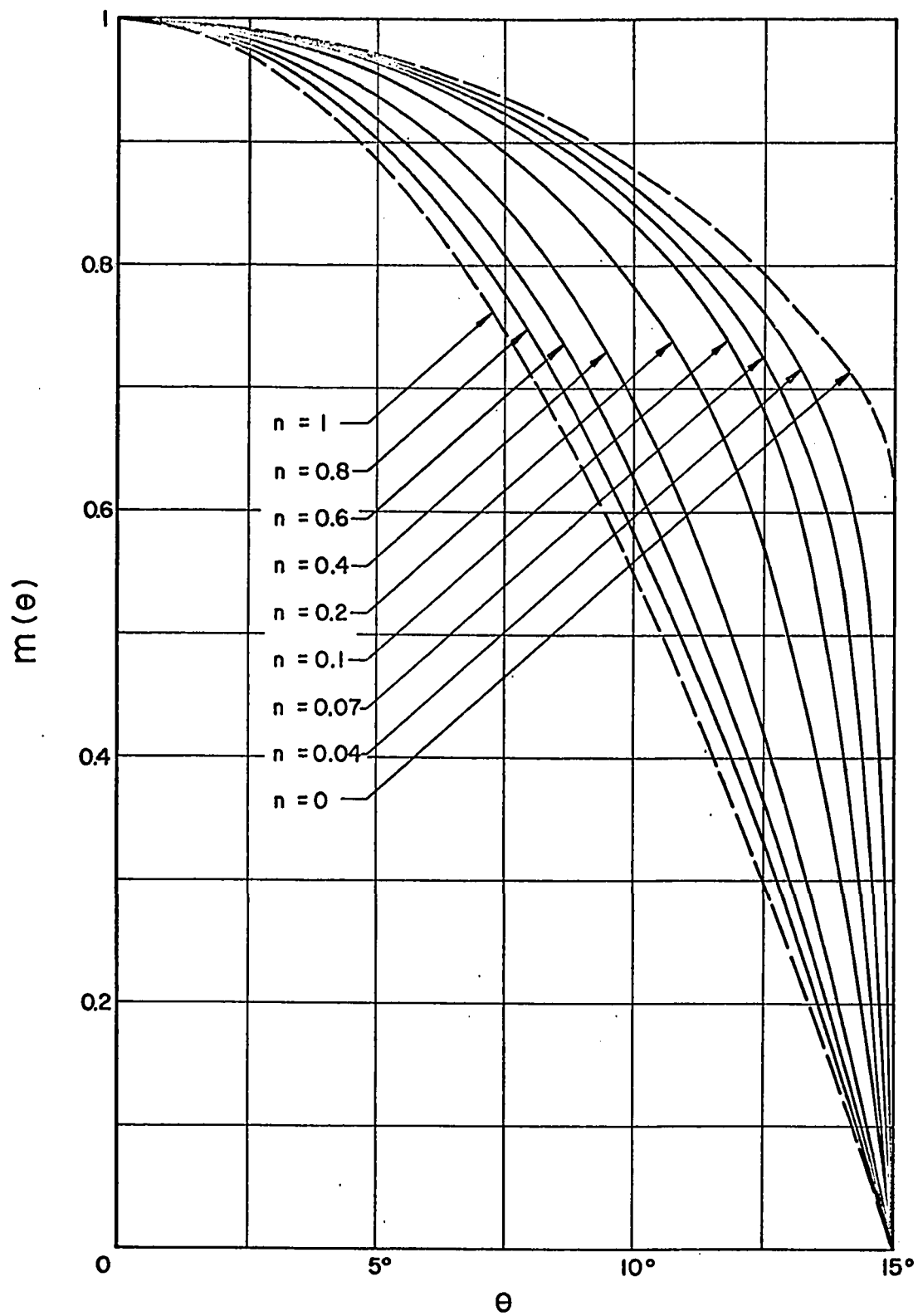


FIGURE 6.II-2

 $m(\theta)$ VERSUS $\theta : \alpha = 15^\circ$

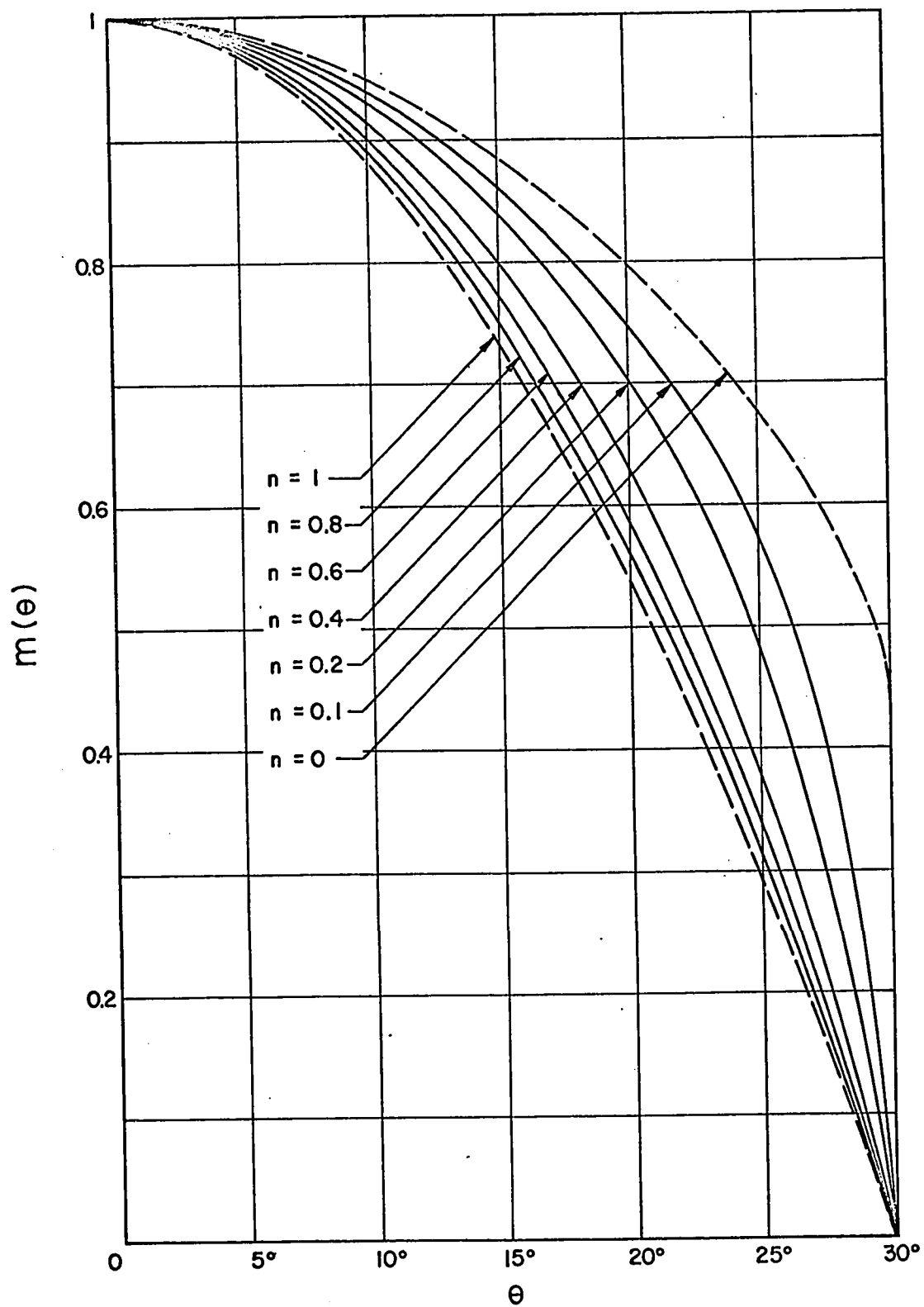


FIGURE 6.II-3
 $m(\theta)$ VERSUS θ : $\alpha = 30^\circ$

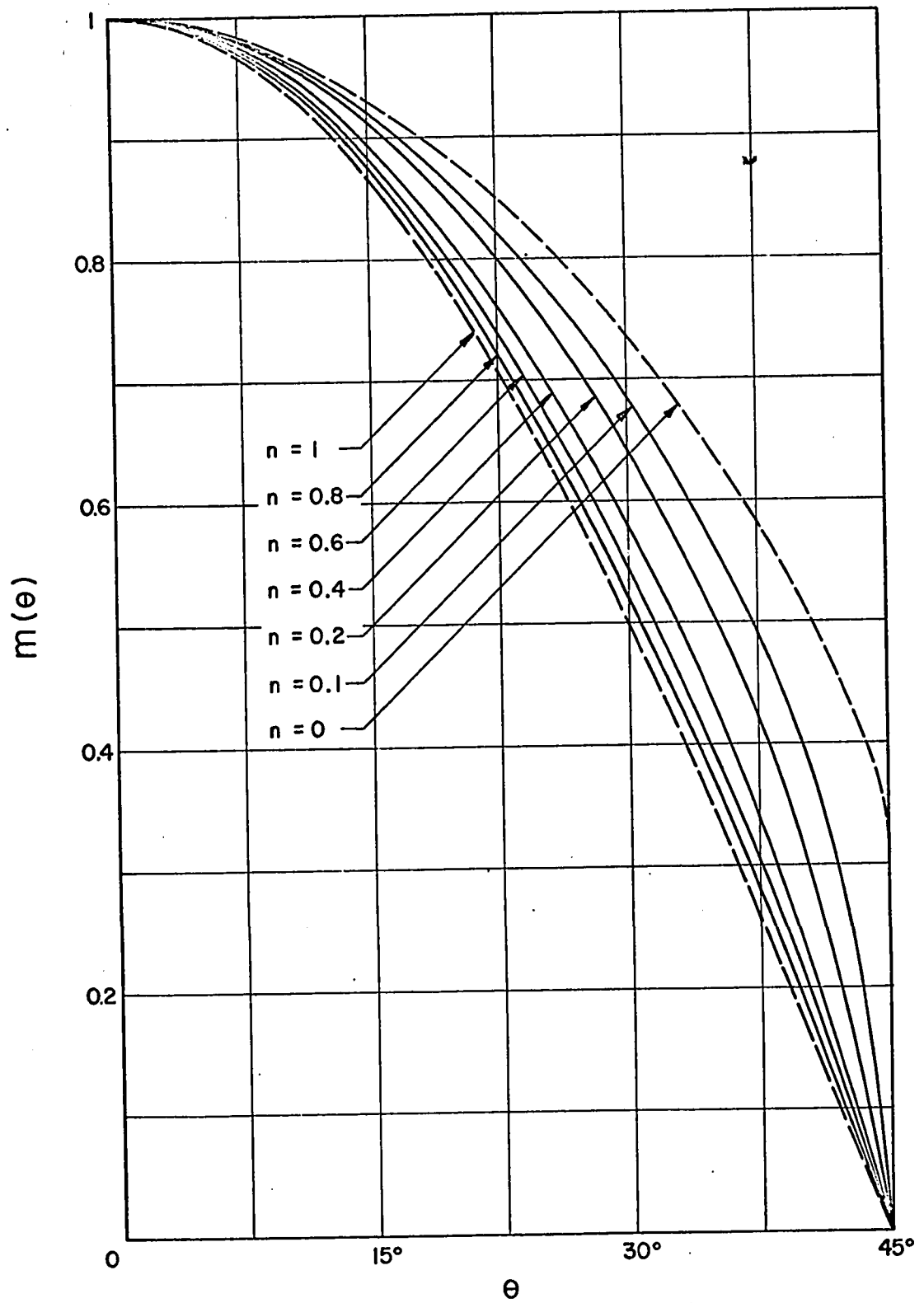


FIGURE 6.II-4

 $m(\theta)$ VERSUS θ : $\alpha = 45^\circ$

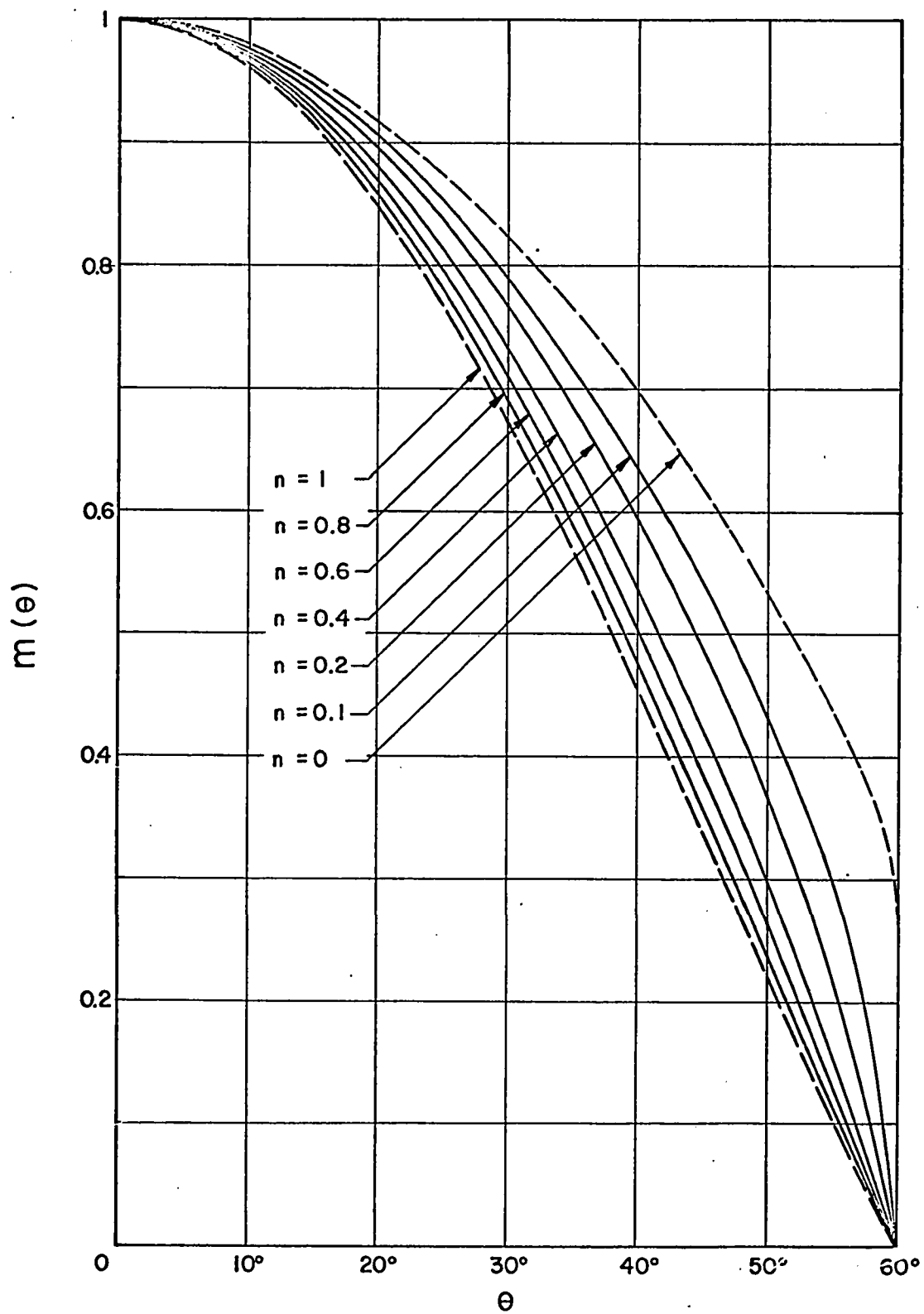


FIGURE 6.II-5

 $m(\theta)$ VERSUS θ : $\alpha = 60^\circ$

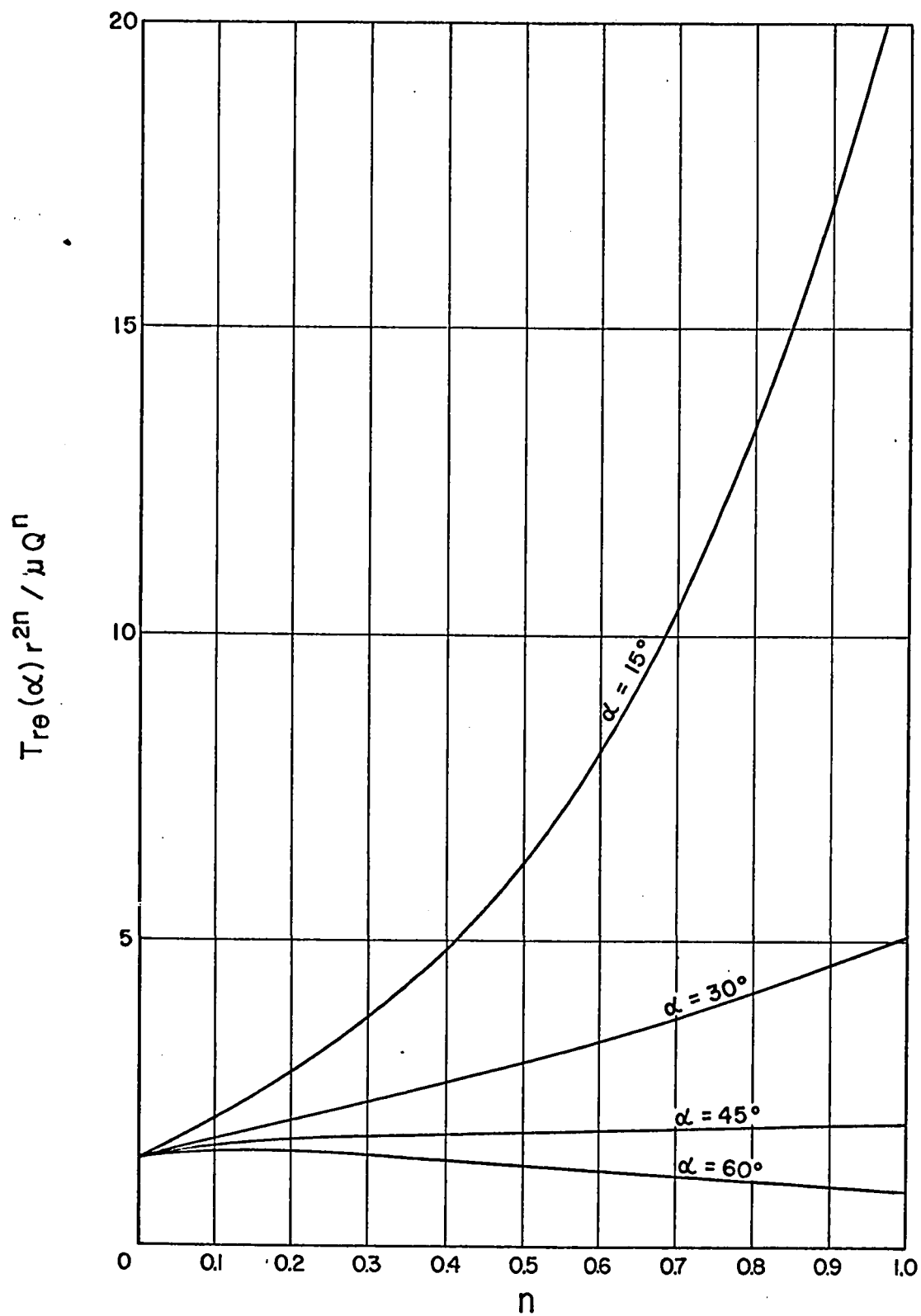


FIGURE 6.II-6
 $T_{re}(\alpha) r^{2n} / \mu Q^n$ VERSUS n

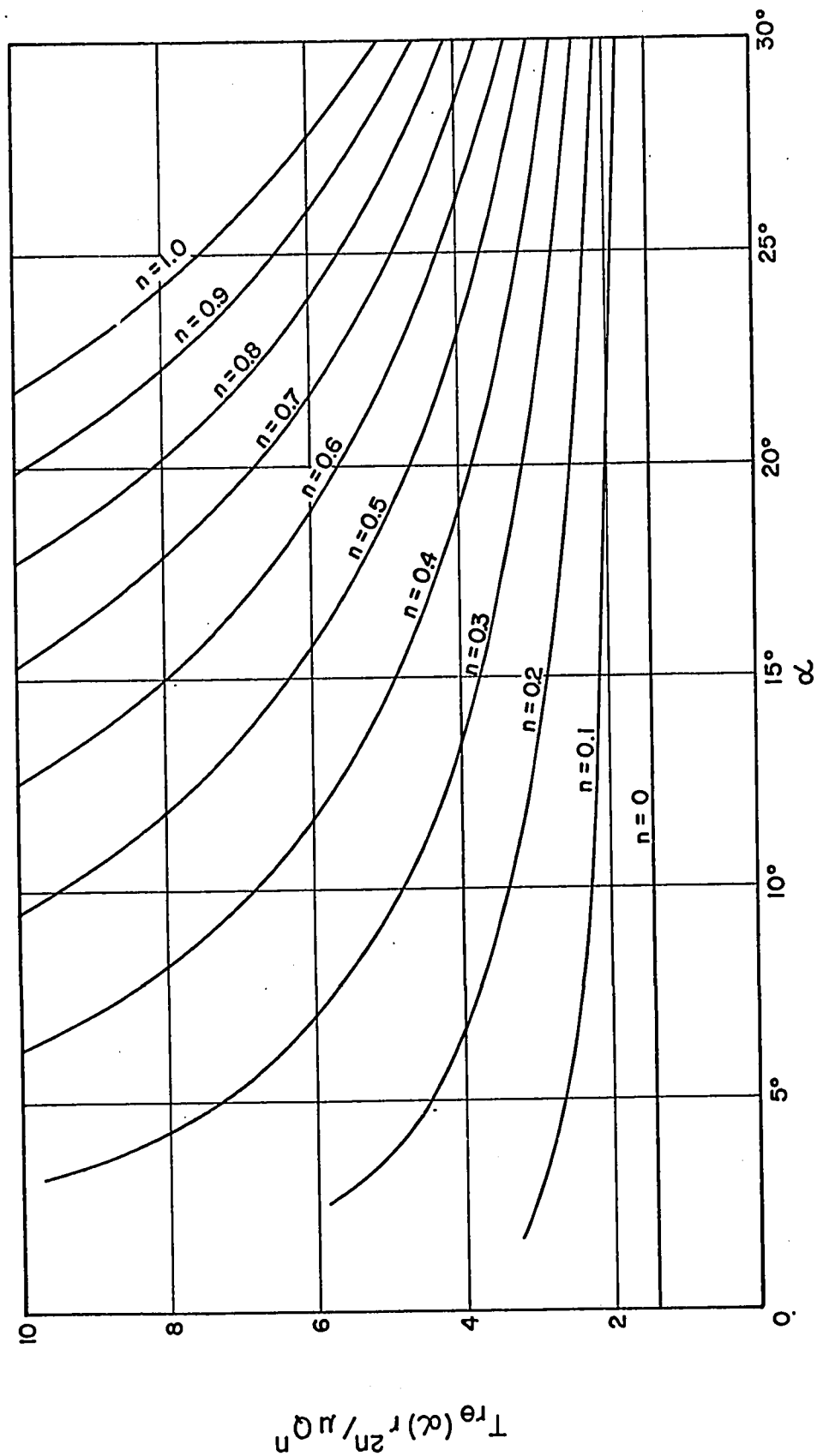


FIGURE 6.II-7
 $T_{re}(\alpha) r^{2n} / \mu Q^n$ VERSUS α

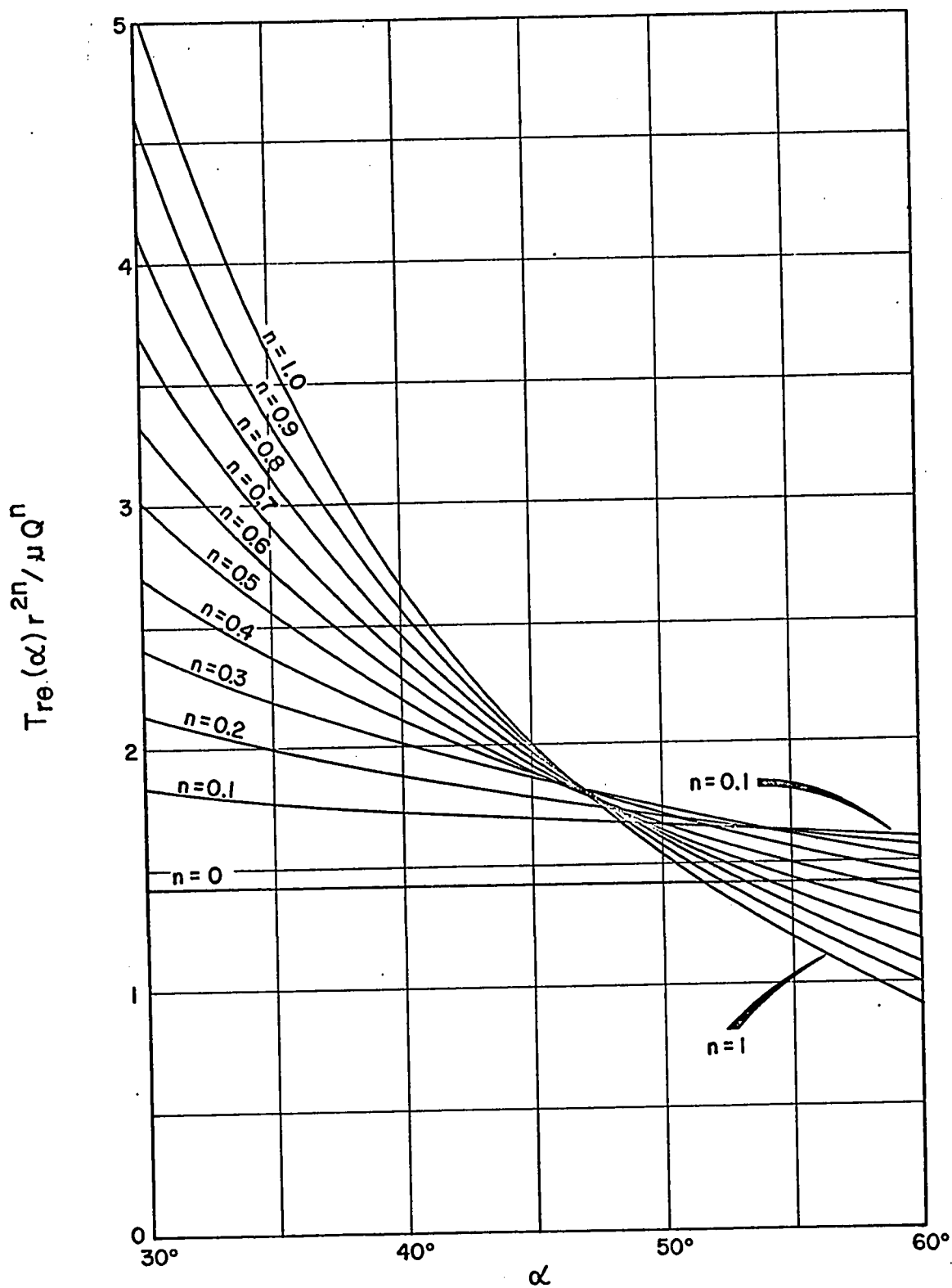


FIGURE 6.II-8
 $T_{re}(\alpha) r^{2n} / \mu Q^n$ VERSUS α

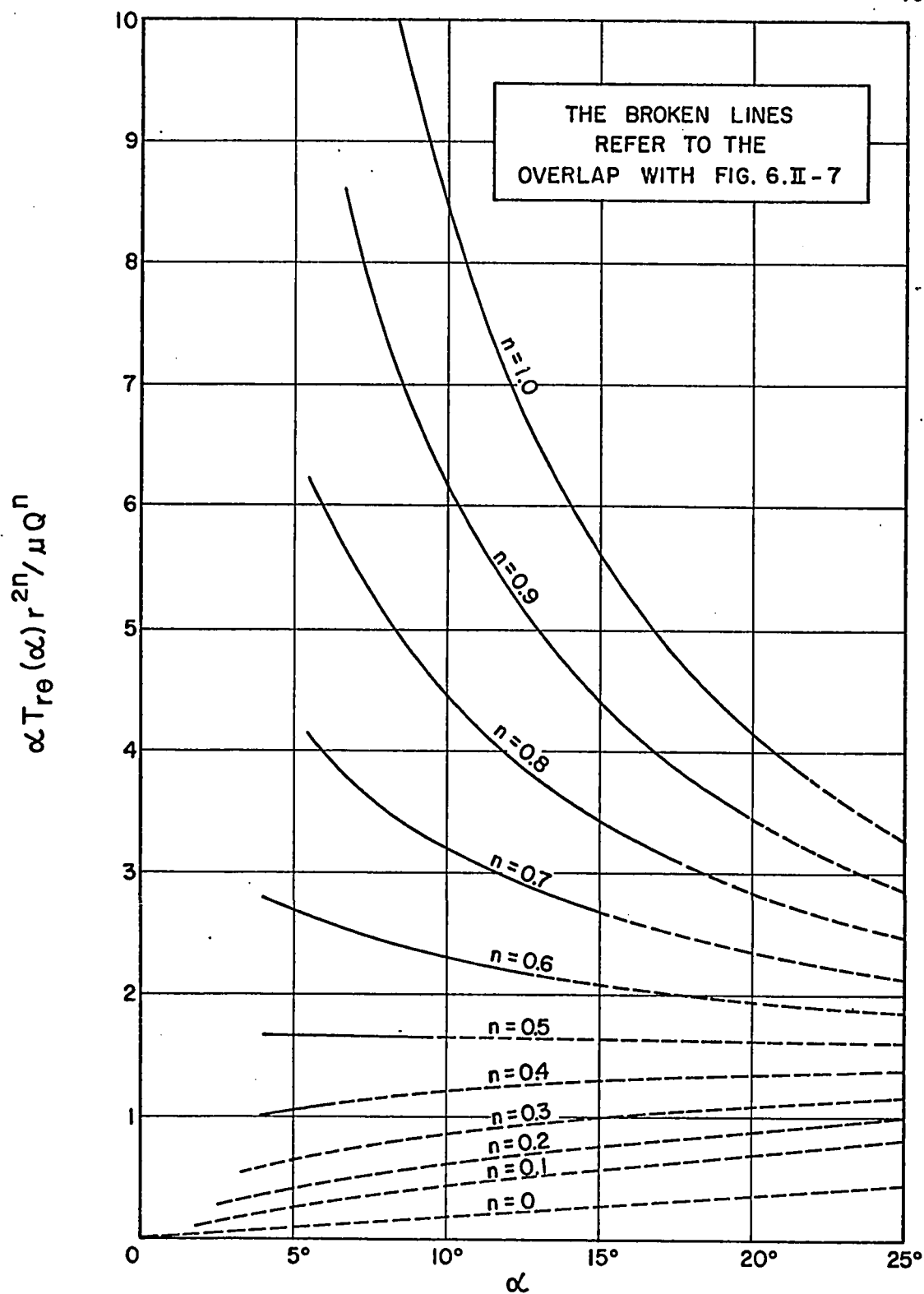


FIGURE 6.II-9

 $\alpha T_{re}(\alpha) r^{2n} / \mu Q^n$ VERSUS α

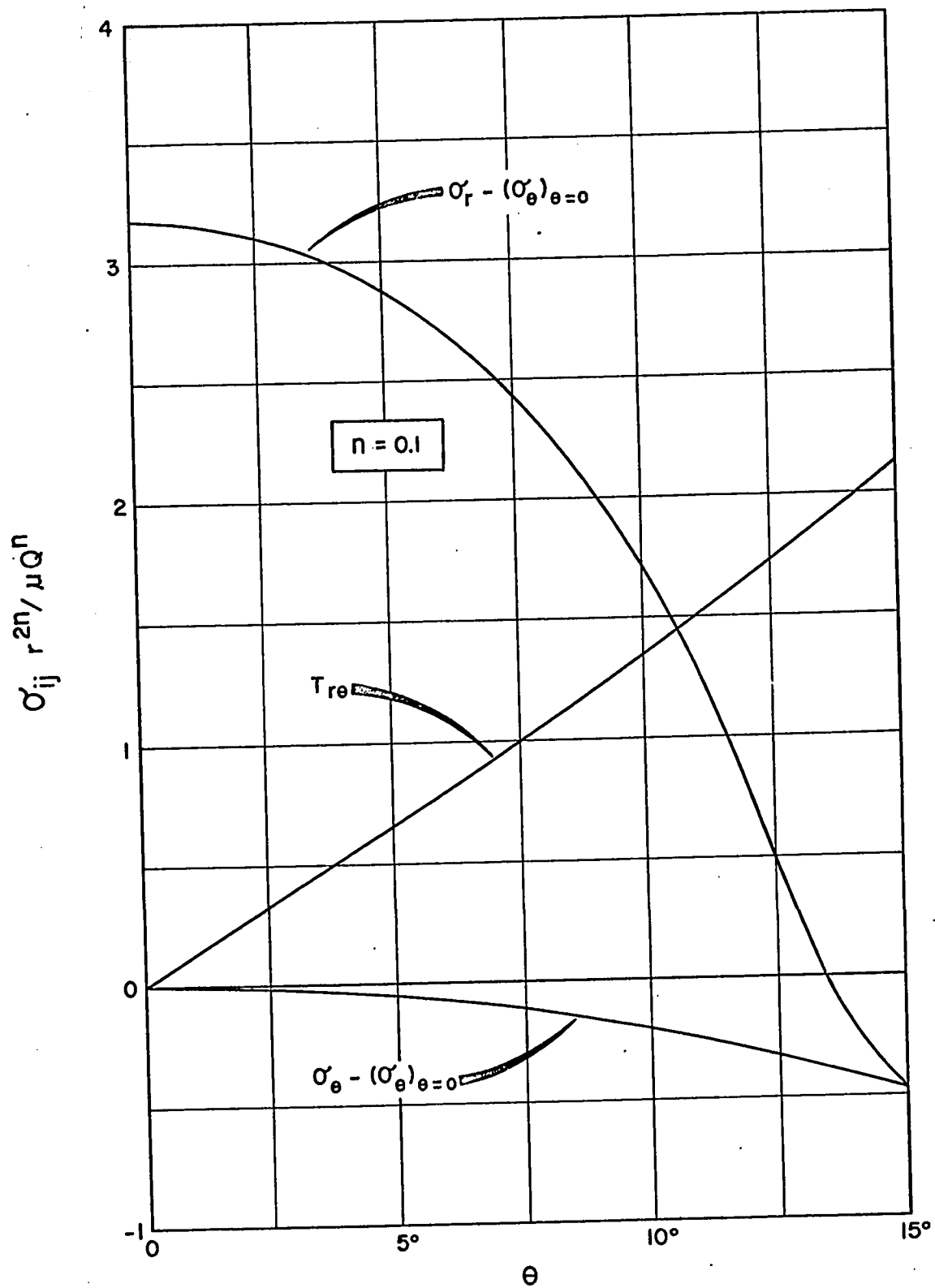


FIGURE 6.II-10
 $\sigma_{ij} r^{2n} / \mu Q^n$ VERSUS θ : $\alpha = 15^\circ$

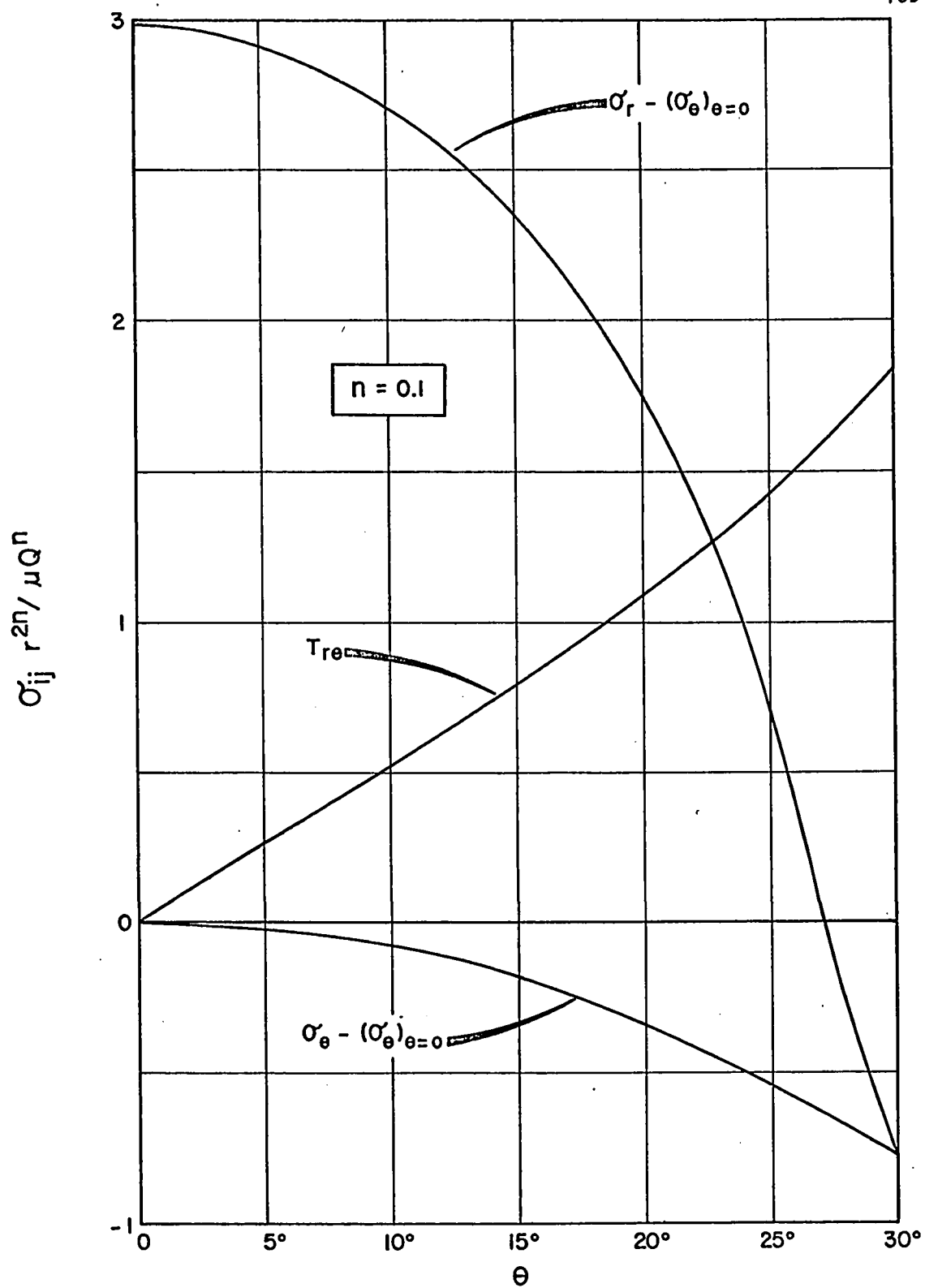


FIGURE 6.II-II

$\sigma_{ij} r^{2n} / \mu Q^n$ VERSUS θ : $\alpha = 30^\circ$

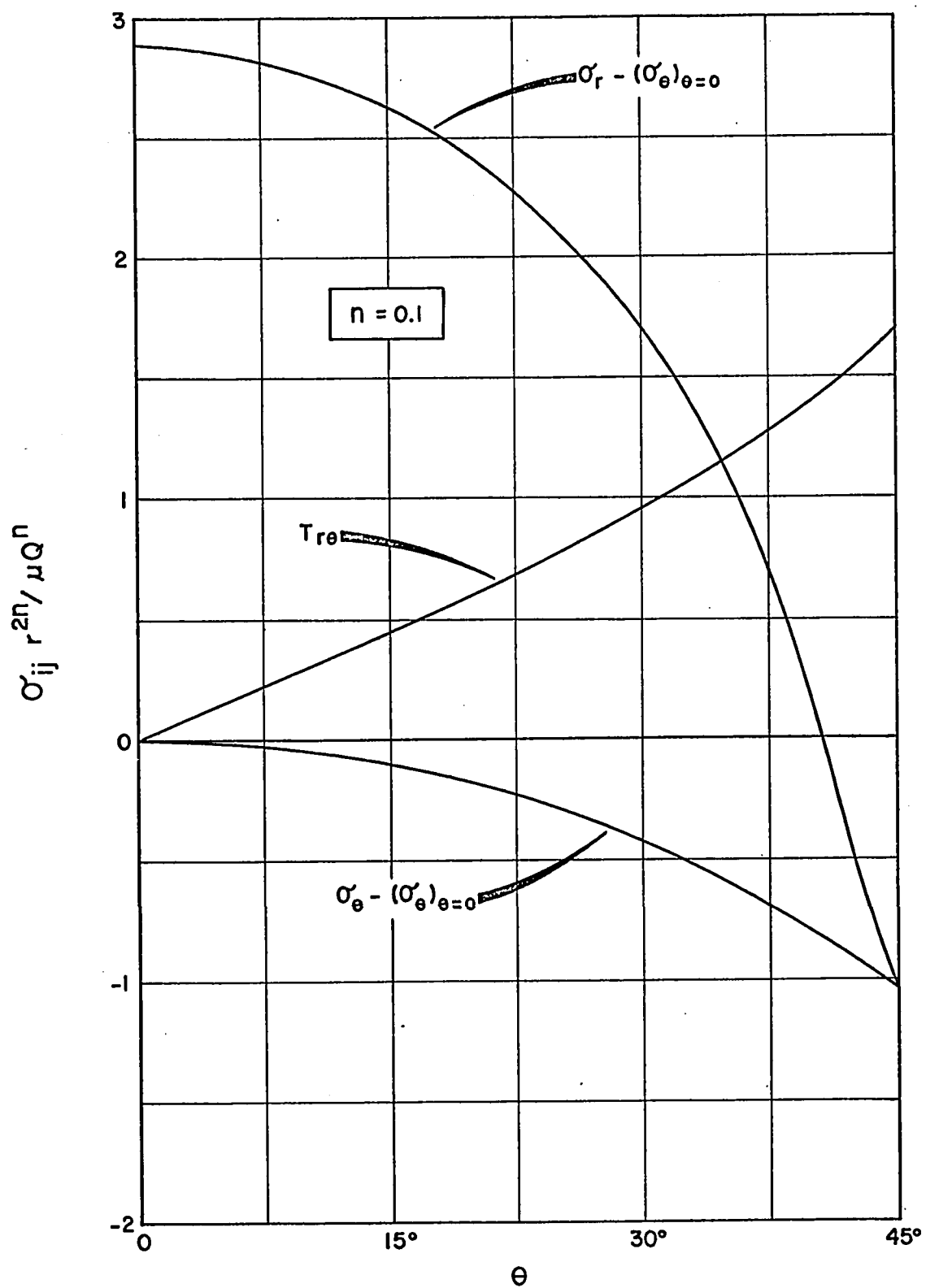


FIGURE 6.II-12

$\sigma_{ij} r^{2n} / \mu Q^n$ VERSUS θ : $\alpha = 45^\circ$

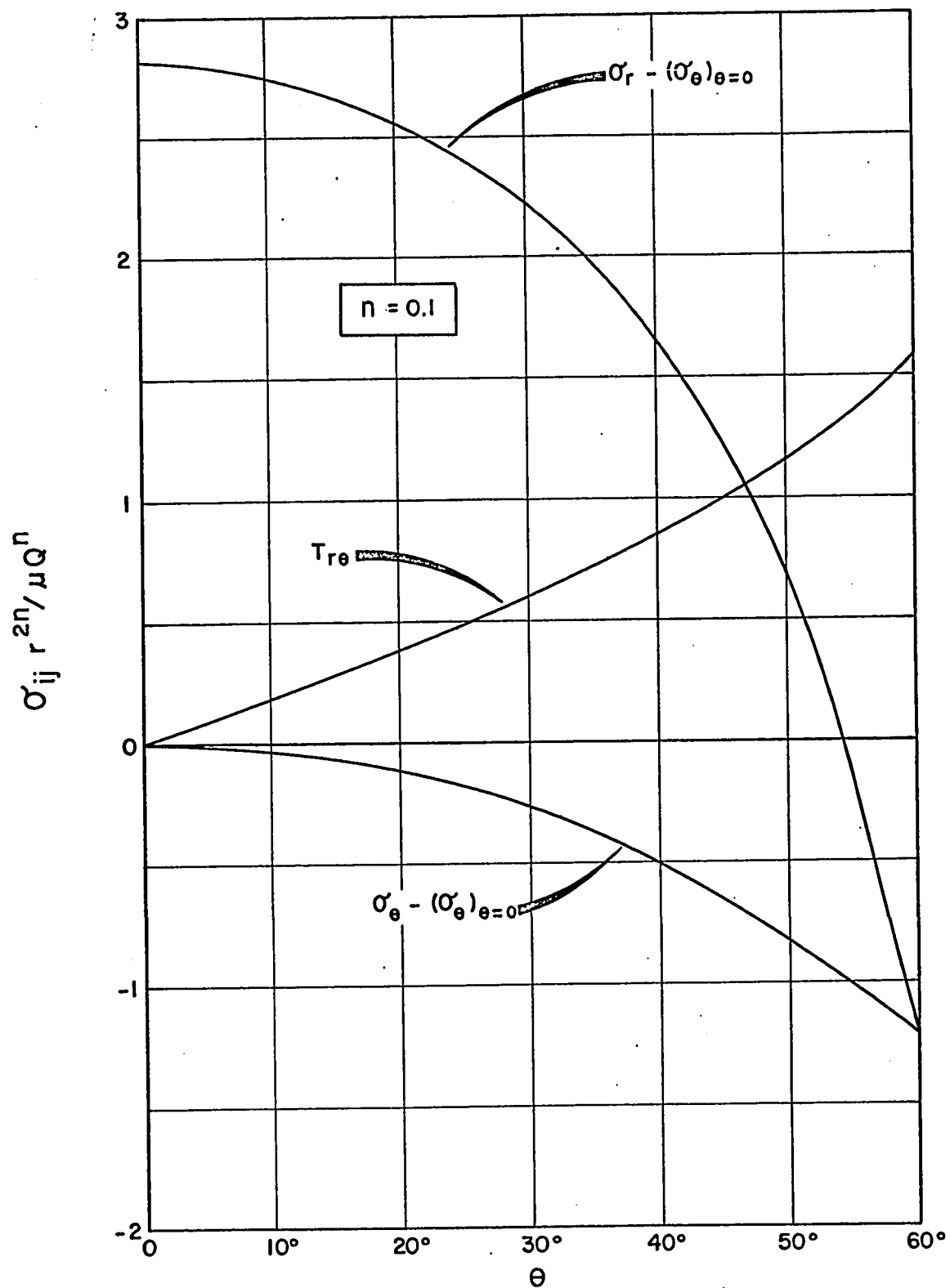


FIGURE 6.II-13

 $\sigma_{ij} r^{2n} / \mu Q^n$ VERSUS θ : $\alpha = 60^\circ$

RESULTS
OF
AXIALLY SYMMETRIC PSEUDO-PLASTIC FLOW
IN A CIRCULAR CONE

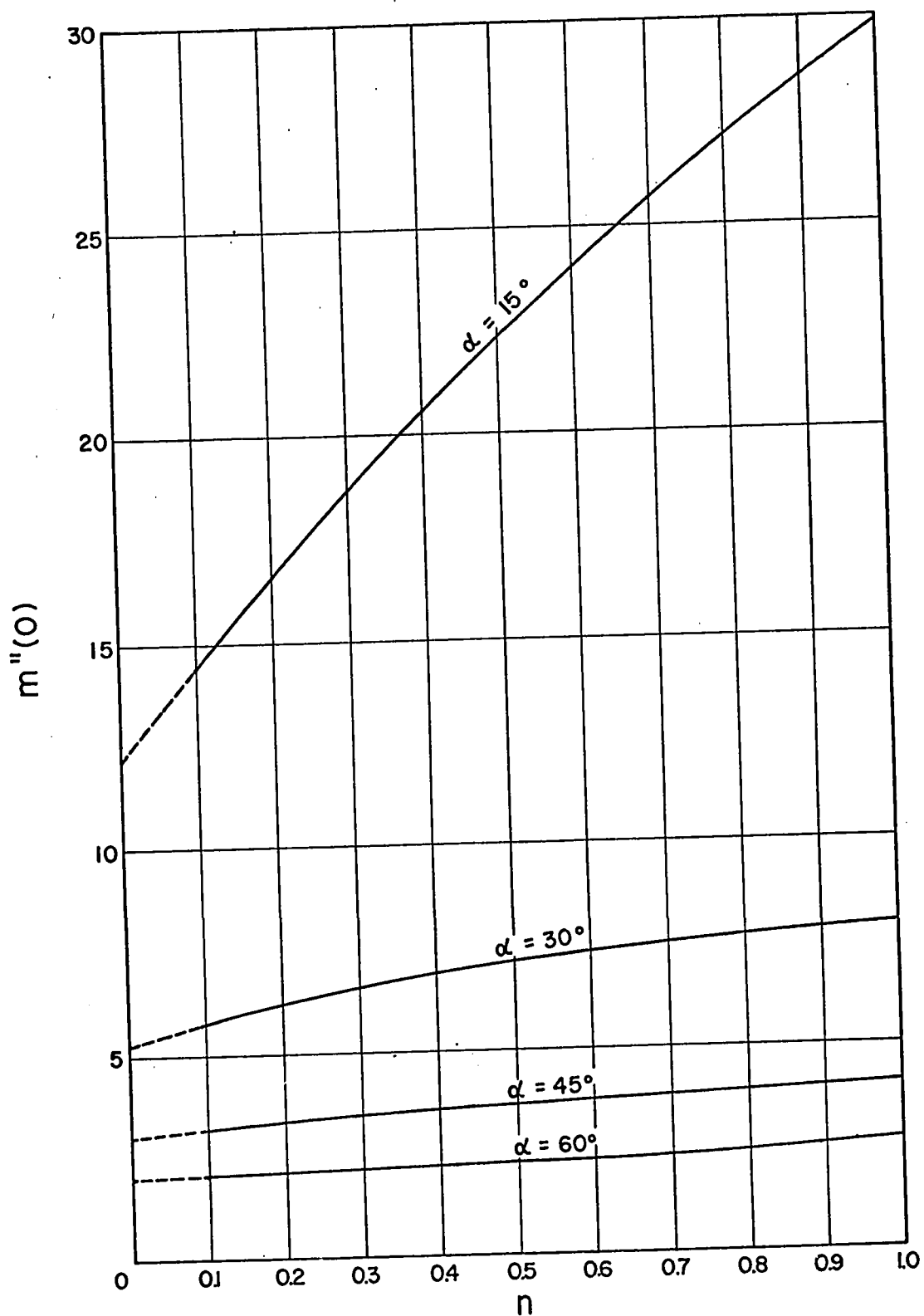


FIGURE 6. III-1
 $m''(0)$ VERSUS n

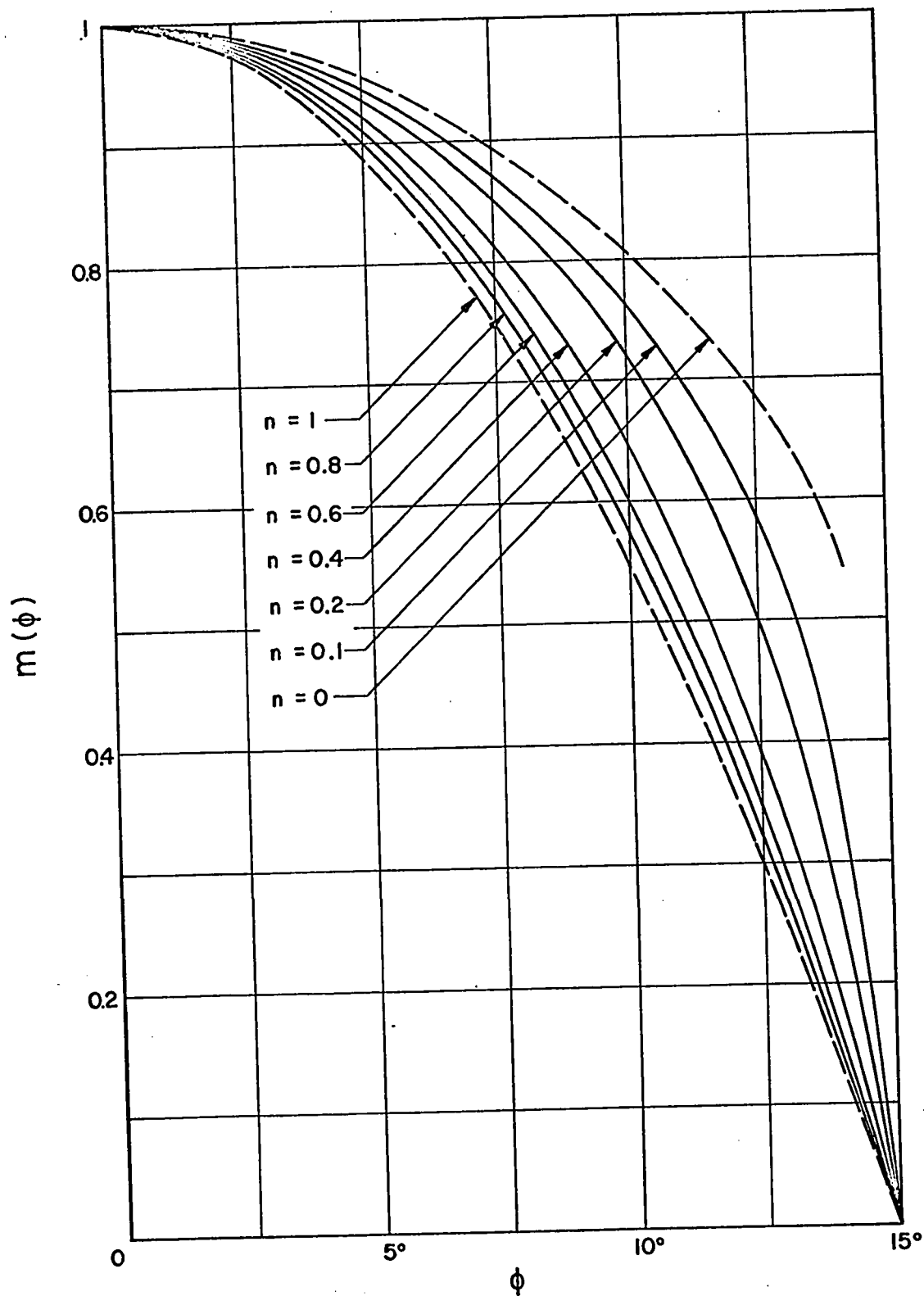


FIGURE 6.III-2

$m(\phi)$ VERSUS $\phi : \alpha = 15^\circ$

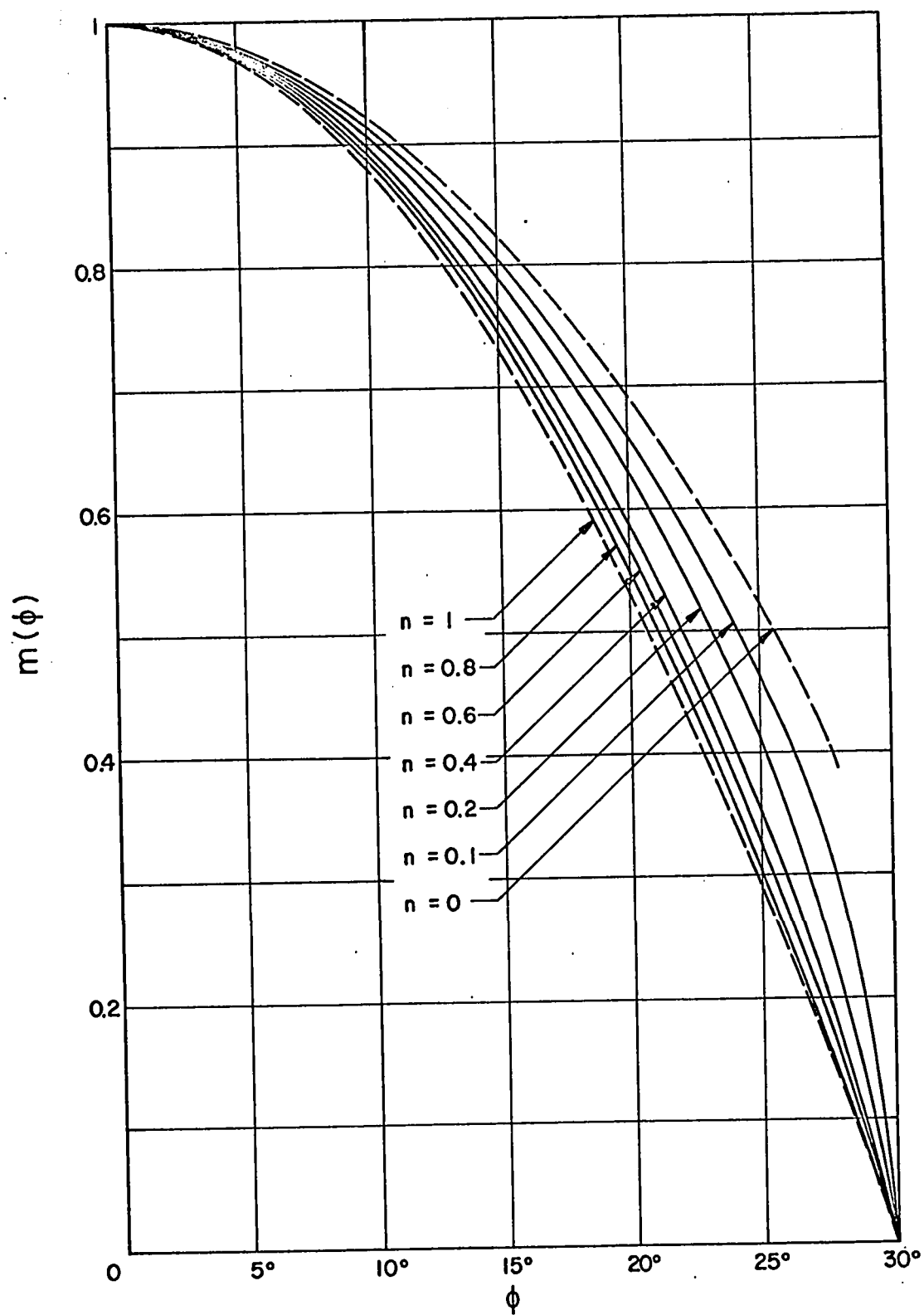


FIGURE 6.III-3

$m(\phi)$ VERSUS ϕ : $\alpha = 30^\circ$

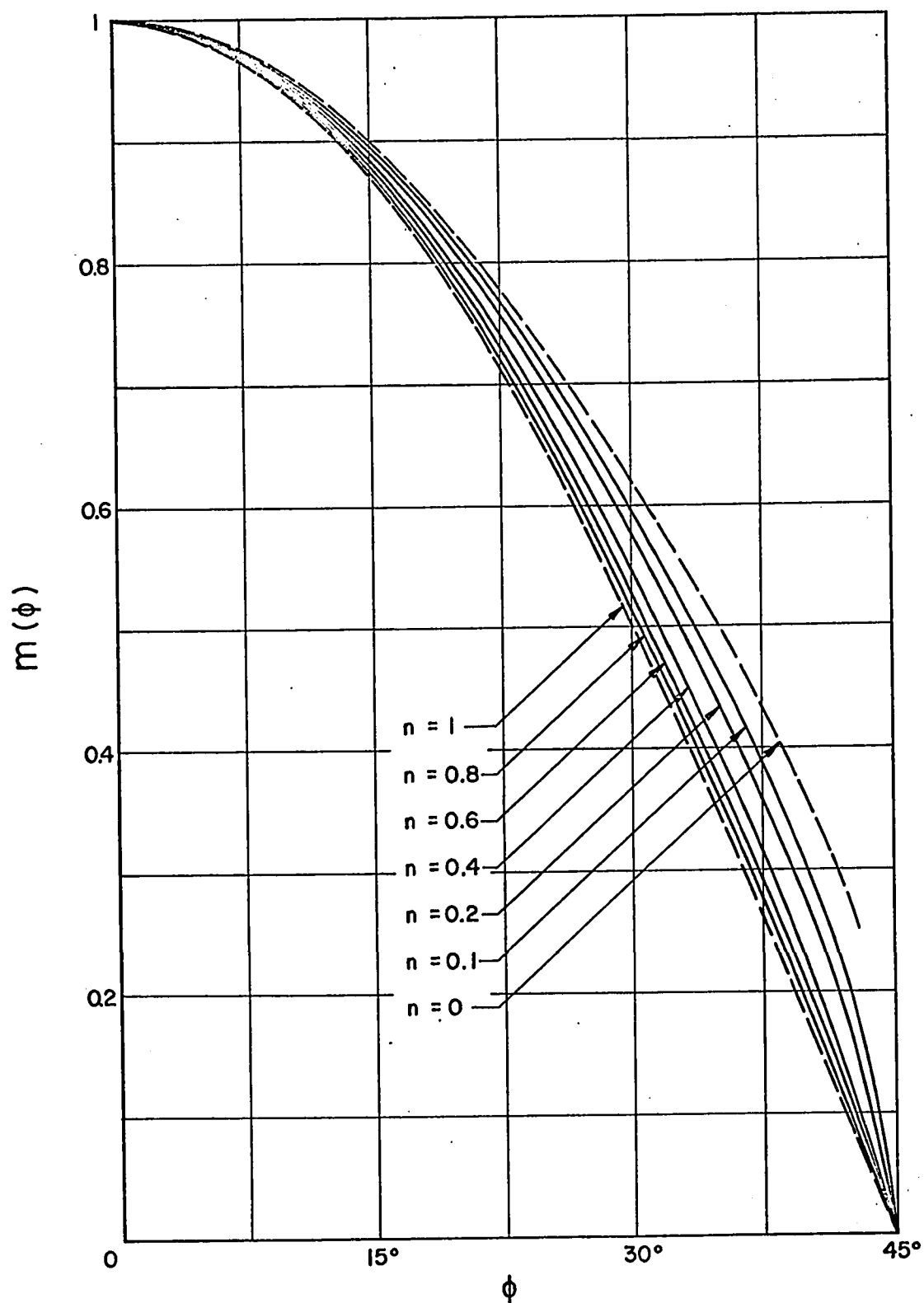


FIGURE 6.III-4

 $m(\phi)$ VERSUS ϕ : $\alpha = 45^\circ$

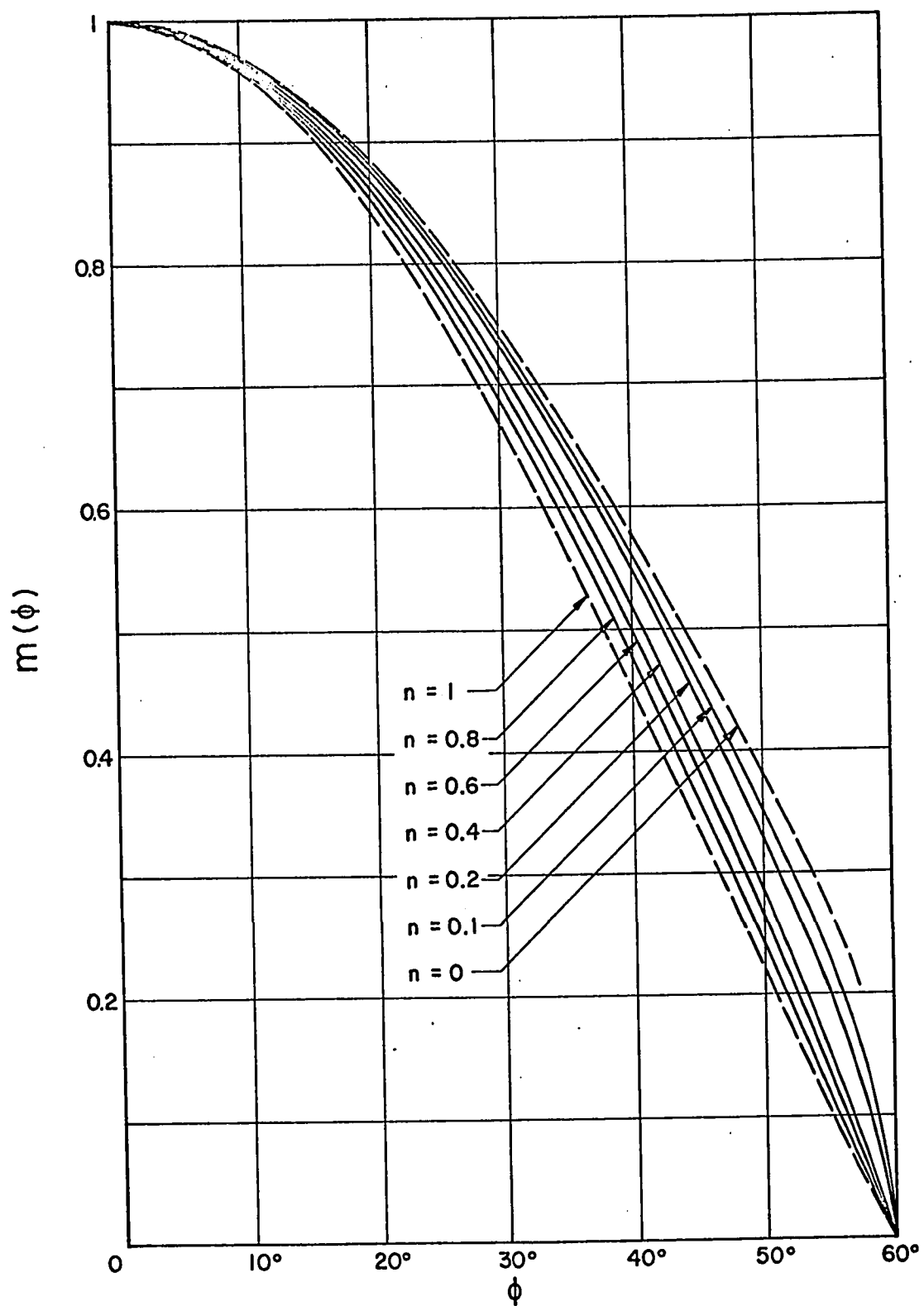


FIGURE 6.III-5

 $m(\phi)$ VERSUS ϕ : $\alpha = 60^\circ$

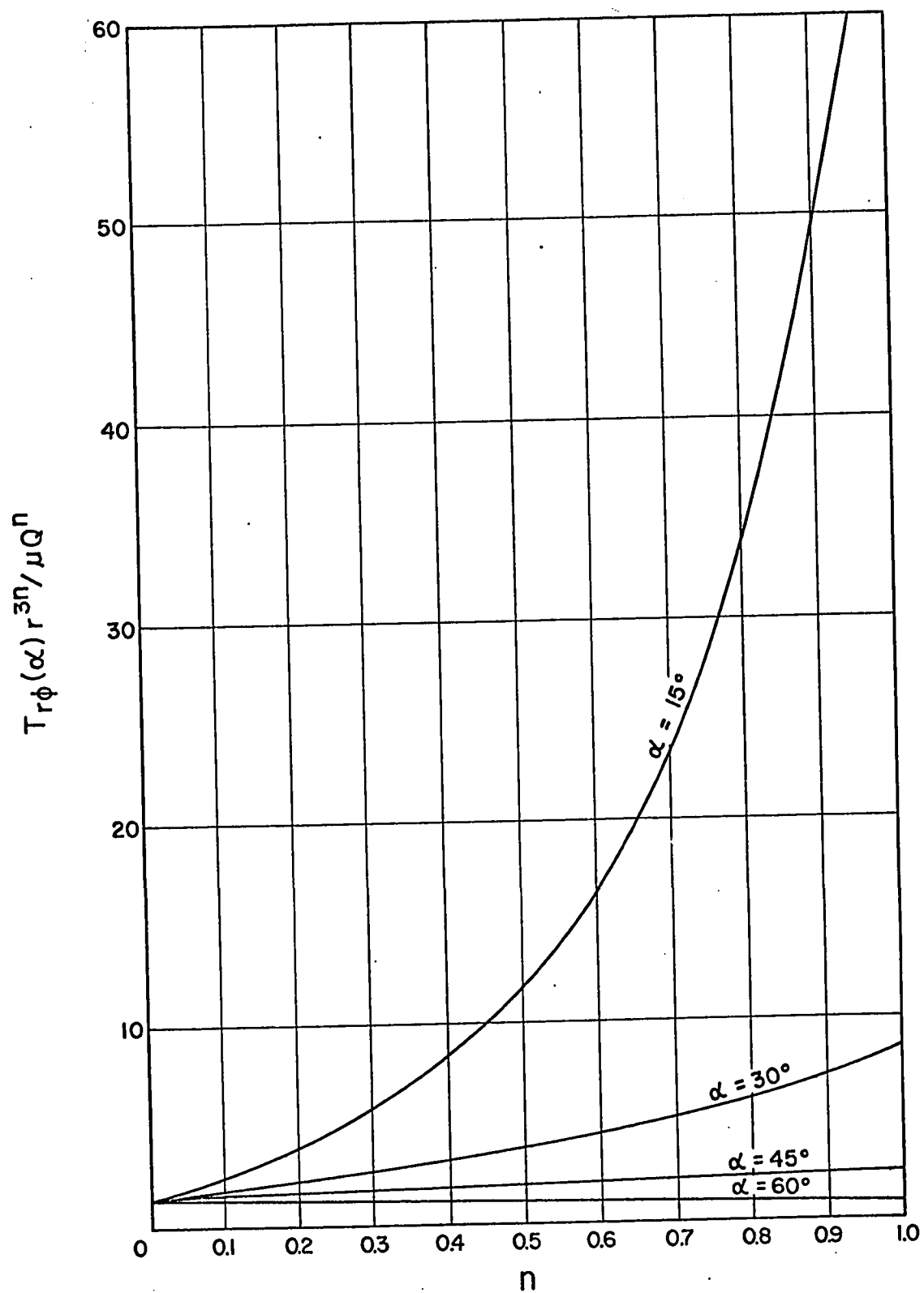


FIGURE 6.III-6

 $T_{r\phi}(\alpha) r^{3n} / \mu Q^n$ VERSUS n

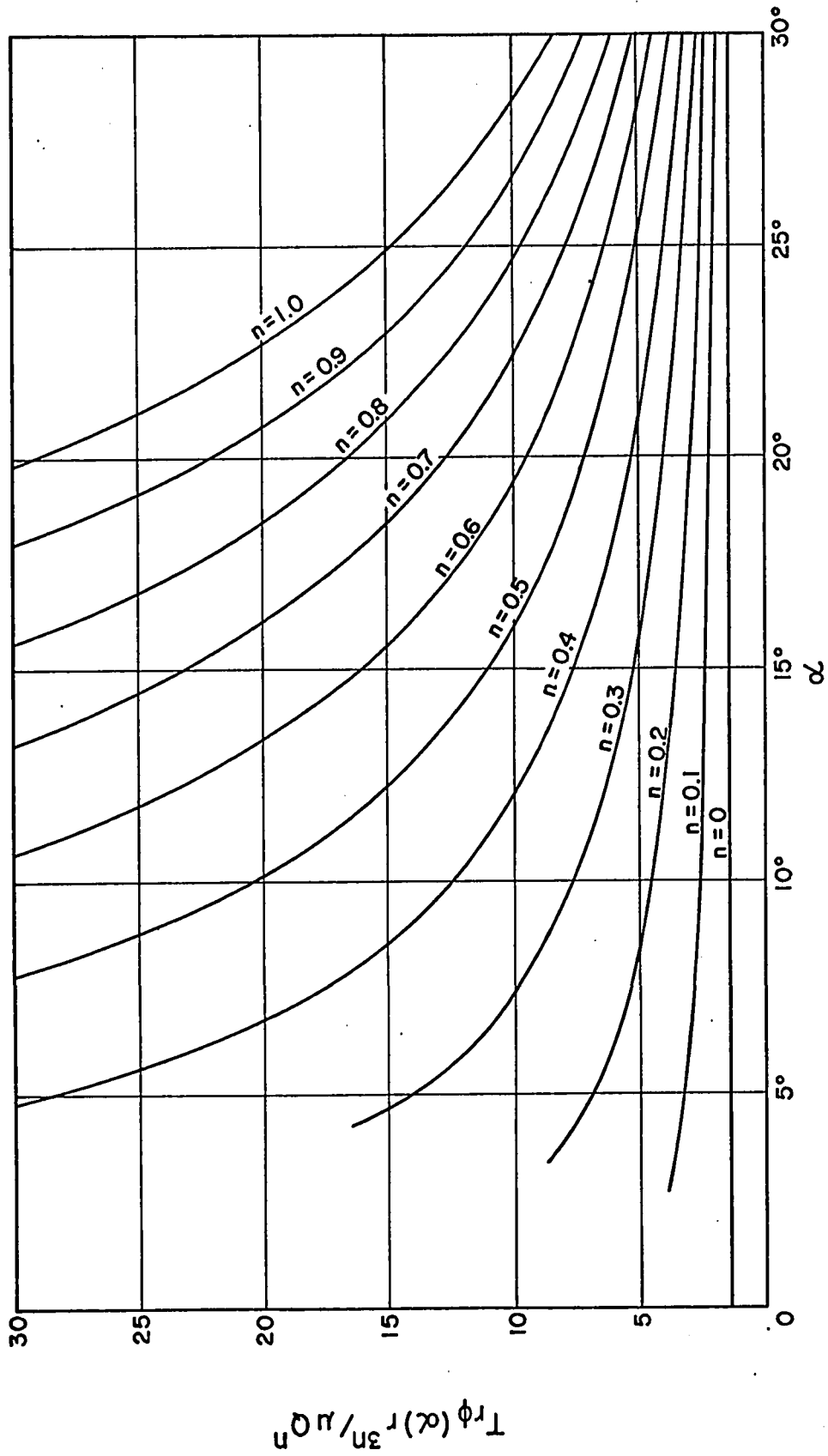


FIGURE 6.Ⅲ-7
 $Tr\phi(\alpha) r^{3n} / \mu Q^n$ VERSUS α

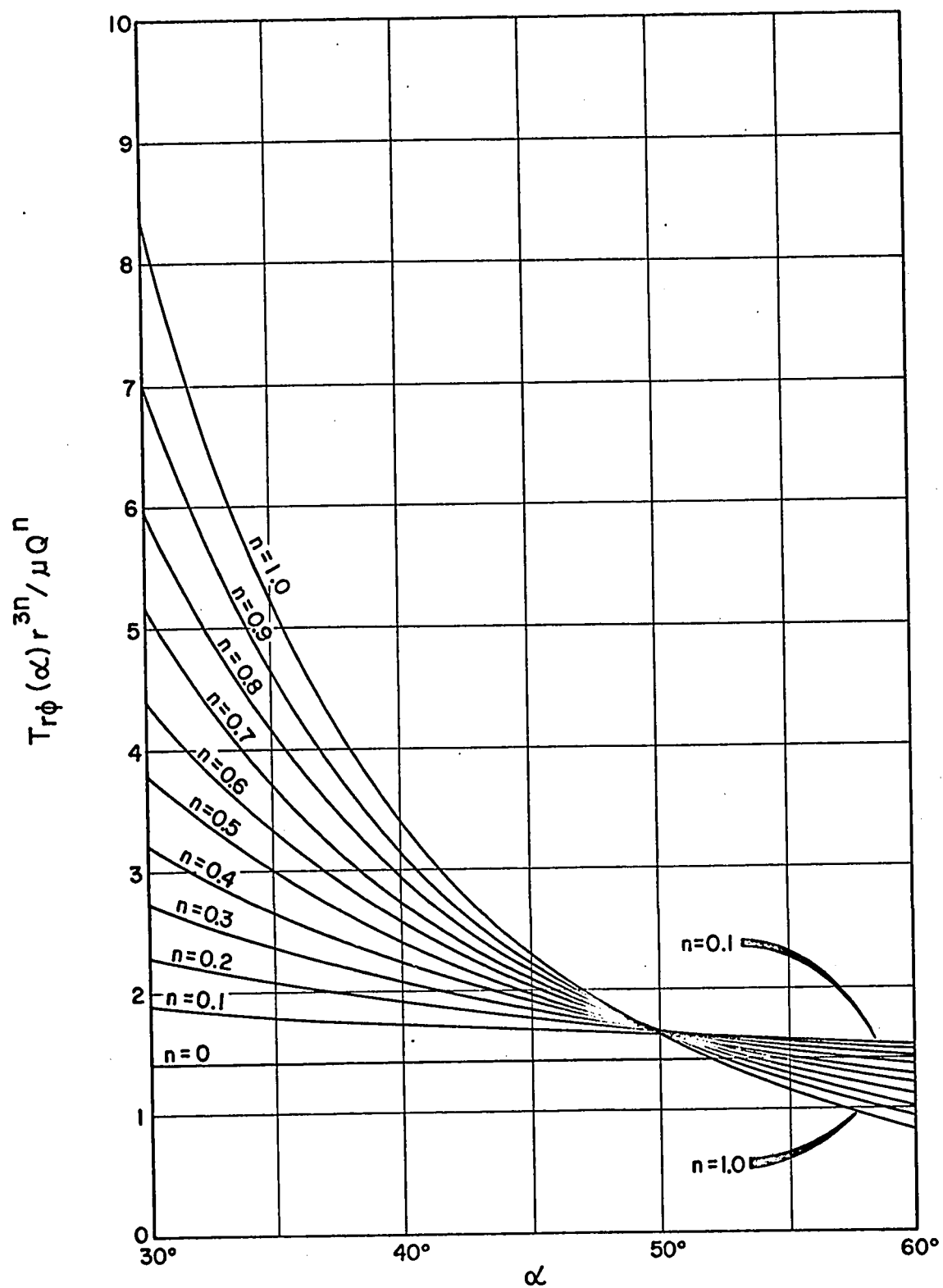


FIGURE 6. III-8
 $\text{Tr}\phi(\alpha) r^{3n} / \mu Q^n$ VERSUS α

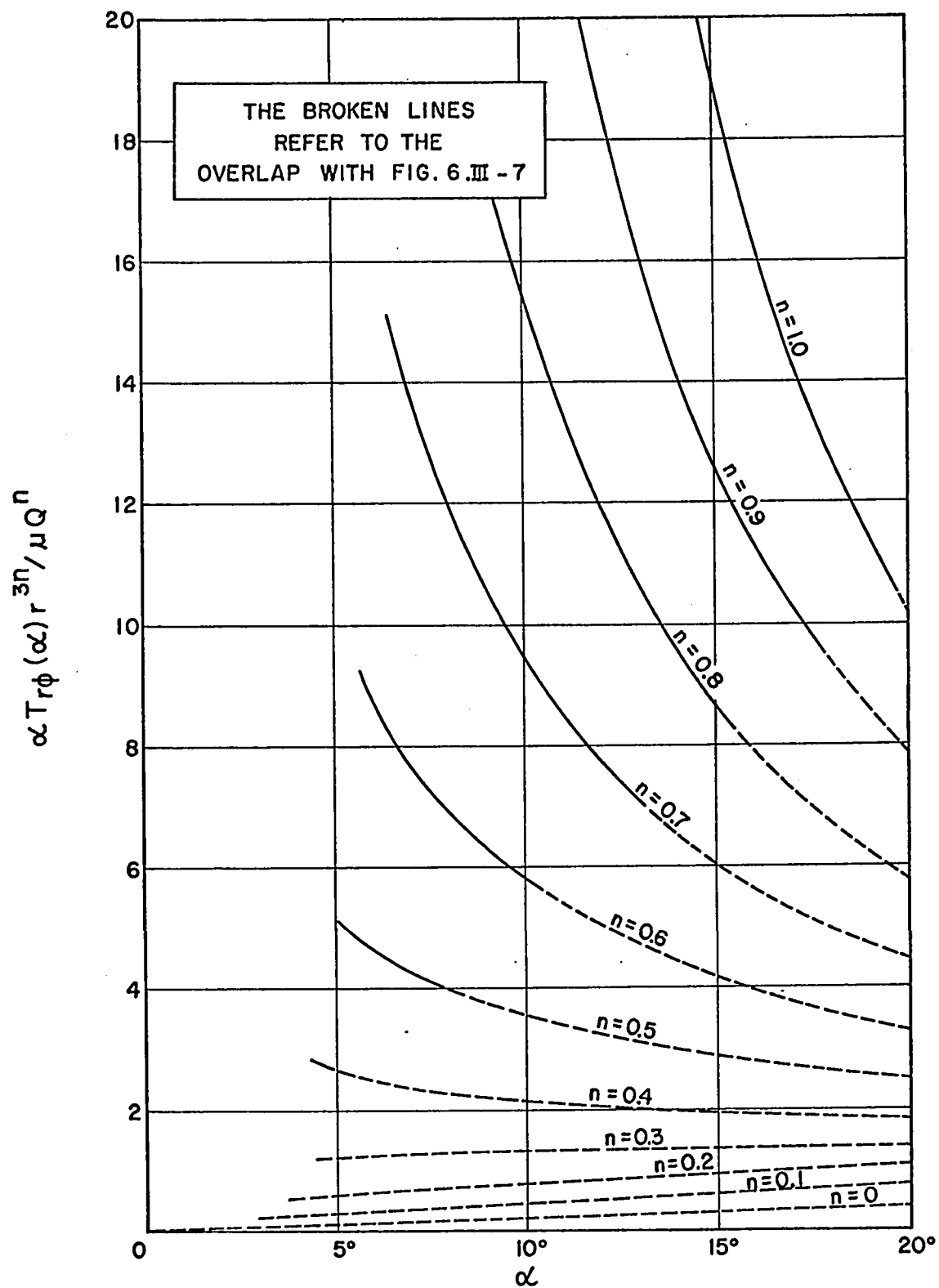


FIGURE 6.III-9

$\alpha T_{r\phi}(\alpha) r^{3n} / \mu Q^n$ VERSUS α

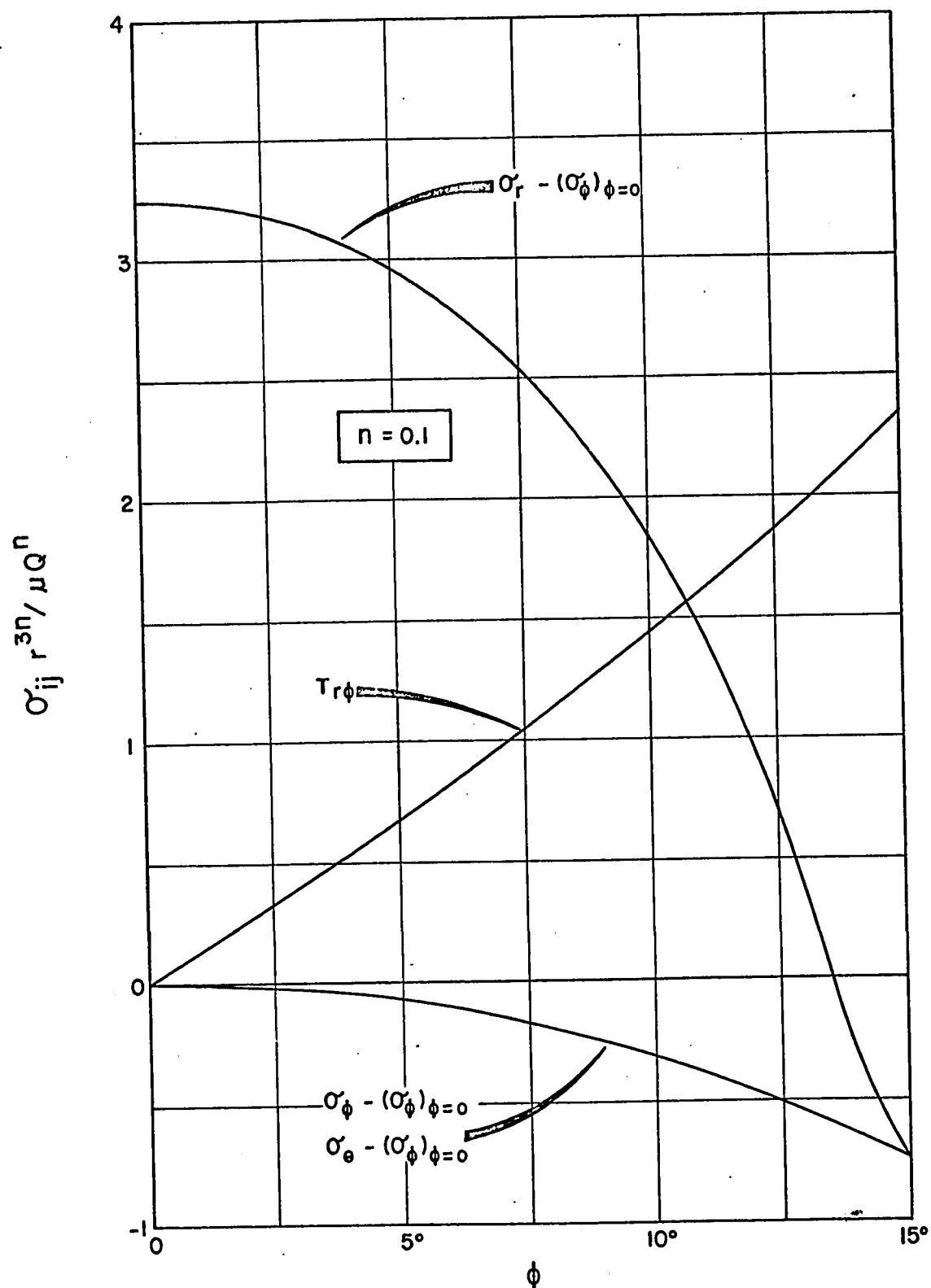


FIGURE 6.III-10

$\sigma_{ij} r^{3n} / \mu Q^n$ VERSUS $\phi : \alpha = 15^\circ$

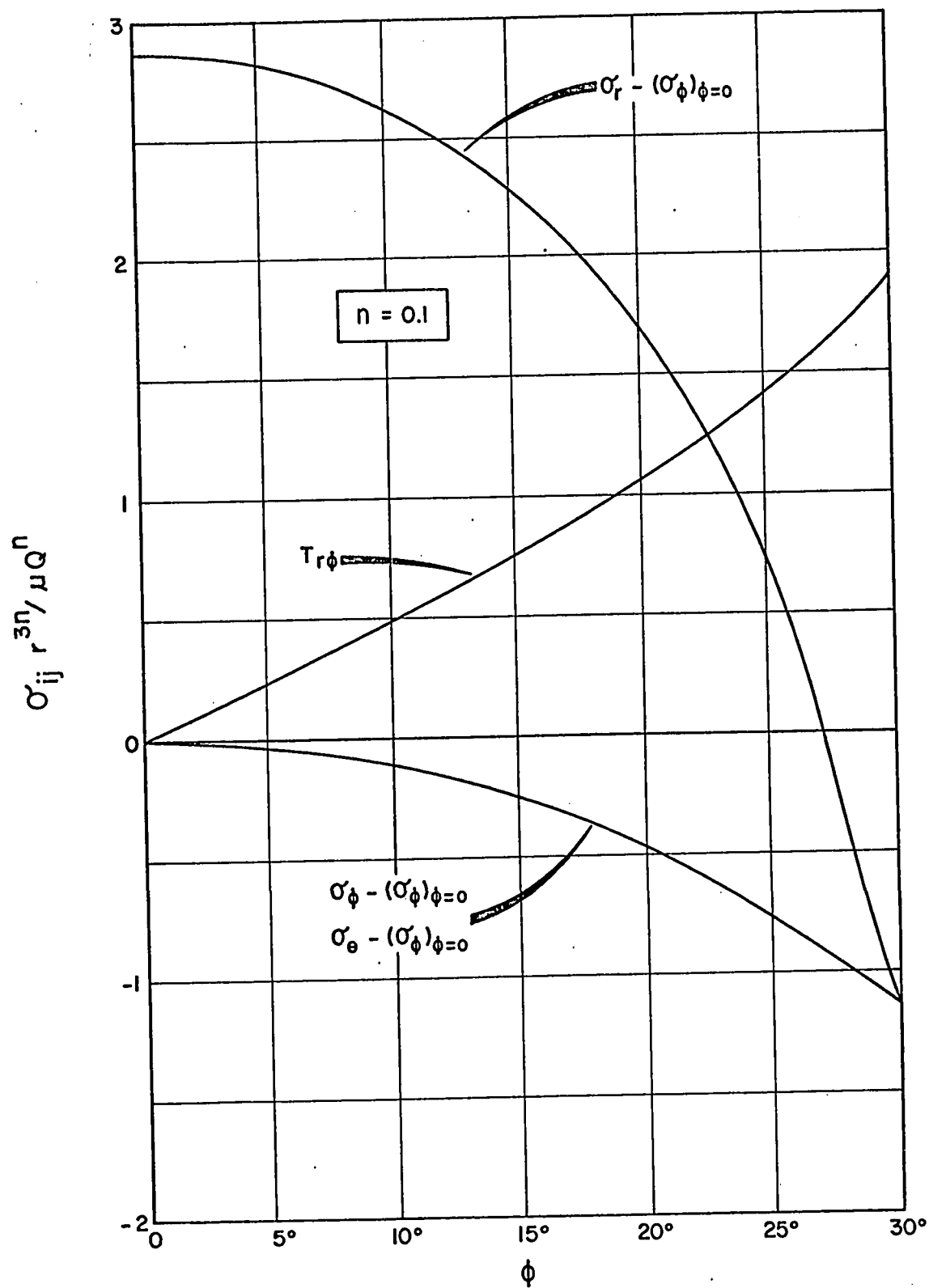


FIGURE 6.III-11

$$\sigma'_{ij} r^{3n} / \mu Q^n \text{ VERSUS } \phi : \alpha = 30^\circ$$

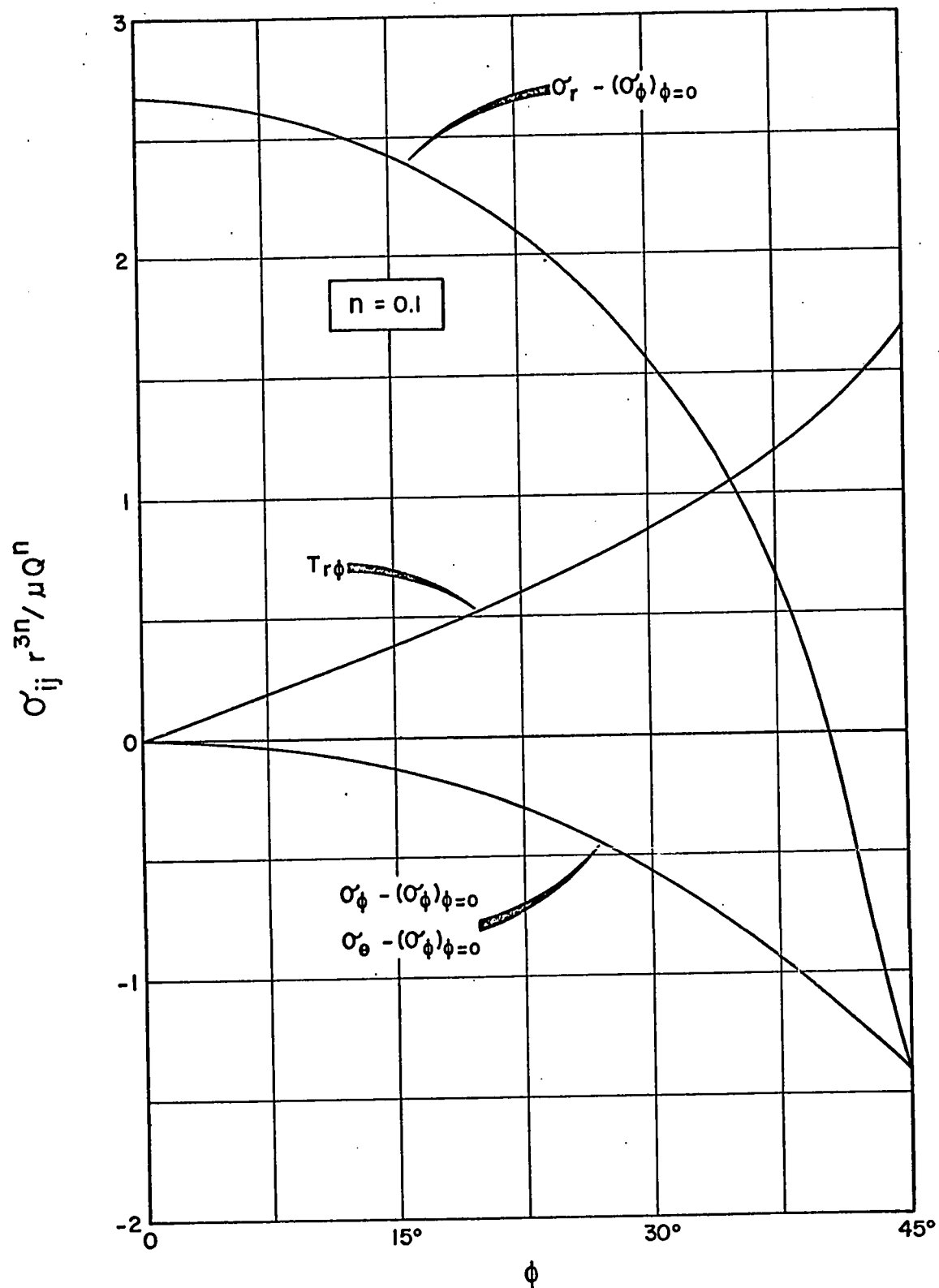


FIGURE 6.III-12

$\sigma'_{ij} r^{3n} / \mu Q^n$ VERSUS ϕ : $\alpha = 45^\circ$

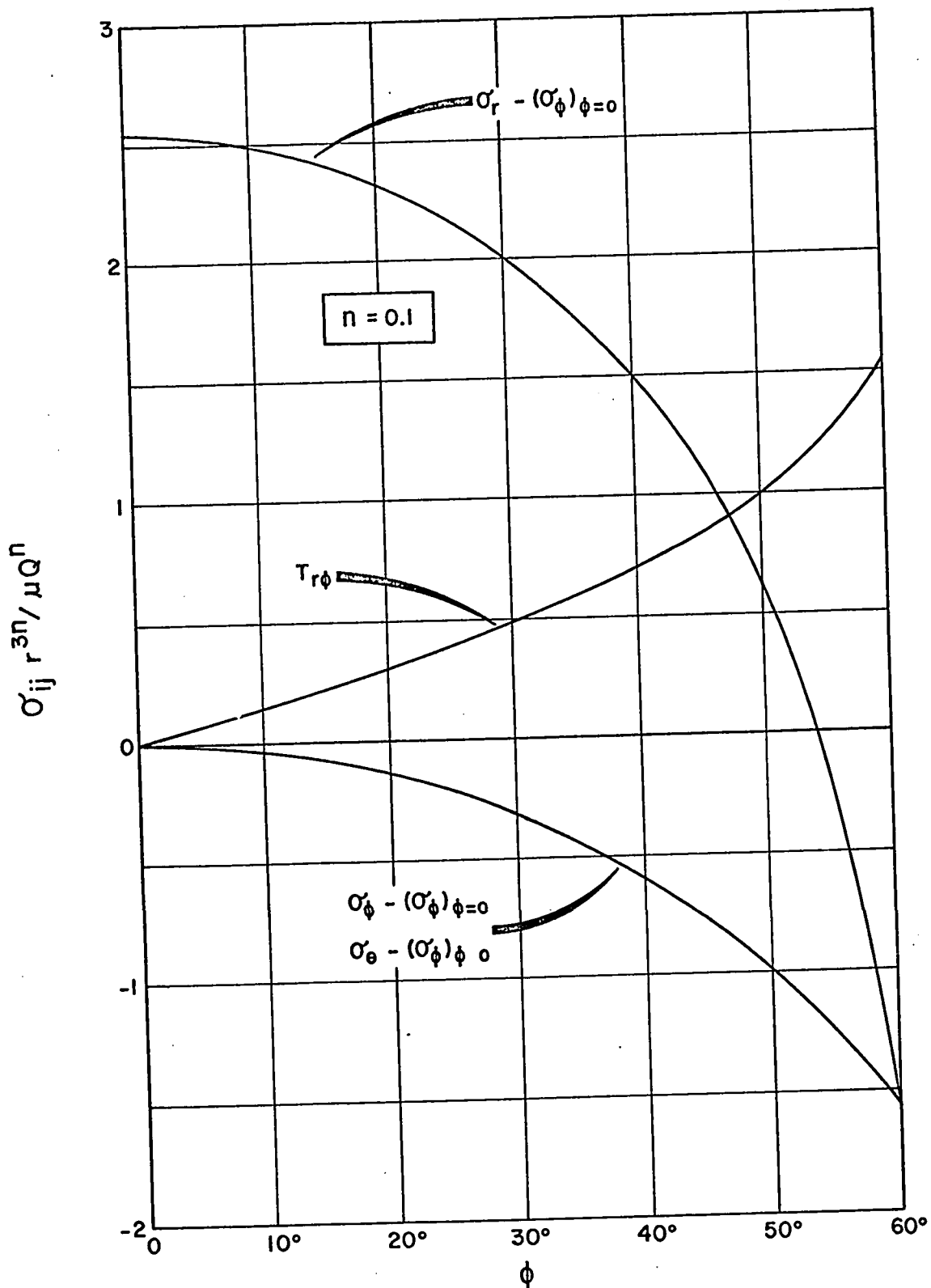


FIGURE 6.III-13

 $\sigma'_{ij} r^{3n} / \mu Q^n$ VERSUS ϕ : $\alpha = 60^\circ$

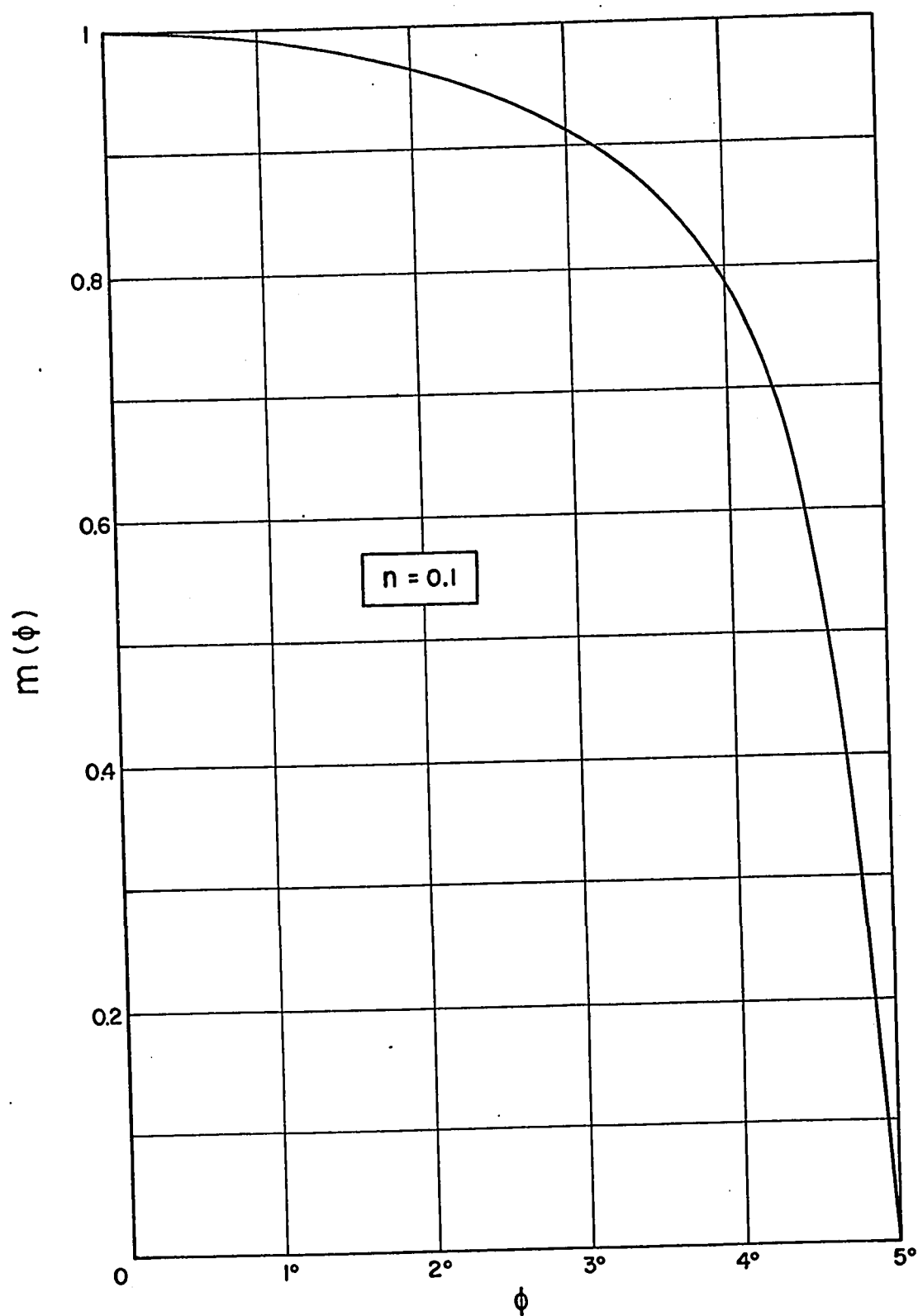


FIGURE 6.III-14

 $m(\phi)$ VERSUS ϕ : $\alpha = 5^\circ$

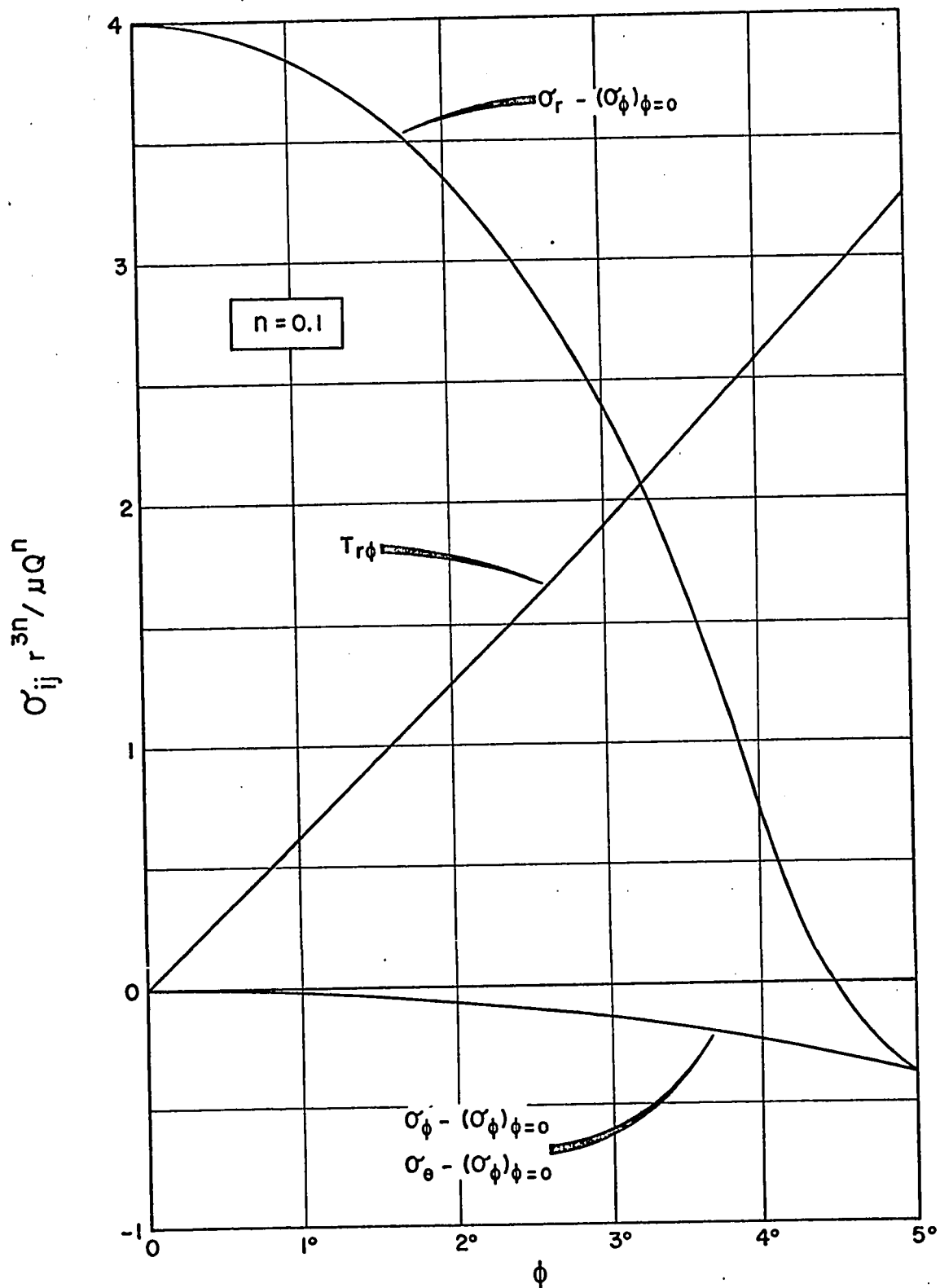


FIGURE 6.III-15

$\sigma_{ij} r^{3n} / \mu Q^n$ VERSUS ϕ : $\alpha = 5^\circ$

6.2 Error Analysis of the Numerical Results

An analysis of the errors involved in the numerical procedure used is facilitated by the discussion presented in the Appendix.

It is shown in the Appendix that, if the solutions y_i are known at $x = X$, the accuracy of the step-by-step integration procedure for n first order ordinary differential equations is controlled by means of a test value δ ;

$$\delta = \frac{1}{15} \sum_{i=1}^n a_i \cdot |y_i^{(1)} - y_i^{(2)}| , \quad (6.1)$$

where $y_i^{(1)}$ are the function values at $x = X + 2h$, which are obtained by using the increment $\Delta x = h$ twice, and $y_i^{(2)}$ are the function values at $x = X + 2h$ as calculated in one step with the increment $\Delta x = 2h$. The coefficients a_i are the error weights, which have to be chosen such that

$$\sum_{i=1}^n a_i = 1 .$$

The equations governing the pseudo-plastic flow problems were shown to consist of three first order ordinary differential equations, both for the plane and the axially symmetric flow. In order that the local truncation errors in the function values y_i are of equal weight, the error weights were chosen to be

$$a_1 = a_2 = a_3 = \frac{1}{3} .$$

The maximum truncation error, therefore, which could possibly occur in the required function at $x = X + 2h$, as obtained in two steps with an increment $\Delta x = h$ for each step, becomes from equations (A.25) and (6.1)

$$2\epsilon = \delta.$$

This test value δ , for the control of accuracy, was chosen to be 10^{-6} for the execution of the program. The maximum truncation error at each station in the sequence of solution is therefore $10^{-6}/2$; consequently, the total maximum error over the entire range, that is from $\phi = 0$ to $\phi = \alpha$, is

$$E_{\text{Total}} = \frac{N \times 10^{-6}}{2}, \quad (6.2)$$

where N is the number of stations needed to reach $\phi = \alpha$. As an example, the solution to the axially symmetric converging flow problem with $\alpha = 30^\circ$, and $n = 2/3$, required 128 stations, hence substitution of

$$N = 128$$

in equation (6.2) yields for the total maximum error in the required function, for this particular case,

$$E_{\text{Total}} = 6.4 \times 10^{-5}$$

over the entire range. The errors involved in the numerical procedure indicate how closely the exact solution is approximated; however, no matter how good this approximation may be, the errors do not indicate the validity of the solution in a physical sense. The validity of a solution, as applied to a physical problem, is dictated by the mathematical model used, and the approximations made in order to obtain that solution.

6.3 Objections to the Power Law Model

The behavior of the pseudo-plastic material, which is the mathematical model considered in this thesis, is based on the generalization of the Ostwald's power law model, and is given by equation (1.6), which is

$$s_{ij} = 2\mu(d_{mn} d_{mn})^{\frac{n-1}{2}} d_{ij} . \quad (1.6)$$

As mentioned previously in this thesis, Reiner (24) has raised major objections to the use of this model. The objections, regarding the behavior of the apparent coefficient of viscosity, are

(i) for zero strain rates, the apparent coefficient of viscosity is infinite, and

(ii) for infinite strain rates, this coefficient becomes zero.

This behavior of the coefficient of viscosity, in its limiting cases, can be shown by consideration of FIG. 4.1. In this plot, the slope of the flow curve is a measure of the apparent coefficient of viscosity, and from equation (4.10) there obtains

$$\frac{dJ}{dI} = 2^{\frac{n-1}{2}} n\mu I^{n-1},$$

where, as previously mentioned, I and J are the strain rate and stress invariants, respectively. The case $n = 1$, corresponding to the Newtonian viscous liquid, reduces to

$$\frac{dJ}{dI} = \mu,$$

where μ is the Newtonian coefficient of viscosity. However, for values of n in the range

$$0 < n < 1,$$

this equation gives an infinite coefficient of viscosity for $I = 0$, and for $I = \infty$ this coefficient becomes zero. Therefore, it must be concluded that for application of the solutions to any physical problem, the power law model is useful only for a certain range of I ; this range must be chosen such that the limiting cases, and thus these objections, are excluded.

In the application of the axially symmetric solutions to wire drawing processes, the objection of an infinite viscosity is removed by the assumption that the material does not yield until some critical point on the flow curve is reached; this assumption has already been discussed in CHAPTER IV. Furthermore, since the flow of materials in experimental investigations is finite, the other objection is removed as well.

The two objections dealt with so far are termed by Reiner (24) as the "zero" and "infinity" objections, respectively. As previously mentioned in CHAPTER I, an obvious defect in the power law model is that the dimensions of μ depend on the value n . This defect, termed by Reiner as the "dimension" objection, has no serious draw-backs if experiments, dealing with curve fitting, are carried out for the particular material under consideration.

Although objections were raised to the use of the power law model, this model is nevertheless of importance in certain physical applications, such as the extrusion of plastics.

6.4 Wire Drawing and Hydraulic Extrusion

In CHAPTER IV the velocity and stress fields, obtained in CHAPTER III, for axially symmetric converging flow in a circular cone were applied to wire drawing and hydraulic extrusion.

The application of solutions, based on the power law model, to wire drawing seems to be unjustifiable, since this model describes a material which flows under any anisotropic stress, no matter how small; nevertheless, it is of academic interest and thus merits investigation. Furthermore, since an assumption is made, stipulating a "yield limit" for this pseudo-plastic material, thus rendering the so obtained model as a rate dependent material with a definite yield criterion, the results of wire drawing become of physical interest. These results become even more important if experimental investigations, involving the fitting of flow curves for rate dependent materials, are carried out. The application to hydraulic extrusion does not meet with this "yielding" problem, and should be of major importance in the extrusion of plastics.

The assumption was made that yielding does not occur until the stress invariant J reaches some value J_0 , which is point P on the flow curve, see FIG. 4.2. The part of the flow curve from the origin, 0, to this critical point P, with coordinates I_0 and J_0/μ , could therefore be considered as the behavior of the material before plastic flow of the entire region ABCD, see FIG. 4.3, first becomes possible. Since in this thesis these preliminary effects are not taken into consideration, it is immaterial how the flow curve behaves until that critical point P is reached, and hence the assumed flow curve, as shown in FIG. 4.2, should be acceptable.

Since the experimental investigation, dealing with hydraulic extrusions, was carried out with a die with a semi-angle of 5° , the velocity profile and stress distributions for the axially symmetric converging flow for that semi-angle, with $n = 0.1$, are presented in FIGS. 6.III-14 and 6.III-15 respectively.

In the application of the pseudo-plastic flow fields to wire drawing, the maximum reductions are dictated by the condition that yielding does not occur in the drawn material. The results of the relationships between the so obtained maximum reductions and semi-angle α are shown in FIG. 6.A-1. This investigation of the maximum reductions alone may not be conclusive however, the fact that the assumption is made that the material adheres to the walls of the die may result in negative normal stresses at the die, if the reductions become too large. The numerical results show that for any reduction, and z_1 fixed, the die pressure at A, see FIG. 6.1, decreases as z_0 increases; the die pressure remains positive

there until $z_0 = Z$ is reached, for which the die pressure at A is zero. A further increase in z_0 , and hence in the reduction, causes the die pressure at A to change sign, thus resulting in a negative normal stress at that point. This condition is not physically tenable, and hence another criterion for the maximum reduction is obtained.

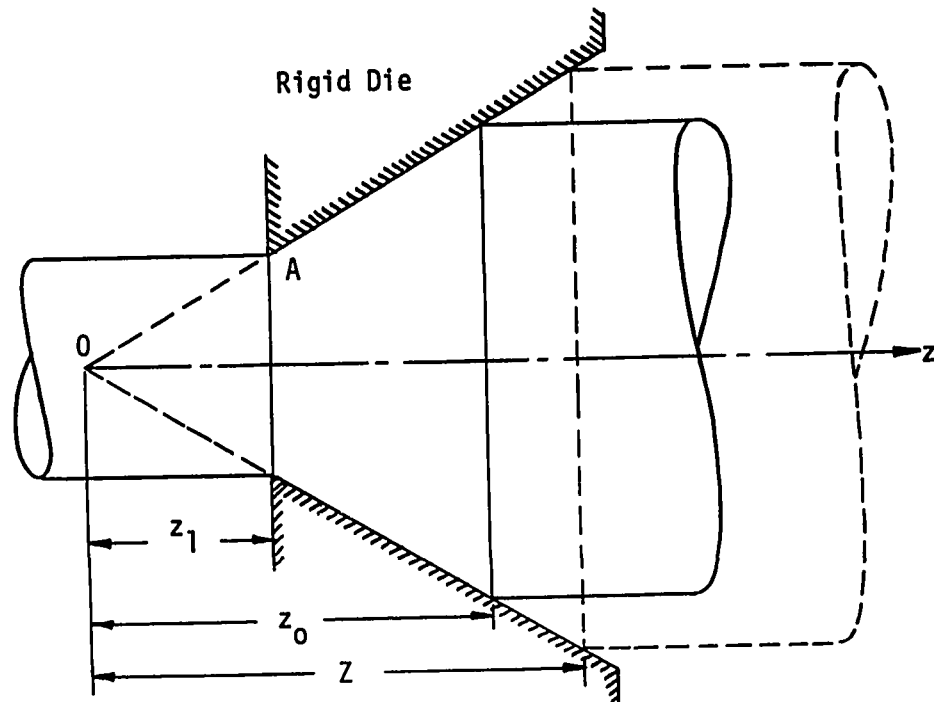


FIGURE 6.1

Possible Negative Normal Stresses at the Walls

The relation for the maximum reduction, based on the condition that

$$P_{\text{die}} \Big|_{z=z_1} = 0,$$

is facilitated by equation (4.15), which, using equations (4.14) and (4.20) gives

$$R_{\max} = 1 - \left[\frac{(2-3n)\{nm'\sin\phi + m'\cos\phi\}_{\phi=\alpha}}{2\{nm'\sin\phi + (1-3n)m'\cos\phi\}_{\phi=\alpha}} \right]^{\frac{2}{3n}}$$

as the maximum reduction which ensures that no negative normal stresses occur at the die. The results of these maximum reductions are presented for various semi-angles in FIG. 6.A-1. Clearly, from the numerical results presented in FIG. 6.A-1, the maximum reduction based on the condition that no negative normal stresses occur at the die dictates the maximum reductions possible. It is interesting to note that the special case $n = 0$, considered by Shield (31), gives a maximum reduction of 63% for any semi-angle, if the shear stress $\tau_{r\phi}$ is identically zero throughout the entire flow region; this maximum reduction is based on the condition that yielding does not occur in the drawn material. It can be shown that, for this particular case, the die pressure is positive along the entire length of the walls. However, Shield did not investigate the possibility of negative normal stresses at the die, not even for the case where $\tau_{r\phi}$ does not vanish identically in the region of flow.

The relationship between the ram pressure and semi-angle α for various reductions is presented in FIG. 6.A-3 for the hydraulic extrusion process. Similar results for the wire drawing process have been presented in FIG. 6.A-2, where in this case the drawing stress is considered; the maximum reductions based on the two criteria, discussed previously, are also shown in this figure. It is noted from FIGS. 6.A-2 and

6.A-3 that both the drawing stress and the ram pressure are monotonically decreasing functions of the semi-angle α . However, Evans and Avitzur (40) found that for a rigid perfectly plastic solid there exists a definite minimum for both the drawing stress and the ram pressure as functions of the semi-angle α . This minimum is denoted by the optimum semi-die angle, and is that semi-angle for which both the drawing stress and the ram pressure are a minimum. This distinct difference can probably be attributed to the fact that the material under consideration in this thesis is rate dependent to a significant extent. It would be of interest to investigate the relationship between the ram pressure and semi-angle α for extrusion of plastics, since these materials are rate dependent.

RESULTS
OF
WIRE DRAWING
AND
HYDRAULIC EXTRUSION

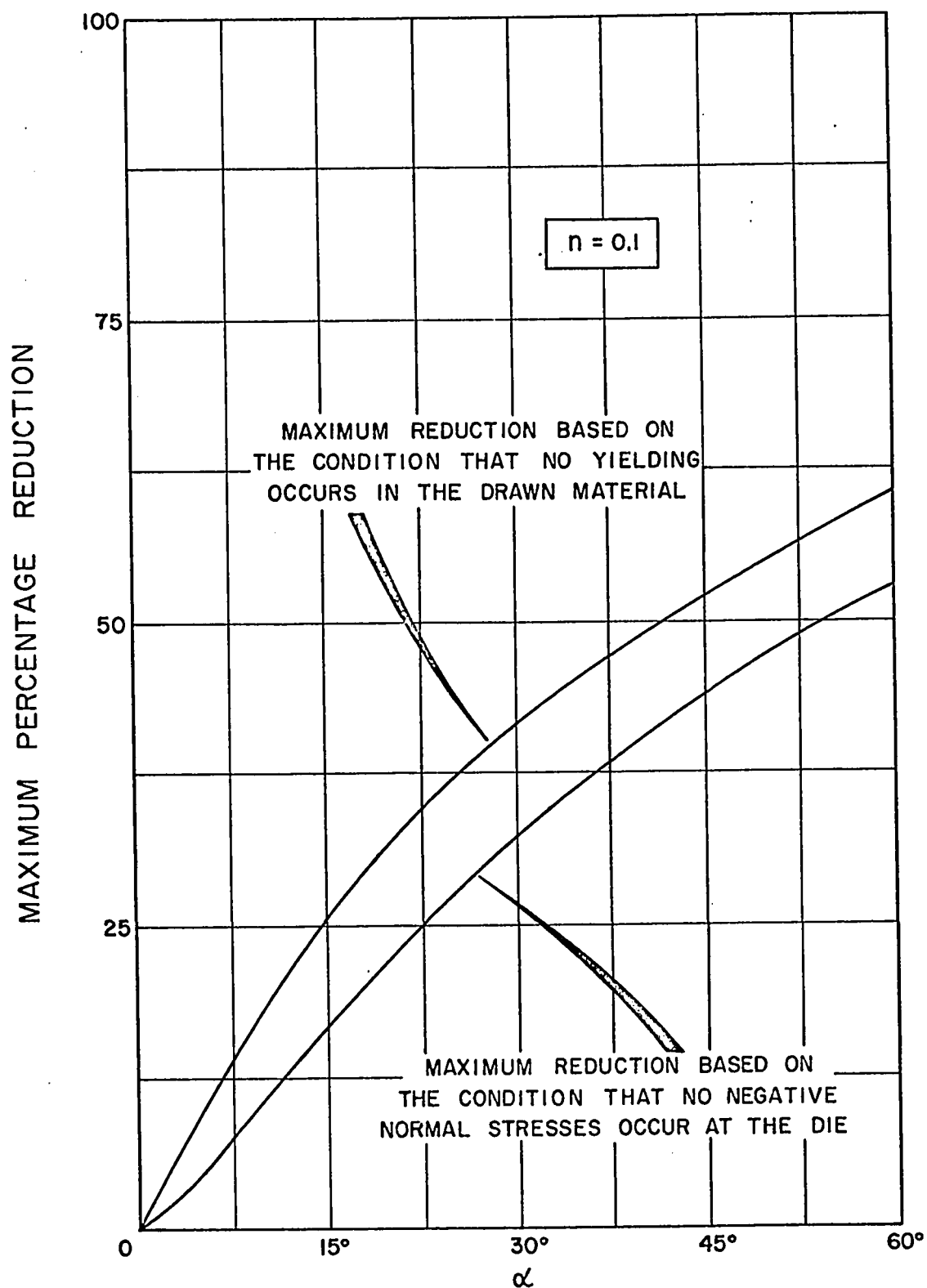


FIGURE 6.A-1
MAXIMUM PERCENTAGE REDUCTION VERSUS α

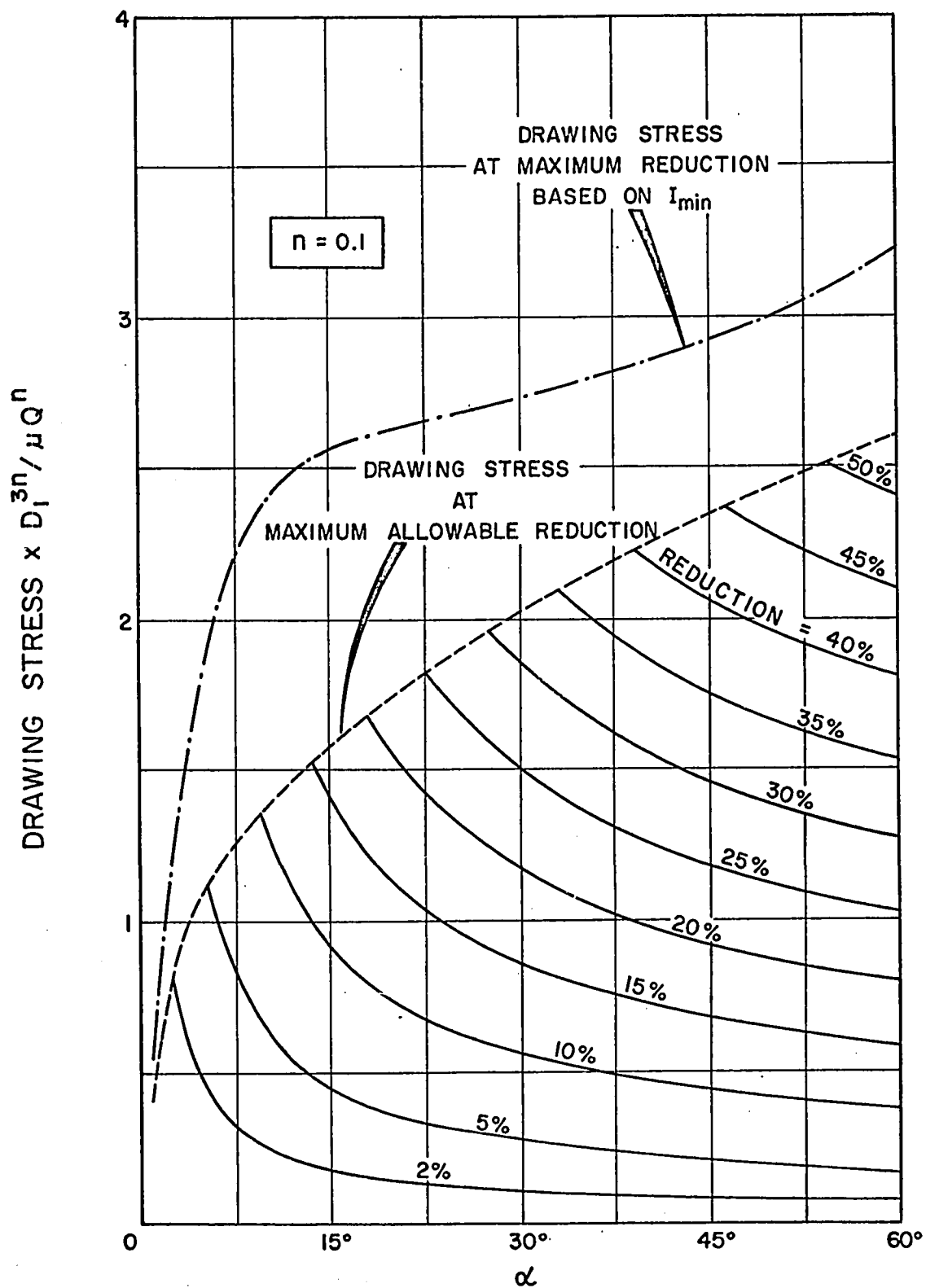


FIGURE 6.A-2
DRAWING STRESS $\times D_1^{3n} / \mu Q^n$ VERSUS α

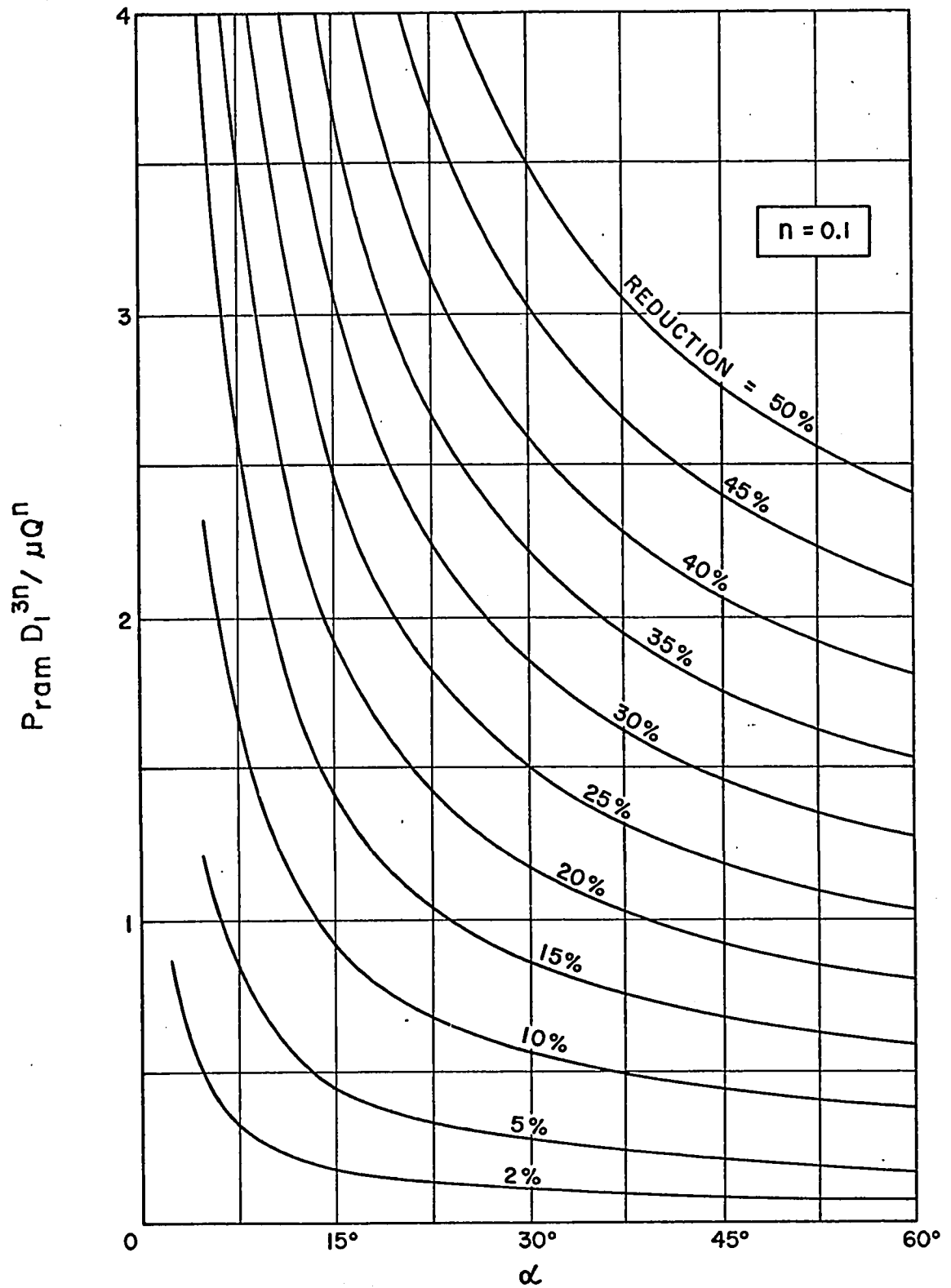


FIGURE 6.A-3
 $P_{ram} D_1^{3n} / \mu Q^n$ VERSUS α

6.5 Suggestions for Future Work

Various results have been presented for the pseudo-plastic flow problems, considered in this thesis, however a solution for the Bingham solid was not obtained. It is of importance, therefore, to discuss a method which could possibly yield an approximate solution to the flow of a Bingham solid in a circular cone. To this end this chapter is concluded with a brief discussion of this method.

It was shown in CHAPTER II that no radial, steady, quasi-static flow solutions exist for the plane flow of a Bingham solid, without body forces, in a converging channel, or for the axially symmetric converging flow in a circular cone, at least if the solid is assumed incompressible.

The limiting cases of the Bingham solid, however, the Newtonian viscous liquid and the perfectly plastic von Mises solid, do indeed yield radial flow solutions to the problems mentioned above. Furthermore, it is clear that in a long channel or cone the velocity profile near the entry section should closely approximate that of the perfectly plastic von Mises solid, whereas close to the exit section, the viscous terms dominate and hence the solution there should be approximately that of the Newtonian viscous liquid.

It is the purpose of this concluding section to outline briefly a method which might yield an approximate solution for the flow of a Bingham solid in a circular cone of small semi-angle and of finite length. This method was successfully applied by Sutterby (37) to the axially symmetric converging, steady, incompressible Newtonian viscous flow in a circular cone of finite length, and of small semi-angle, with specified

conditions at the inlet section.

Let the flow of a Bingham solid in a circular cone, of length L , be described by spherical polar coordinates, (r, ϕ, θ) ; the z -axis is taken along the axis of symmetry, see FIG. 6.2. Further necessary notation is also shown in this figure.

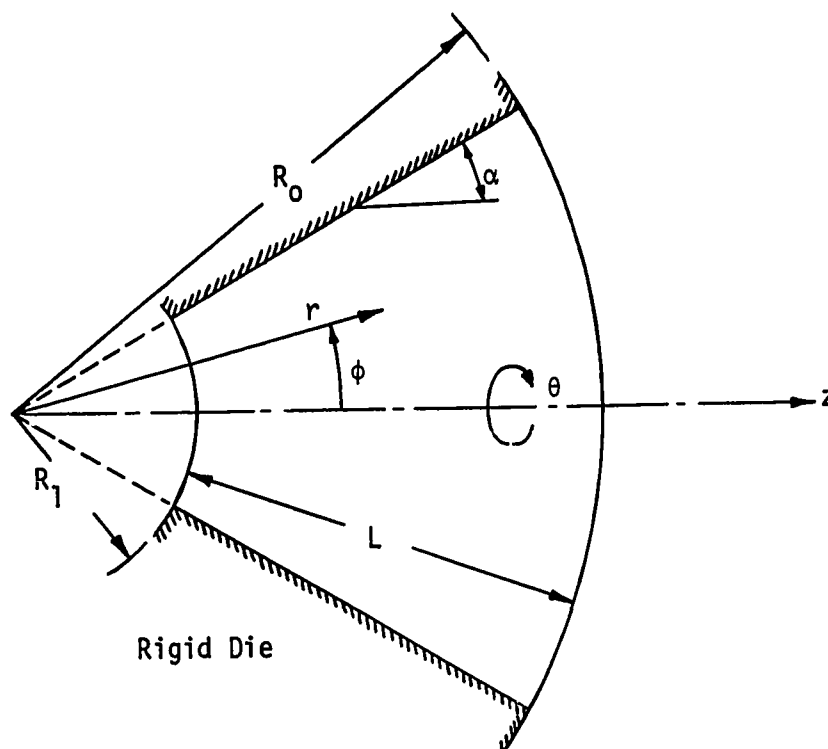


FIGURE 6.2

The Cone of Finite Length

Since no radial flow exist for the Bingham solid, the flow must consist of a tangential component as well. The flow field, therefore, consists of a radial velocity $v_r = v_r(r, \phi)$, a tangential velocity $v_\phi = v_\phi(r, \phi)$, and $v_\theta = 0$. From equations (2.1), there obtains for the

components of the strain rate tensor

$$\begin{aligned}
 d_r &= \frac{\partial v_r}{\partial r} , \\
 d_\phi &= \frac{v_r}{r} + \frac{1}{r} \frac{\partial v_\phi}{\partial \phi} , \\
 d_\theta &= \frac{v_r}{r} + \frac{v_\phi \cot \phi}{r} , \\
 d_{r\phi} &= \frac{1}{2r} \frac{\partial v_r}{\partial \phi} + \frac{1}{2} \frac{\partial v_\phi}{\partial r} .
 \end{aligned} \tag{6.3}$$

The equation of continuity becomes

$$\frac{1}{r} \frac{\partial}{\partial r} (r^2 v_r) + \frac{1}{\sin \phi} \frac{\partial}{\partial \phi} (v_\phi \sin \phi) = 0. \tag{6.4}$$

The strain rate invariant,

$$I = \sqrt{2d_{mn} d_{mn}} , \tag{6.5}$$

is obtained from the strain rate relations (6.3). Similarly, the stress deviator components are found by substitution of equations (6.3) and (6.5) in the constitutive equations (1.4). These expressions are very complex, and will not be reproduced here. The equations of motion, assuming steady flow, and without body forces, are

$$\frac{\partial p}{\partial r} + \rho \left(v_r \frac{\partial v_r}{\partial r} + \frac{v_\phi}{r} \frac{\partial v_r}{\partial \phi} \right) = \frac{\partial s_r}{\partial r} + \frac{3s_r}{r} + \frac{1}{r} \left(\frac{\partial s_{r\phi}}{\partial \phi} + s_{r\phi} \cot \phi \right),$$

$$\frac{\partial p}{\partial \phi} + \rho(rv_r \frac{\partial v_\phi}{\partial r} + v_\phi \frac{\partial v_r}{\partial \phi}) = \frac{\partial s_\phi}{\partial \phi} + r \frac{\partial s_{r\phi}}{\partial r} + 3s_{r\phi} . \quad (6.6)$$

Substitution of the stress deviators in equations (6.6), results in a set of equations, which along with equation (6.4) constitute three equations for the three unknowns p , v_r , and v_ϕ .

If the circular cone under consideration is of small semi-angle α , then it may be assumed that the streamlines are only slightly curved. Consequently, v_ϕ is small compared to v_r , and furthermore, $\sin\phi$ and $\cos\phi$ may be replaced by ϕ and 1, respectively. With these approximations, the governing equations are simplified to some extent.

The resulting equations of motion are of the following form

$$\frac{\partial p}{\partial r} + \rho F + kG + \mu H = 0 , \quad (6.7)$$

$$\frac{\partial p}{\partial \phi} + \rho \bar{F} + k\bar{G} + \mu\bar{H} = 0 ,$$

and the equation of continuity becomes

$$r \frac{\partial v_r}{\partial r} + 2v_r + \frac{\partial v_\phi}{\partial \phi} + \frac{v_\phi}{\phi} = 0 , \quad (6.8)$$

where the functions F , G , H , \bar{F} , \bar{G} , and \bar{H} are functions of r and ϕ , and of the velocity components and their derivatives with respect to r and ϕ up to and including their second order. The volume flow condition, for small semi-angles, becomes

$$Q = 2\pi r^2 \int_0^\alpha v_r \phi d\phi. \quad (6.9)$$

The problem reduces to the solution of equations (6.7) and (6.8) subject to the volume flow condition (6.9), and the following boundary conditions:

from symmetry,

$$\frac{\partial v_r}{\partial \phi} = 0, \quad v_\phi = 0, \quad \text{at } \phi = 0,$$

and since there is no flow across the walls of the die,

$$v_\phi = 0 \quad \text{at } \phi = \alpha,$$

and finally the assumed no-slip boundary condition

$$v_r = 0, \quad \text{at } \phi = \alpha.$$

In this method the velocity profile at the entry section, that is $r = R_0$, is assumed to be that of the Bingham solid in a circular tube, and the pressure is assumed to be constant there. Consequently, the inlet conditions are

$$\text{at } r = R_0: \quad v_\phi = 0, \quad p = p_0, \quad \text{and } v_r \text{ is as given by the}$$

Bingham solution in a circular tube. A finite difference analysis can

now be applied to the region of deformation.

It is noted that the complexity of the system is more pronounced than that for the Newtonian viscous flow. This may be a defect in this method, as applied to flow of materials with a less simple constitutive equation. A more thorough theoretical investigation is therefore required; if a solution is obtained, these results should be of major importance for hydraulic extrusion and wire drawing processes.

BIBLIOGRAPHY

1. A.G. Fredrickson, "Principles and Applications of Rheology",
Prentice-Hall, Inc., Englewood Cliffs, N.J., 1964, Chap. 1.
2. M. Reiner, "Rheology", Handbuch der Physik (edited by S. Flügge),
Springer-Verlag, Berlin, 1958, vol. 6, p. 542.
3. G.W. Scott Blair, "A Survey of General and Applied Rheology", Sir
Isaac Pitman & Sons, Ltd., 2nd edition, 1949, p. 3.
4. A. Cemal Eringen, "Mechanics of Continua", John Wiley & Sons, Inc.,
New York. London. Sydney, 1967, Chap. 5.
5. M. Reiner, "Rheology", Handbuch der Physik (Edited by S. Flügge),
Springer-Verlag, Berlin, 1958, vol. 6, p. 447.
6. M. Reiner, "Rheology", Handbuch der Physik (Edited by S. Flügge),
Springer-Verlag, Berlin, 1958, vol. 6, p. 456.
7. W.L. Wilkinson, "Non-Newtonian Fluids"; Fluid Mechanics, Mixing and
Heat Transfer, Pergamon Press, London. Oxford. New York.
Paris, 1960, Chap. 1.
8. M. Reiner, "Rheology", Handbuch der Physik (Edited by S. Flügge),
Springer-Verlag, Berlin, 1958, vol. 6, p. 457.
9. E.C. Bingham and H. Green, "Paint, a Plastic Material and not a
Viscous Liquid"; The Measurement of its Mobility and Yield
Value, Proc. ASTM, 19 (1919), p. 640.
10. R.B. Bird, W.E. Stewart, E.N. Lightfoot, "Transport Phenomena",
John Wiley & Sons, Inc., New York, 1960, p. 11.

11. K. Hohenemser and W. Prager, "Über die Ansätze der Mechanik Isotroper Kontinua", Zeitschrift für Angewandte Mathematik und Mechanik, vol. 12 (1932). pp. 216-226.
12. W. Prager, "On Slow Visco-Plastic Flow", Studies in Mathematics and Mechanics, Academic Press, New York, 1954, p. 208.
13. M. Reiner, "Deformation and Flow"; An Elementary Introduction to Theoretical Rheology, Interscience Publishers, Inc., New York, 1960, p. 124.
14. J.G. Oldroyd, "Two-Dimensional Plastic Flow of a Bingham Solid", Proceedings Cambridge Philosophical Society, Vol. 43 (1947), pp. 383-395; "Rectilinear Plastic Flow of a Bingham Solid", ibid., Vol. 43 (1947), pp. 396-405, 521-532; vol. 44 (1948), pp. 200-213.
15. R.L. Carlson, "Compression of a Visco-Plastic Disk", Journal of Basic Engineering, vol. 86 (1964), p. 700.
16. W. Prager, "Linearization in Visco-Plasticity", Oesterreichisches Ingenieur-Archiv. Vol. 15 (1961), pp. 152-157.
17. J.B. Haddow, "On the Compression of a Thin Disk", International Journal of Mechanical Sciences, vol. 7 (1965).
18. J.B. Haddow, "A Linearized Theory of Visco-Plasticity", International Journal of Solids & Structures, vol. 3 (1967), pp. 533-542.
19. T.M. Hrudey, "Bending of Rate Sensitive Circular Plates", M.Sc. thesis - Department of Mechanical Engineering, University of Alberta, Edmonton, Alberta.

20. W. Prager, "On Slow Visco-Plastic Flow", *Studies in Mathematics and Mechanics*, Academic Press, New York, 1954, pp. 212-216.
21. J.B. Haddow and H. Luming, "An Extension of One of the Extremum Principles for a Bingham Solid", *Applied Scientific Research*, vol. 15, Section A, pp. 81-85.
22. M. Reiner, "Rheology", *Handbuch der Physik* (Edited by S. Flügge), Springer-Verlag, Berlin, 1958, vol. 6, p. 494.
23. M. Reiner, "Rheology", *Handbuch der Physik* (Edited by S. Flügge), Springer-Verlag, Berlin, 1958, vol. 6, p. 488.
24. M. Reiner, "Deformation and Flow"; *An elementary Introduction to Theoretical Rheology*, Interscience Publishers, Inc., New York, 1960, pp. 245-247.
25. R. Hill, "New Horizons in the Mechanics of Solids", *Journal of the Mechanics and Physics of Solids*, 1956, Vol. 5, p. 67.
26. L. Rosenhead, "The Steady Two-Dimensional Radial Flow of Viscous Fluid between two Inclined Plane Walls", *Proc. Royal Society A*, vol. 175, p. 436.
27. W.E. Langlois, "Slow Viscous Flow", The Macmillan Company, New York, 1964, pp. 109-110.
28. N.Ch. Pattabhi Ramacharyulu, "Slow Steady Flow of an Idealized Elastico-Viscous Liquid through a Cone with a Source/Sink at the Vertex", *ZAMM* 47 (1967), Heft 1, pp. 12-13.
29. A. Nadai, "Über die gleit und Verzweigungsflächen einiger Gleichgewichtszustände de bildsamer Massen und die Nachspannungen bleibend verzerrter Körper". *Zeits.f. Phys.* 30, 106 (1924).

30. R. Hill, "The Mathematical Theory of Plasticity", Clarendon Press, Oxford, 1950, pp. 209-212.
31. R.T. Shield, "Plastic Flow in a Converging Channel", Journal of the Mechanics and Physics of Solids, Pergamon Press Ltd., London, vol. 3, 1955, pp. 246-258.
32. R.I. Tanner, "Non-Newtonian Fluid Parameter Estimation using Conical Flows", I. and E.C. Fundamentals, vol. 5, 1966, Published by American Chemical Society, Washington D.C., pp. 55-59.
33. G.K. Batchelor, "An Introduction to Fluid Dynamics", Cambridge - University Press, 1967, pp. 217-218.
34. G. Sachs, "Zur Theorie des Zichvorganges", Zeitschrift für Angewandte Mathematik und Mechanik, Band 7, 1927, Kleine Mitteilungen, p. 235-236.
35. H. Luming, "A Study on Visco-Plasticity", Ph.D. thesis - Department of Mechanical Engineering, University of Alberta, Edmonton, Alberta.
36. W. Prager, "Introduction to Mechanics of Continua", Ginn and Company, 1961, p. 141.
37. J.L. Sutterby, "Finite Difference Analysis of Viscous Laminar Flow in Conical Tubes," Applied Scientific Research - Section A, vol. 15, 1965-66, Martinus Nyhoff, The Hague, pp. 241-252.
38. W.J. Harrison, "The Pressure in a Viscous Liquid Moving through a Channel with Diverging Boundaries", Proc. of the Camb. Phil. Soc., vol. 19, 1916-1919, pp. 307-312.

39. W.N. Bond, "Viscous Flow through Wide-Angled cones", Philosophical Magazine and Journal of Science, vol. 50, Sixth Series, 1925, pp. 1058-1066.
40. W. Evans and B. Avitzur, "Measurement of Friction in Drawing, Extrusion, and Rolling", Transactions of the A.S.M.E., Journal of Lubrication Technology, vol. 90, Series F, Number 1, Jan. 1968, pp. 72-80.
41. S. Gill, "A Process for the Step-by-Step Integration of Differential Equations in an Automatic Digital Computing Machine", Proc. Camb. Phil. Soc., vol. 47, 1951, pp. 96-108.
42. E.L. Ince, "Ordinary Differential Equations", Dover Publications, 1956, Appendix B, pp. 540-547.
43. Subroutine DRKGS from IBM System/360 Scientific Subroutine Package.

APPENDIX

NUMERICAL INTEGRATION OF ORDINARY DIFFERENTIAL EQUATIONS

A.1 Introduction

The governing equations of CHAPTERS III and IV were integrated by Gill's variation of the Runge-Kutta fourth order method (41). This is a self starting integration procedure which is applicable to a system of n first order ordinary differential equations. The following explanation first considers a single differential equation, this is then generalized to a system of ordinary differential equations, and finally the accuracy of the method is indicated.

A.2 The First Order Ordinary Differential Equation

Consider the single first order ordinary differential equation

$$\frac{dy}{dx} = f(x,y).$$

The initial condition is $y = Y$ at $x = X$ and suppose that y is required at $x = X + h$, where h is small. One possible procedure is to consider the Taylor series expansion about the point P , with coordinates (X,Y) ,

$$y - Y = \delta y = h \left(\frac{dy}{dx} \right)_P + \frac{h^2}{2!} \left(\frac{d^2y}{dx^2} \right)_P + \frac{h^3}{3!} \left(\frac{d^3y}{dx^3} \right)_P + \dots, \quad (A.1)$$

where the coefficients are calculated from

$$\frac{dy}{dx} = f(x,y) ,$$

$$\frac{d^2y}{dx^2} = \frac{\partial f}{\partial x} + f \frac{\partial f}{\partial y} , \text{ etc.}$$

The complexity of the coefficients renders this process impracticable.

An alternative procedure, introduced by Runge and modified by Kutta, proceeds as follows:

Define, following Gill's notation,

$$k_0 = hf(X,Y) ,$$

$$k_1 = hf(X + mh, Y + mk_0) ,$$

$$k_2 = hf(X + nh, Y + (n-r)k_0 + rk_1) ,$$

$$k_3 = hf(X + ph, Y + (p-s-t)k_0 + sk_1 + tk_2) ,$$

and construct

$$\delta y = ak_0 + bk_1 + ck_2 + dk_3 . \quad (A.2)$$

FIGURE A.1 indicates the geometrical nature of this procedure. The six constants m, n, p, r, s, t , and the four weighting factors a, b, c , and d are chosen such that the terms up to and including $O(h^4)$ in the Taylor series expansion of equation (A.1) agree with the corresponding terms in the expansion of equation (A.2).

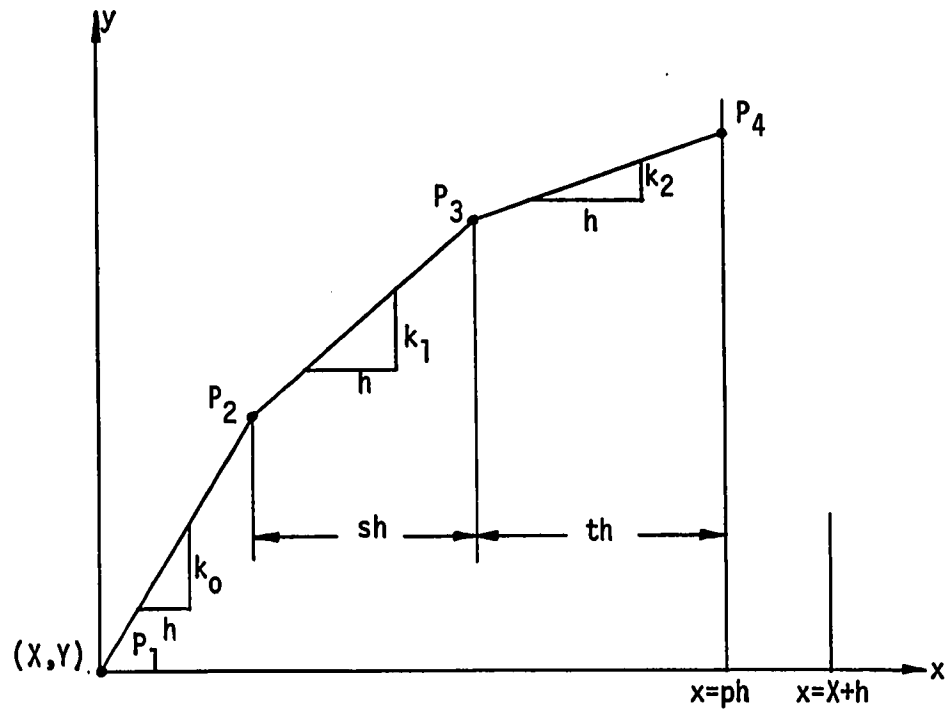


FIGURE A.1

Geometrical Construction of δy

A.3 Equations Governing the Constants and Weighting Factors

The Taylor series expansion of equation (A.2) requires the expansions of the weighting functions k_0 , k_1 , k_2 , and k_3 . These expansions are obtained by making use of the Taylor series expansion in two variables (42)

$$f(x+p, y+q) = f(x, y) + \bar{D}f(x, y) + \frac{\bar{D}^2}{2!} f(x, y) + \frac{\bar{D}^3}{3!} f(x, y) + \dots,$$

where the operator \bar{D} is given by

$$\bar{D}^r = (p \frac{\partial}{\partial x} + q \frac{\partial}{\partial y})^r .$$

With the introduction of the notation

$$f_0 = f(X,Y),$$

the expression for k_0 becomes

$$k_0 = hf_0 .$$

Letting $D = \frac{\partial}{\partial x} + f_0 \frac{\partial}{\partial y} ,$

then

$$mh \frac{\partial}{\partial x} + mk_0 \frac{\partial}{\partial y} = mh \left(\frac{\partial}{\partial x} + f_0 \frac{\partial}{\partial y} \right) = mh D ,$$

consequently

$$k_1 = h \left[f + mhDf + \frac{m^2 h^2 D^2 f}{2!} + \frac{m^3 h^3 D^3 f}{3!} + \dots \right]_p .$$

To evaluate k_2 , then

$$nh \frac{\partial}{\partial x} + [(n-r)k_0 + rk_1] \frac{\partial}{\partial y} = nhD + r(k_1 - k_0) \frac{\partial}{\partial y} =$$

$$nhD + mrh^2 \left[Df + \frac{mhD^2f}{2!} + \frac{m^2h^2D^3f}{3!} + \dots \right]_p \frac{\partial}{\partial y},$$

consequently

$$k_2 = h \left[f + nhDf + \frac{n^2h^2D^2f}{2!} + \frac{n^3h^3D^3f}{3!} + \dots \right. \\ \left. + mrh^2 \left\{ f_y Df + \frac{mh}{2!} f_y D^2f + nhDf \cdot Df_y + \dots \right\} \right]_p,$$

where

$$f_y = \frac{\partial f}{\partial y}.$$

Similarly to evaluate k_3 ,

$$ph \frac{\partial}{\partial x} + [(p-s-t)k_0 + sk_1 + tk_2] = phD + [s(k_1 - k_0) + t(k_2 - k_0)] \frac{\partial}{\partial y} = \\ phD + [h^2ms \left\{ Df + \frac{mhD^2f}{2!} + \frac{m^2h^2D^3f}{3!} + \dots \right\} \\ + h^2nt \left\{ Df + \frac{nhD^2f}{2!} + \frac{n^2h^2D^3f}{3!} + \dots \right\} \\ + h^3tmr \left\{ f_y Df + \frac{mh}{2!} f_y D^2f + nhDf \cdot Df_y + \dots \right\}]_p \frac{\partial}{\partial y},$$

consequently

$$k_3 = h \left[f + phDf + \frac{p^2h^2D^2f}{2!} + \frac{p^3h^3D^3f}{3!} + \dots \right. \\ \left. + h^2(msDf + tnDf)f_y + \frac{h^3}{2!} (sm^2D^2f + 2tmrf_y Df + tn^2D^2f) f_y \right]$$

$$+ h^3(psmDf + ptnDf) Df_y + \dots]_p .$$

The expansion of equation (A.1) becomes

$$\begin{aligned} \delta y = [hf + \frac{h^2}{2!} Df + \frac{h^3}{3!} (D^2f + f_y Df) + \\ \frac{h^4}{4!} (D^3f + f_y D^2f + f_y^2 Df + 3Df Df_y) + \dots]_{x=X} \end{aligned} \quad (A.3)$$

The equations connecting the constants and the weighting factors are obtained by equating the eight terms in the expansion of δy , equation (A.3), to the corresponding terms in the expansion of $\delta y = ak_0 + bk_1 + ck_2 + dk_3$. There results the equations

$$a + b + c + d = 1 ,$$

$$bm + cn + dp = 1/2 ,$$

$$bm^2 + cn^2 + dp^2 = 1/3 ,$$

(A.4)

$$bm^3 + cn^3 + dp^3 = 1/4 ,$$

$$crm + dsm + dtn = 1/6 ,$$

$$crm^2 + dsm^2 + dtn^2 = 1/12 ,$$

$$drmn + dsmp + dtnp = 1/8 ,$$

$$dtrm = 1/24 .$$

The set of equations (A.4) represent eight constraints on the ten unknowns a, b, \dots, s, t , consequently two further consistent relations may be imposed; this may be done in various ways, but first it is shown that $p = 1$.

A.4 Determination of the Constants and Weighting Factors

Adding the second of the set of equations (A.4) multiplied by mp and the third multiplied by $-(m+p)$ to the fourth equation, gives

$$cn(m-n)(p-n) = \frac{mp}{2} - \frac{m+p}{3} + \frac{1}{4} . \quad (A.5)$$

Multiplying the fifth equation by p and subtracting from this the seventh equation,

$$cmr(p-n) = \frac{p}{6} - \frac{1}{8} . \quad (A.6)$$

Similarly from the fifth and sixth,

$$dnt(n-m) = \frac{1}{12} - \frac{m}{6} . \quad (A.7)$$

Eliminating d between equation (A.7) and the eighth of the set of equations (A.4),

$$mr = \frac{n(m-n)}{2(2m-1)} . \quad (A.8)$$

Substituting equation (A.8) in equation (A.6),

$$cn(p-n)(m-n) = (2m-1)\left(\frac{p}{3} - \frac{1}{4}\right) . \quad (\text{A.9})$$

Comparing equation (A.9) with equation (A.5) gives

$$mp = m . \quad (\text{A.10})$$

From the eighth of the set of equations (A.4)

$$m \neq 0 ,$$

hence the solution to equation (A.10) reduces to

$$p = 1 .$$

The values of a , b , c , and d are determined from the first four of the set of equations (A.4),

$$a + b + c + d = 1 ,$$

$$bm + cn + d = \frac{1}{2} ,$$

$$bm^2 + cn^2 + d = \frac{1}{3} , \quad (\text{A.11})$$

$$bm^3 + cn^3 + d = \frac{1}{4} ,$$

since $p = 1$. This set of equations yields a unique solution for a , b , c , and d , if the coefficient determinant is non-zero that is if

$$mn(m-n)(n-1)(1-m) \neq 0 . \quad (\text{A.12})$$

Solving the set of equations (A.11);

$$\begin{aligned} a &= \frac{1}{2} + \frac{1 - 2(m+n)}{12mn} , \\ b &= \frac{2n-1}{12m(n-m)(1-m)} , \\ c &= \frac{1-2m}{12n(n-m)(1-n)} , \\ d &= \frac{1}{2} + \frac{2(m+n) - 3}{12(1-m)(1-n)} . \end{aligned} \quad (\text{A.13})$$

Finally, the constants r , s , and t are determined from the fifth, sixth and seventh of the set of equations (A.4),

$$\begin{aligned} crm + dsm + dtn &= \frac{1}{6} , \\ crm^2 + dsm^2 + dtn^2 &= \frac{1}{12} , \\ crmn + dsm + dtn &= \frac{1}{8} . \end{aligned} \quad (\text{A.14})$$

Once again a unique solution is obtained if the coefficient determinant of the set of equations (A.14)

$$cd^2m^2n(n-m)(n-1) \neq 0 . \quad (\text{A.15})$$

Consequently, the unique solution to r , s , and t is

$$\begin{aligned} r &= \frac{n(n-m)}{2m(1-2m)} , \\ s &= \frac{(1-m)\{m+n-1-(2n-1)^2\}}{2m(n-m)\{6mn-4(m+n)+3\}} , \\ t &= \frac{(1-2m)(1-m)(1-n)}{n(n-m)\{6mn-4(m+n)+3\}} . \end{aligned}$$

The parameters m and n may be assigned in any manner consistent with the previous equations. Let the interval h be divided into three equal parts, then

$$\begin{aligned} m &= \frac{1}{3} , \\ n &= \frac{2}{3} . \end{aligned} \quad (\text{A.16})$$

Substitution of equations (A.16) in the set of equations (A.13) yields

$$a = \frac{1}{8} ,$$

$$b = \frac{3}{8} ,$$

$$c = \frac{3}{8} ,$$

$$d = \frac{1}{8} .$$

Similarly the constants r , s , and t are

$$r = 1 ,$$

$$s = - 1 ,$$

$$t = 1 .$$

The weighting functions obtained are

$$k_0 = hf(X, Y) ,$$

$$k_1 = hf\left(X + \frac{h}{3}, Y + \frac{k_0}{3}\right) ,$$

$$k_2 = hf\left(X + \frac{2h}{3}, Y - \frac{k_0}{3} + k_1\right) ,$$

$$k_3 = hf(X + h, Y + k_0 - k_1 + k_2) ,$$

and the increment in y becomes

$$\delta y = \frac{1}{8} (k_0 + 3k_1 + 3k_2 + k_3) .$$

The formulae for the k 's and the increment in y thus obtained are those

due to Kutta (42).

Another useful choice for the parameters m and n is facilitated by setting the determinants (A.12) and (A.15) equal to zero. The case of interest

$$m = n \tag{A.17}$$

is considered. Substitution of equation (A.17) in equations (A.13) further imposes the conditions

$$m = \frac{1}{2} ,$$

$$n = \frac{1}{2} ,$$

in order that b and c remain finite. Substituting these values for m and n into the first and fourth of the set of equations (A.11) yields

$$a = \frac{1}{6} ,$$

$$d = \frac{1}{6} .$$

Either b or c is now arbitrary but not both, since the condition

$$a + b + c + d = 1$$

is to be satisfied. Assuming that

$$b = \frac{1}{3} ,$$

$$c = \frac{1}{3} ,$$

equations (A.14) give

$$r = \frac{1}{2} ,$$

$$s = 0 ,$$

$$t = 1 .$$

The constants and weighting factors thus obtained give rise to a set of formulae, originally due to Runge (42), for the k 's and an increment in y ;

$$k_0 = hf(X, Y) ,$$

$$k_1 = hf\left(X + \frac{h}{2}, Y + \frac{k_0}{2}\right) ,$$

$$k_2 = hf\left(X + \frac{h}{2}, Y + \frac{k_1}{2}\right) ,$$

$$k_3 = hf(X + h, Y + k_2) ,$$

and the increment in y becomes

$$\delta y = \frac{1}{6} (k_0 + 2k_1 + 2k_2 + k_3) .$$

Two methods of evaluation of the constants have been considered, namely those due to Kutta and Runge. Another approach, due to Gill (41), is based on the number of storage registers needed in the calculation of each step. Gill's variation will now be considered by application to a system of ordinary differential equations.

A.5 The System of First Order Ordinary Differential Equations

The consideration of the system of equations is facilitated by the preceeding discussion of a single first order ordinary differential equation. The system of equations is

$$\frac{dy_i}{dx} = f_i(x, y_j) ; i, j = 1, 2, \dots, n ,$$

with the initial values of Y_1, Y_2, \dots, Y_n at $x = X$. The weighting functions for the system are expressed as

$$k_{i0} = hf_i(X, Y_1, Y_2, \dots) ,$$

$$k_{i1} = hf_i(X + mh, Y_1 + mk_{10}, Y_2 + mk_{20}, \dots) ,$$

$$k_{i2} = hf_i(X + nh, Y_1 + (n-r)k_{10} + rk_{11}, Y_2 + (n-r)k_{20} + rk_{21}, \dots) ,$$

$$k_{i3} = hf_i(X + ph, Y_1 + (p-s-t)k_{10} + sk_{11} + tk_{22}, \dots) ,$$

and the fourth order approximation is

$$\delta y_i = ak_{i0} + bk_{i1} + ck_{i2} + dk_{i3} .$$

Gill has introduced a notation which simplifies the theory and is also better adapted to computer programming techniques. Let

$$x = y_0 , \quad (A.18)$$

then the system of equations becomes

$$\begin{aligned} \frac{dy_i}{dx} &= f_i(y_j) ; & i &= 1, 2, \dots, n, \\ & & j &= 0, 1, \dots, n, \end{aligned}$$

where $f_0 \equiv 1$. Under the transformation (A.18) the weighting functions are obtained as

$$k_{i0} = hf_i(Y_j) ,$$

$$k_{i1} = hf_i(Y_j + mk_{j0}) ,$$

$$k_{i2} = hf_i(Y_j + (n-r)k_{j0} + rk_{j1}) ,$$

$$k_{i3} = hf_i(Y_j + (p-s-t)k_{j0} + sk_{j1} + tk_{j2}) ,$$

where $i = 1, 2, \dots, n$, and $j = 0, 1, \dots, n$.

The Taylor series expansion for

$$\delta y_i = y_i(X + h) - y_i(X)$$

about the initial condition is now obtained. The manipulations are considerably simplified by the introduction of the notation

$$f_i = f_i(Y_j) ,$$

and

(A.19)

$$f_i^j = \left(\frac{\partial f_i}{\partial y_j} \right)_{(X, Y_j)} ,$$

where

$$i = 1, 2, \dots, n ,$$

$$j = 0, 1, \dots, n .$$

The Taylor series expansion, as given by

$$\begin{aligned} \delta y_i = y_i(X+h) - y_i(X) &= h \left(\frac{dy_i}{dx} \right)_{(X, Y_i)} + \frac{h^2}{2!} \left(\frac{d^2 y_i}{dx^2} \right)_{(X, Y_i)} \\ &+ \frac{h^3}{3!} \left(\frac{d^3 y_i}{dx^3} \right)_{(X, Y_i)} + \dots, \end{aligned}$$

becomes with the notation of (A.19)

$$\begin{aligned} \delta y_i = y_i(X+h) - y_i(X) = hf_i + \frac{h^2}{2!} f_j f_i^j + \\ \frac{h^3}{3!} (f_j f_k f_i^{jk} + f_k f_i^j f_j^k) + \end{aligned} \quad (A.20)$$

$$\frac{h^4}{4!} (f_j f_k f_l f_i^{jkl} + 3f_j f_k f_l^k f_i^{jl} + f_j f_k f_l^{jk} f_i^l + f_j f_k^j f_l^k f_i^l) + \dots$$

Taylor series expansions are also required for the weighting functions k_{i0} , k_{i1} , k_{i2} , and k_{i3} ; the expression for k_{i0} simply reduces to

$$k_{i0} = hf_i. \quad (A.21)$$

The expansion of k_{i1} is obtained from

$$f_i(Y_j + mk_{j0}) = f_j(Y_j) + mk_{j0} \left(\frac{df_i}{dy_j} \right)_{Y_j} + \frac{m^2 k_{j0} k_{p0}}{2!} \left(\frac{d^2 f_i}{dy_j dy_p} \right)_{Y_j} + \dots \quad (A.22)$$

Substituting equation (A.21) in the expansion (A.22) gives

$$\begin{aligned} k_{i1} = hf_i(Y_j + mk_{j0}) = hf_i + mh^2 f_j f_i^j + \frac{m^2 h^3}{2} f_j f_k f_i^{jk} \\ + \frac{m^3 h^4}{6} f_j f_k f_l f_i^{jkl} + \dots \end{aligned}$$

The substitutions and manipulations required to find the expansions for k_{i2} and k_{i3} are complicated, and it serves no purpose to reproduce them here. However, it can be shown that the equality of the eight terms in equation (A.20) and the corresponding ones in the expansion of $\delta y_i = ak_{i0} + bk_{i1} + ck_{i2} + dk_{i3}$ leads to the set of equations (A.4) previously given for a single equation. Table A.1, extracted from Gill's paper (41), indicates the typical terms as well as their coefficients.

TABLE A.1
Typical Terms and their Coefficients

Term	Coefficient in	
	$\delta y_i = y_i(X+h) - y_i(X)$	$\delta y_i = ak_{i0} + bk_{i1} + ck_{i2} + dk_{i3}$
hf_i	1	$a + b + c + d$
$h^2 f_{j i} f_i^j$	1/2	$bm + cn + dp$
$h^3 f_{j k i} f_i^{jk}$	1/6	$1/2(bm^2 + cn^2 + dp^2)$
$h^3 f_{j k} f_i^j f_i^k$	1/6	$crm + d(sm + tn)$
$h^4 f_{j k l i} f_i^{jkl}$	1/24	$1/6(bm^3 + cn^3 + dp^3)$
$h^4 f_{j k l} f_i^k f_i^{jl}$	1/8	$crm + d(sm + tn) p$
$h^4 f_{j k l} f_i^{jk} f_i^l$	1/24	$1/2\{crm^2 + d(sm^2 + tn^2)\}$
$h^4 f_{j k l} f_i^k f_i^l$	1/24	$dtrm$

A.6 Gill's Variation of the Runge-Kutta Fourth Order Method

The procedure Gill used in removing the indeterminacy of the constants is now discussed; the purpose of this procedure, as previously noted, is to minimize the number of storage registers required for auto-

matic machine computations. Further, Gill chose the parameters such that the accuracy was the highest attainable.

In starting out the integration procedure $n + 1$ registers are required to store the quantities Y_j , $j = 0, 1, \dots, n$. At the end of the first stage an extra register is required to store the quantity k_{j0} . During the second stage, the quantities $Y_j + mk_{j0}$ and k_{j1} are to be stored. Before proceeding, however, the quantities $Y_j + (n-r)k_{j0}$, $Y_j + (p-s-t)k_{j0}$ and $Y_j + ak_{j0}$ should be stored as well since they are needed in the following stages. These five quantities are linearly dependent and can be represented by three. For the third stage the quantities $Y_j + (n-r)k_{j0} + rk_{j1}$, $Y_j + (p-s-t)k_{j0} + sk_{j1}$, $Y_j + ak_{j0} + bk_{j1}$, and k_{j2} need to be stored, therefore, four registers are required. At the final stage the quantities to be stored are three in number, namely

$$Y_j + (p-s-t)k_{j0} + sk_{j1} + tk_{j2}, Y_j + ak_{j0} + bk_{j1} + ck_{j2}, \text{ and } k_{j3}.$$

So in general three storage registers are enough except at the third stage, where four are needed. This draw-back can be overcome by making the first three linearly dependent; this condition implies that

$$\begin{vmatrix} 1 & n-r & r \\ 1 & p-s-t & s \\ 1 & a & b \end{vmatrix} = 0,$$

which reduces to

$$[p - (s+t)](b-r) + (n-r)(s-b) + a(r-s) = 0. \quad (\text{A.23})$$

The system of equations to be solved, therefore, reduces to the set of equations (A.4) and in addition equation (A.23).

It has been shown previously that $p = 1$; then, if m and n are constrained to be equal to $1/2$, a set of equations is obtained, which for completeness is shown below

$$a + b + c + d = 1 ,$$

$$b + c + 2d = 1 ,$$

$$b + c + 4d = 4/3 ,$$

$$b + c + 8d = 2 , \quad (\text{A.24})$$

$$cr + ds + dt = 1/3 ,$$

$$cr + ds + dt = 1/3 ,$$

$$cr + 2ds + 2dt = 1/2 ,$$

$$dtr = 1/12 ,$$

$$[1 - (s+t)](b-r) + \left(\frac{1}{2} - r\right)(s-b) + a(r-s) = 0 .$$

Solving the set of equations (A.24), gives

$$a = 1/6 ,$$

$$b = \frac{1}{3} [1 \mp \sqrt{\frac{1}{2}}] ,$$

$$c = \frac{1}{3} [1 \pm \sqrt{\frac{1}{2}}] ,$$

$$d = 1/6 ,$$

and

$$r = 1 \mp \sqrt{\frac{1}{2}} ,$$

$$s = \mp \sqrt{\frac{1}{2}} ,$$

$$t = 1 \pm \sqrt{\frac{1}{2}} ,$$

with

$$m = n = 1/2 ,$$

$$p = 1 .$$

Gill has shown that in making the error in the term of $O(h^5)$ in the Taylor

series expansion the least, and thus obtaining maximum accuracy, the upper sign of the square root should be used. The formulae, due to Gill, then become

$$k_{i0} = hf_i(y_{00}, y_{10}, y_{20}, \dots) ,$$

$$k_{i1} = hf_i(y_{01}, y_{11}, y_{21}, \dots) ,$$

$$k_{i2} = hf_i(y_{02}, y_{12}, y_{22}, \dots) ,$$

$$k_{i3} = hf_i(y_{03}, y_{13}, y_{23}, \dots) ,$$

where

$$y_{i0} = Y_i ,$$

$$y_{i1} = Y_i + \frac{1}{2} k_{i0} ,$$

$$y_{i2} = Y_i + \left[-\frac{1}{2} + \sqrt{\frac{1}{2}}\right] k_{i0} + \left[1 - \sqrt{\frac{1}{2}}\right] k_{i1} ,$$

$$y_{i3} = Y_i + \left[-\sqrt{\frac{1}{2}}\right] k_{i1} + \left[1 + \sqrt{\frac{1}{2}}\right] k_{i2} ,$$

and the accepted value of y_i at the end of the step is

$$y_{i4} = Y_i + \frac{1}{6} k_{i0} + \frac{1}{3} \left[1 - \sqrt{\frac{1}{2}}\right] k_{i1} + \frac{1}{3} \left[1 + \sqrt{\frac{1}{2}}\right] k_{i2} + \frac{1}{6} k_{i3} ,$$

where

$$i = 0, 1, \dots, n.$$

A subroutine based on Gill's variation of the Runge-Kutta fourth order method (43) has been prepared, and is shown in the body of this Appendix.

Up to now no mention has been made about the errors encountered in using this process; this is done in the next section.

A.7 Brief Discussion on the Accuracy of the Method

In order to discuss the results qualitatively, it is necessary that some estimate is made of the errors due to rounding-off and truncation. The latter are caused by the fact that terms of $O(h^5)$ and higher are neglected in the Taylor series expansion about the initial values.

Gill has discussed the rounding-off errors of such quantities as $\sqrt{\frac{1}{2}}$ and $\frac{1}{6}$ at length. However, since the program is written in double precision, that is the calculations are performed carrying 16 significant figures, it is reasonable to assume that the errors introduced due to rounding-off are negligible.

Truncation errors or estimates thereof are not accounted for in the program. In order to overcome this disadvantage, control of accuracy is accomplished by adjusting the increment in x ; a comparison is then made between the function values obtained at $x = X + 2h$ by firstly using the increment $\Delta x = h$ in two stages and secondly by using double the increment, $\Delta x = 2h$, in a single stage.

Returning now to the single first order equation

$$\frac{dy}{dx} = f(x,y) .$$

Suppose that the initial condition is $y = Y$ at $x = X$, and that the function value is required at $x = X + 2h$, where h is small. Let the error, due to truncation, of the function value at $x = X + h$ be denoted by ϵ . Since terms $O(h^5)$ are neglected in the Taylor series expansion,

$$\epsilon = ch^5$$

approximately, where c is some constant. The error in the function value at $x = X + 2h$, as calculated in two stages, is then

$$2\epsilon = 2ch^5 .$$

Secondly, the increment $\Delta x = 2h$ is used and consequently the error in the function value at $x = X + 2h$, as obtained in a single stage, is given by

$$\epsilon' = 32ch^5 ,$$

consequently

$$2\epsilon = 2ch^5 = \frac{1}{15} (\epsilon' - 2\epsilon) . \quad (A.25)$$

From the preceding discussion, this may be written as

$$2\varepsilon = \frac{1}{15} [y^{(2)} - y^{(1)}] ,$$

where $y^{(1)}(X + 2h)$ is the function value obtained in two stages with the increment $\Delta x = h$, and $y^{(2)}(X + 2h)$ is the function value calculated in one stage with the increment $\Delta x = 2h$. This discussion of the truncation errors may readily be extended to a system of ordinary differential equations.

In the subroutine a test value δ is generated for the control of accuracy and is defined as

$$\delta = \frac{1}{15} \sum_{i=1}^n a_i \cdot |y_i^{(1)} - y_i^{(2)}| ,$$

where $y_i^{(1)}$ and $y_i^{(2)}$ have the same meaning as before, and the coefficients a_i are the error-weights. The test value δ is an approximate measure of the local truncation error at the point $x = X + 2h$, and may be specified arbitrarily at the start of the program. The test value δ is denoted by DELT in the subroutine. For completeness the subroutine based on Gill's variation of the Runge-Kutta fourth order method is now presented.

A.8 Subroutine DRKGS

SUBROUTINE DRKGS

PURPOSE

TO SOLVE A SYSTEM OF FIRST ORDER ORDINARY DIFFERENTIAL EQUATIONS WITH GIVEN INITIAL VALUES.

USAGE

CALL DRKGS(PRMT,Y,DERY,NDIM,IHLF,FCT,OUTP,AUX)

PARAMETERS FCT AND OUTP REQUIRE AN EXTERNAL STATEMENT.

DESCRIPTION OF PARAMETERS

- PRMT - DOUBLE PRECISION INPUT AND OUTPUT VECTOR WITH DIMENSION GREATER THAN OR EQUAL TO 5, WHICH SPECIFIES THE PARAMETERS OF THE INTERVAL AND OF ACCURACY AND WHICH SERVES FOR COMMUNICATION BETWEEN OUTPUT SUBROUTINE (FURNISHED BY THE USER) AND SUBROUTINE DRKGS. EXCEPT PRMT(5) THE COMPONENTS ARE NOT DESTROYED BY SUBROUTINE DRKGS AND THEY ARE
- PRMT(1)- LOWER BOUND OF THE INTERVAL (INPUT),
 PRMT(2)- UPPER BOUND OF THE INTERVAL (INPUT),
 PRMT(3)- INITIAL INCREMENT OF THE INDEPENDENT VARIABLE (INPUT),
 PRMT(4)- UPPER ERROR BOUND (INPUT). IF ABSOLUTE ERROR IS GREATER THAN PRMT(4), INCREMENT GETS HALVED. IF INCREMENT IS LESS THAN PRMT(3) AND ABSOLUTE ERROR LESS THAN PRMT(4)/50, INCREMENT GETS DOUBLED. THE USER MAY CHANGE PRMT(4), BY MEANS OF HIS OUTPUT SUBROUTINE.
- PRMT(5)- NO INPUT PARAMETER. SUBROUTINE DRKGS INITIALIZES PRMT(5)=0. IF THE USER WANTS TO TERMINATE SUBROUTINE DRKGS AT ANY OUTPUT POINT, HE HAS TO CHANGE PRMT(5) TO NON-ZERO BY MEANS OF SUBROUTINE OUTP. FURTHER COMPONENTS OF VECTOR PRMT ARE FEASIBLE IF ITS DIMENSION IS DEFINED GREATER THAN 5. HOWEVER SUBROUTINE DRKGS DOES NOT REQUIRE AND CHANGE THEM. NEVERTHELESS THEY MAY BE USEFUL FOR HANDING RESULT VALUES TO THE MAIN PROGRAM (CALLING DRKGS) WHICH ARE OBTAINED BY SPECIAL MANIPULATIONS WITH OUTPUT DATA IN SUBROUTINE OUTP.
- Y - DOUBLE PRECISION INPUT VECTOR OF INITIAL VALUES (DESTROYED). LATERON Y IS THE RESULTING VECTOR OF DEPENDENT VARIABLES COMPUTED AT INTERMEDIATE POINTS X.
- DERY - DOUBLE PRECISION INPUT VECTOR OF ERROR WEIGHTS (DESTROYED). THE SUM OF ITS COMPONENTS MUST BE EQUAL TO 1. LATERON DERY IS THE VECTOR OF DERIVATIVES, WHICH BELONG TO FUNCTION VALUES Y AT INTERMEDIATE POINTS X.

- NDIM - AN INPUT VALUE, WHICH SPECIFIES THE NUMBER OF EQUATIONS IN THE SYSTEM.
- IHLF - AN OUTPUT VALUE, WHICH SPECIFIES THE NUMBER OF BISECTIONS OF THE INITIAL INCREMENT. IF IHLF GETS GREATER THAN 10, SUBROUTINE DRKGS RETURNS WITH ERROR MESSAGE IHLF=11 INTO MAIN PROGRAM. ERROR MESSAGE IHLF=12 OR IHLF=13 APPEARS IN CASE PRMT(3)=0 OR IN CASE SIGN(PRMT(3)).NE.SIGN(PRMT(2)-PRMT(1)) RESPECTIVELY.
- FCT - THE NAME OF AN EXTERNAL SUBROUTINE USED. THIS SUBROUTINE COMPUTES THE RIGHT HAND SIDES DERY OF THE SYSTEM TO GIVEN VALUES X AND Y. ITS PARAMETER LIST MUST BE X,Y,DERY. SUBROUTINE FCT SHOULD NOT DESTROY X AND Y.
- OUTP - THE NAME OF AN EXTERNAL OUTPUT SUBROUTINE USED. ITS PARAMETER LIST MUST BE X,Y,DERY,IHLF,NDIM,PRMT. NONE OF THESE PARAMETERS (EXCEPT, IF NECESSARY, PRMT(4),PRMT(5),...) SHOULD BE CHANGED BY SUBROUTINE OUTP. IF PRMT(5) IS CHANGED TO NON-ZERO, SUBROUTINE DRKGS IS TERMINATED.
- AUX - DOUBLE PRECISION AUXILIARY STORAGE ARRAY WITH 8 ROWS AND NDIM COLUMNS.

REMARKS

- THE PROCEDURE TERMINATES AND RETURNS TO CALLING PROGRAM, IF
- (1) MORE THAN 10 BISECTIONS OF THE INITIAL INCREMENT ARE NECESSARY TO GET SATISFACTORY ACCURACY (ERROR MESSAGE IHLF=11),
 - (2) INITIAL INCREMENT IS EQUAL TO 0 OR HAS WRONG SIGN (ERROR MESSAGES IHLF=12 OR IHLF=13),
 - (3) THE WHOLE INTEGRATION INTERVAL IS WORKED THROUGH,
 - (4) SUBROUTINE OUTP HAS CHANGED PRMT(5) TO NON-ZERO.

SUBROUTINES AND FUNCTION SUBPROGRAMS REQUIRED

THE EXTERNAL SUBROUTINES FCT(X,Y,DERY) AND OUTP(X,Y,DERY,IHLF,NDIM,PRMT) MUST BE FURNISHED BY THE USER.

METHOD

EVALUATION IS DONE BY MEANS OF FOURTH ORDER RUNGE-KUTTA FORMULAE IN THE MODIFICATION DUE TO GILL. ACCURACY IS TESTED COMPARING THE RESULTS OF THE PROCEDURE WITH SINGLE AND DOUBLE INCREMENT.

SUBROUTINE DRKGS AUTOMATICALLY ADJUSTS THE INCREMENT DURING THE WHOLE COMPUTATION BY HALVING OR DOUBLING. IF MORE THAN 10 BISECTIONS OF THE INCREMENT ARE NECESSARY TO GET SATISFACTORY ACCURACY, THE SUBROUTINE RETURNS WITH ERROR MESSAGE IHLF = 11 INTO MAIN PROGRAM.

TO GET FULL FLEXIBILITY IN OUTPUT, AN OUTPUT SUBROUTINE MUST BE FURNISHED BY THE USER.

FOR REFERENCE, SEE

RALSTON/WILF, MATHEMATICAL METHODS FOR DIGITAL COMPUTERS,
WILEY, NEW YORK/LONDON, 1960, PP. 110-120.

```

SUBROUTINE DRKGS(PRMT,Y,DERY,NDIM,IHLF,AUX)
DIMENSION Y(1),DERY(1),AUX(8,1),A(4),B(4),C(4),PRMT(1)
DOUBLE PRECISION PRMT,Y,DERY,AUX,A,B,C,X,XEND,H,AJ,BJ,CJ,R1,R2,
1DELT
DO 1 I=1,NDIM
1 AUX(8,I)=.06666666666666667DO*DERY(I)
X=PRMT(1)
XEND=PRMT(2)
H=PRMT(3)
PRMT(5)=0.DO
CALL FCT(X,Y,DERY)
ERROR TEST
IF(H*(XEND-X))38,37,2

```

PREPARATIONS FOR RUNGE-KUTTA METHOD

```

2 A(1)=.5DO
A(2)=.29289321881345248DO
A(3)=1.7071067811865475DO
A(4)=.16666666666666667DO
B(1)=2.DO
B(2)=1.DO
B(3)=1.DO
B(4)=2.DO
C(1)=.5DO
C(2)=.29289321881345248DO
C(3)=1.7071067811865475DO
C(4)=.5DO

```

PREPARATIONS FOR FIRST RUNGE-KUTTA STEP

```

DO 3 I=1,NDIM
AUX(1,I)=Y(I)
AUX(2,I)=DERY(I)
AUX(3,I)=0.DO
3 AUX(6,I)=0.DO
IREC=0
H=H+H
IHLF=-1
ISTEP=0
IEND=0

```

START OF A RUNGE-KUTTA STEP

```

4 IF((X+H-XEND)*H)7,6,5
5 H=XEND-X
6 IEND=1

```

RECORDING OF INITIAL VALUES OF THIS STEP

```

7 CALL OUTP(X,Y,DERY,IREC,NDIM,PRMT)

```

```

      IF(PRMT(5))40,8,40
8  ITEST=0
9  ISTEP=ISTEP+1

```

```

      START OF INNERMOST RUNGE-KUTTA LOOP
      J=1
10  AJ=A(J)
      BJ=B(J)
      CJ=C(J)
      DO 11 I=1,NDIM
      R1=H*DERY(I)
      R2=AJ*(R1-BJ*AUX(6,I))
      Y(I)=Y(I)+R2
      R2=R2+R2+R2
11  AUX(6,I)=AUX(6,I)+R2-CJ*R1
      IF(J-4)12,15,15
12  J=J+1
      IF(J-3)13,14,13
13  X=X+.5D0*H
14  CALL FCT(X,Y,DERY)
      GO TO 10
      END OF INNERMOST RUNGE-KUTTA LOOP

```

```

      TEST OF ACCURACY
15  IF(ITEST)16,16,20

```

IN CASE ITEST=0 THERE IS NO POSSIBILITY FOR TESTING OF ACCURACY

```

16  DO 17 I=1,NDIM
17  AUX(4,I)=Y(I)
      ITEST=1
      ISTEP=ISTEP+ISTEP-2
18  IHLF=IHLF+1
      X=X-H
      H=.5D0*H
      DO 19 I=1,NDIM
      Y(I)=AUX(1,I)
      DERY(I)=AUX(2,I)
19  AUX(6,I)=AUX(3,I)
      GO TO 9

```

IN CASE ITEST=1 TESTING OF ACCURACY IS POSSIBLE

```

20  IMOD=ISTEP/2
      IF(ISTEP-IMOD-IMOD)21,23,21
21  CALL FCT(X,Y,DERY)
      DO 22 I=1,NDIM
      AUX(5,I)=Y(I)
22  AUX(7,I)=DERY(I)
      GO TO 9

```

```

      COMPUTATION OF TEST VALUE DELT
23  DELT=0.DO
      DO 24 I=1, NDIM
24  DELT=DELT+AUX(8,I)*DABS(AUX(4,I)-Y(I))
      IF(DELT-PRMT(4))28,28,25

      ERROR IS TOO GREAT
25  IF(IHLF-10)26,36,36
26  DO 27 I=1,NDIM
27  AUX(4,I)=AUX(5,I)
      ISTEP=ISTEP+ISTEP-4
      X=X-H
      IEND=0
      GO TO 18

      RESULT VALUES ARE GOOD
28  CALL FCT(X,Y,DERY)
      DO 29 I=1,NDIM
      AUX(1,I)=Y(I)
      AUX(2,I)=DERY(I)
      AUX(3,I)=AUX(6,I)
      Y(I)=AUX(5,I)
29  DERY(I)=AUX(7,I)
      CALL OUTP(X-H,Y,DERY,IHLF,NDIM,PRMT)
      IF(PRMT(5))40,30,40
30  DO 31 I=1,NDIM
      Y(I)=AUX(1,I)
31  DERY(I)=AUX(2,I)
      IREC=IHLF
      IF(IEND)32,32,39

      INCREMENT GETS DOUBLED
32  IHLF=IHLF-1
      ISTEP=ISTEP/2
      H=H+H
      IF(IHLF)4,33,33
33  IMOD=ISTEP/2
      IF(ISTEP-IMOD-IMOD)4,34,4
34  IF(DELT-.02DO*PRMT(4))35,35,4
35  IHLF=IHLF-1
      ISTEP=ISTEP/2
      H=H+H
      GO TO 4

      RETURNS TO CALLING PROGRAM
36  IHLF=11
      CALL FCT(X,Y,DERY)
      GO TO 39
37  IHLF=12
      GO TO 39
38  IHLF=13
39  CALL OUTP(X,Y,DERY,IHLF,NDIM,PRMT)
40  RETURN
      END

```